NAVAL POSTGRADUATE SCHOOL
Monterey , California

THESIS

DESIGN AND INVESTIGATION OF A DIVE PLANE
SLIDING MODE
COMPENSATOR FOR AN AUTONOMOUS UNDER-
WATER VEHICLE.

by

Sur, Joo-No

September 1989

Thesis Advisor   Fotis A. Papoulias
Co-Advisor   Anthony J. Healey

REPORT DOCUMENTATION PAGE

a Report Security Classification Unclassified		1b Restrictive Markings		
a Security Classification Authority		3 Distribution Availability of Report		
b Declassification Downgrading Schedule		Approved for public release; distribution is unlimited.		
Performing Organization Report Number(s)		5 Monitoring Organization Report Number(s)		
a Name of Performing Organization Naval Postgraduate School	6b Office Symbol *(if applicable)* 69	7a Name of Monitoring Organization Naval Postgraduate School		
c Address *(city, state, and ZIP code)* Monterey, CA 93943-5000		7b Address *(city, state, and ZIP code)* Monterey, CA 93943-5000		
a Name of Funding Sponsoring Organization	8b Office Symbol *(if applicable)*	9 Procurement Instrument Identification Number		
c Address *(city, state, and ZIP code)*		10 Source of Funding Numbers		
		Program Element No	Project No	Task No	Work Unit Accession No

1 Title *(include security classification)* DESIGN AND INVESTIGATION OF A DIVE PLANE SLIDING MODE COMPENSATOR FOR AN AUTONOMOUS UNDERWATER VEHICLE.

2 Personal Author(s) Sur, Joo-No

3a Type of Report Master's Thesis	13b Time Covered From To	14 Date of Report *(year, month, day)* September 1989	15 Page Count 130

6 Supplementary Notation The views expressed in this thesis are those of the author and do not reflect the official policy or position of the Department of Defense or the U.S. Government.

7 Cosati Codes			18 Subject Terms *(continue on reverse if necessary and identify by block number)*
ield	Group	Subgroup	word processing, Script, GML, text processing.

9 Abstract *(continue on reverse if necessary and identify by block number)*
   A sliding mode compensator for depth control of an autonomous underwater vehicle (AUV) using depth feedback only s designed. The controller is evaluated for a nominal linear model and optimized by a series of numerical experiments for a umber of depth changing maneuvers. A state observer is used in order to estimate the unmeasurable states together with the liding mode controller. The effects of varying control parameters are discussed. Compensator performance is assessed by umerical simulation of AUV dynamic response based on the full six degrees of freedom nonlinear equations of motion. The xpected robustness of the design is demonstrated by comparison between linear and nonlinear vehicle response character-stics, and by a wide variation in vehicle parameters and hydrodynamic coefficients. Finally, suggestions for design improvement and directions for future research are indicated.

0 Distribution Availability of Abstract ⊠ unclassified unlimited ☐ same as report ☐ DTIC users	21 Abstract Security Classification Unclassified	
2a Name of Responsible Individual Totis A. Papoulias	22b Telephone *(include Area code)* (408) 646-3381	22c Office Symbol 69Pa

D FORM 1473.84 MAR

83 APR edition may be used until exhausted
All other editions are obsolete

security classification of this page

Unclassified

T245493

Design and Investigation of a Dive Plane Sliding Mode
Compensator for an Autonomous Underwater Vehicle.

by

Sur, Joo-No
Lt, Korean Navy
B.S., Naval Academy, 1981
B.S., Seoul National University,1985

Submitted in partial fulfillment of the
requirements for the degree of

MASTER OF SCIENCE IN MECHANICAL ENGEERING

from the

NAVAL POSTGRADUATE SCHOOL
September 1989

ABSTRACT

A sliding mode compensator for depth control of an autonomous underwater vehicle (AUV) using depth feedback only is designed. The controller is evaluated for a nominal linear model and optimized by a series of numerical experiments for a number of depth changing maneuvers. A state observer is used in order to estimate the unmeasurable states together with the sliding mode controller. The effects of varying control parameters are discussed. Compensator performance is assessed by numerical simulation of AUV dynamic response based on the full six degrees of freedom nonlinear equations of motion. The expected robustness of the design is demonstrated by comparison between linear and nonlinear vehicle response characteristics, and by a wide variation in vehicle parameters and hydrodynamic coefficients. Finally, suggestions for design improvement and directions for future research are indicated.

TABLE OF CONTENTS

LIST OF TABLES

LIST OF FIGURES

ACKNOWLEDGEMENTS

I. INTRODUCTION

A. GENERAL

There has been an increased interest recently in the need for autonomous underwater vehicles (AUV) in both Navy and private industry. A variety of unclassified missions includes ASW, decoy, survey, reconnaissance, and ocean engineering work service. As the cost of manned submarine vehicles increases, there are significant advantages to the use of cheaper unmanned vehicles. The AUV should be able to maneuver freely in the ocean enviroment with respect to depth, heading, and speed in order to carry out its missions. Such maneuvering requirements have to be easily accomplished by a low level active control system, and in the presence of environmental and physical uncertainty.

All information concerning the environment of a vehicle is detected by the sensing level of control on-board the vehicle and directed to the high level intelligent system in order to carry out an unmanned mission. The dynamics of underwater vehicles are described by highly nonlinear systems with uncertain coefficients and disturbances that are difficult to measure. Robust control using variable structure systems are reputed to provide accurate control of nonlinear systems despite unmodeled system dynamics and disturbances, leading to the motion that sliding mode compensators should be employed in situations where accurate tracking is desired and where maneuvering parameters of AUV change with operating conditions.

B. AIM OF THIS STUDY

This thesis aims at investigation of the use of sliding mode compensator for AUV depth keeping and changing. The control concept developed here is that of a variable structure system consisting of continuous subsystems together with suitable switching logic. The sliding mode control concept was suggested by V. Utkin [Ref. 1] and recently developed by J.J.E. Slotine [Ref. 2]. Because sliding mode control requires full state feedback, this work has incorporated a state observed based on output measurement resulting in a sliding mode compensator.

The main goal of this thesis is to present a design procedure and estimate robustness of the variable structure compensator in the presence of vehicle non-linearities, modeling errors, uncertainties, and variation of parameters.

C. THESIS OUTLINE

Chapter 2 introduces the basic concept of Liapunov stability and an asymptotically stable condition which is related to energy degeneration with increasing time for a dynamics system. The other sections will discuss how to design a sliding surface and a control law based on a linear model. The last section of the chapter presents a technique to eliminate chattering in order to provide smooth control inputs.

In Chapter 3, vehicle dynamics and a process used to produce a linear state space representation are described. Sliding control law for a linear model is designed using results of the previous chapter. The design is evaluated through computer simulation.

Chapter 4 presents the sliding mode compensator using depth measurements only. A model with perturbed hydrodynamic and geometric parameters is used to estimate the performance of the sliding mode compensator. The chapter ends with a discussion of the robustness of the sliding mode compensator and advantage of the variable structure control system

Finally, Chapter 5 contains a summary, conclusions, and some directions for further research.

II.   THEORETICAL BACKGROUND OF SLIDING MODE CONTROL

A.   GENERAL

The dynamics of underwater vehicles are described by highly nonlinear, high order systems with uncertain models and disturbances that are difficult to model. A new form of sliding mode (Variable Structure System) control has been developed recently, and shown to apply to a large class of nonlinear systems [Ref. 3]. Sliding mode control offers the control designer new possibilities for improving the quality of the control in comparison with a fixed structure system. The basic idea is to design a controller structure which consists of a set of continuous subsystems together with suitable switching logic according to [Ref. 1]. The basic sliding mode control for a SISO system

$$\dot{x} = Ax + Bu$$

$$u = [\pm \Psi x] \tag{2.1}$$

where,   x is the state variable

u is the sliding mode control law

Ψ is a switched feedback gain

A,B are system matrix.

This chapter is devoted to the study of the basic background of the sliding mode theory for the design of a linear controller for the AUV.

B.   LIAPUNOV STABILITY

For a given control system, stability is usually the most important thing to be determined. If the system is linear and time invariant, then, many stability criteria are available, such as the Nyquist stability criterion, the Routh's stability

3

criterion etc. The second method of Liapunov is the most general method for the determination of the stability of nonlinear and time varying systems. Before discussing the sliding mode control, the second method of Liapunov will be discussed in order to understand the sliding condition, which will be discussed in the next section. The basic concept of the second method of Liapunov is that if the system has an asymptotically stable equilibrium state, the stored energy of system decays with increasing time until it finally assumes it's minimum value. In order to explain this, Liapunov introduced the so called Liapunov function, an imaginary energy function which depends on the state variable $(x_1, x_2 ... x_n)$ and time (t). If the Liapunov function is denoted by V(x,t) and it's time derivatives denoted by

$$\dot{V}(x,t) = \frac{dv(x,t)}{dt} \tag{2.2}$$

then the Liapunov function has information as to stability, asymptotic stability or instability of an equilibrium state of the system without solving the state equation. The theorem of the Liapunov function is described in modern control engineering [Ref. 4]. If a system is described by

$$\dot{x} = f(x,t) \tag{2.3}$$

where   x is the state variable and if
$f(0,t) = 0$, for $t_0 < t$.

and there exists a Liapunov function V(x,t) having continuous $\dot{V}(x,t)$ and satisfying the following conditions:

1. V(x,t) is positive definite, and
2. $\dot{V}(x,t)$ is negative definite.

then the equilibrium state at the origin is asymptotically stable. $V(x,t)$ is negative definite which shows that V(x,t) is continually decreasing. So for any system

$$\dot{x} = f(x,u(t)) \tag{2.4}$$

where,   x is the state variable

u(t) is the control law

$x(0,t) = x_0$

and the time derivative of the Liapunov function $V(x,u(t))$ is negative definite, then control law u(t) is guaranteed stable.

C.   DYNAMICS OF SYSTEM WITH SWITCHING

Now consider the case that an asymptotically stable system may consist of two structures neither of which is asymptotically stable.   If the differential equations of the second order system have the following format:

$$\frac{dx_1}{dt} = x_2$$

$$\frac{dx_2}{dt} = Ux_1 \tag{2.5}$$

where   u is a constant $\leq |\Psi^2|$

then the structure of the system is elliptic as described in Figure 1 on page 6. Suppose the system with a positive feedback gain, then structure is aperiodically unstable as shown in Figure 1. The block diagram of the closed loop system with switching gain is illustrated in Figure 2 on page 7. Let us try to combine the advantage of both systems by suitable choice of their structures in the appropri-

5
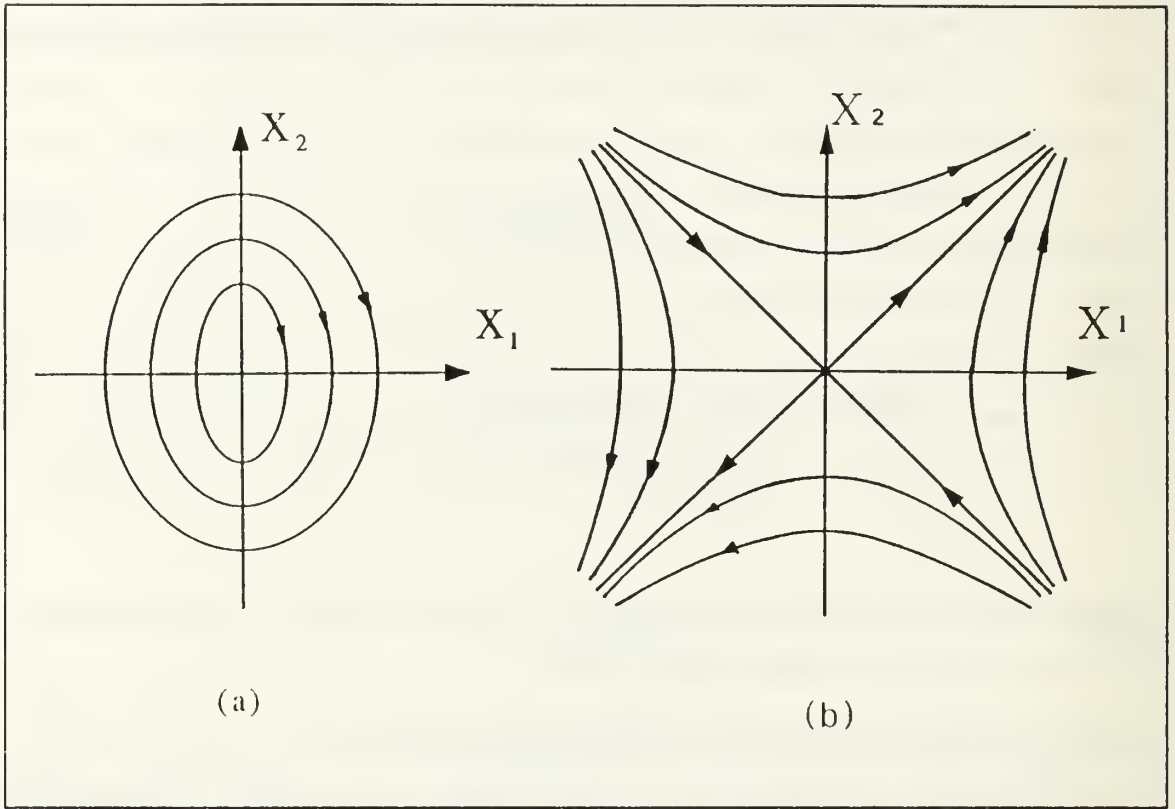
Figure 1.   Asymptotically unstable structure [Ref.5]

ate parts of the phase plane. In order to get the asymptotically stable structures in Figure 3 (b), the phase plane was divided into four pairwise subsections as shown in Figure 3 (a) by the following conditions:

1.   Subsection I   : $x_1 \geq 0$, $x_2 + \Psi' x_1 > 0$

2.   Subsection II   : $x_1 < 0$, $x_2 + \Psi' x_1 \geq 0$

3.   Subsection III   : $x_1 \leq 0$, $x_2 + \Psi' x_1 < 0$

4.   Subsection IV   : $x_1 > 0$, $x_2 + \Psi' x_1 \leq 0$

The good phase trajectory for each phase portrait has been chosen to make asymptotically stable structures as in Figure 3 (b).

This phase plane is separated from one another by the straight line $x_1 = 0$ and $x_2 + \Psi' x_1 = 0$ which we call the switch line or sliding surface. The asymptote

6
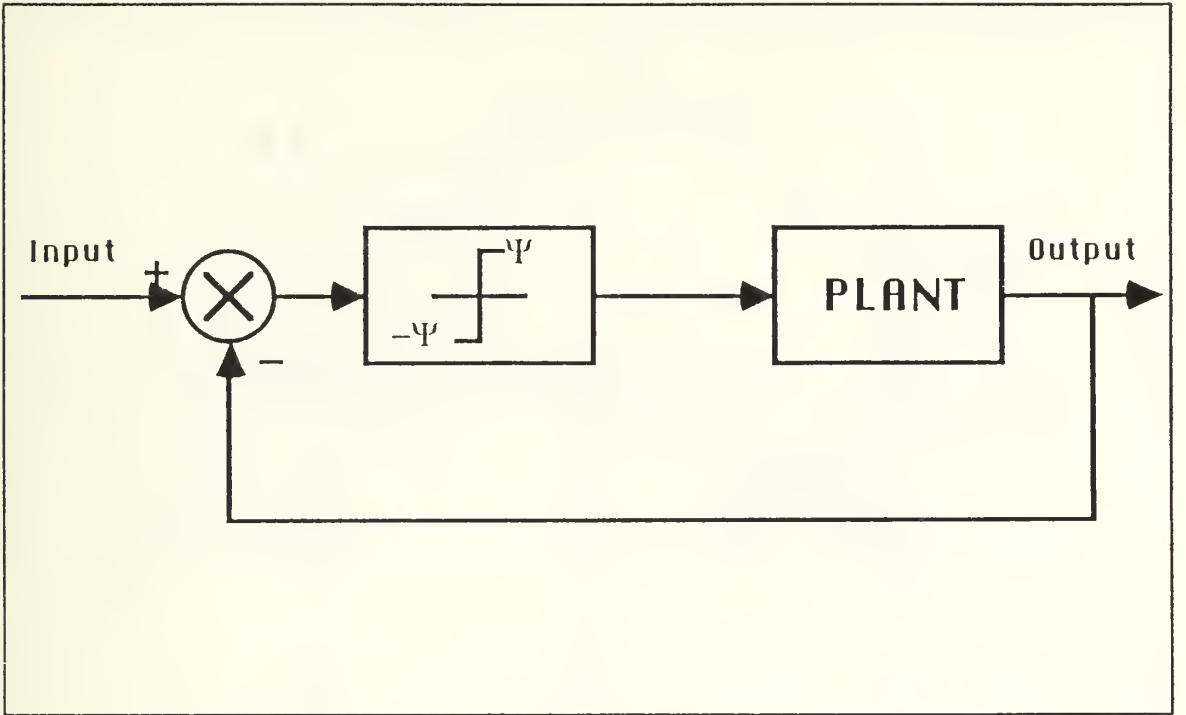
Figure 2. The block diagram with switching gain

$x_2 + \Psi' x_1 = 0$ acts as a switching line for the structure when the trajectory of the subsection I is reached. The structure of the system can be switched by using this line instantaneously from elliptic to hyperbolic in this case. This switching line is very important in sliding mode control. Once the system state trajectory approaches the switching line, and in order to keep the trajectory on the sliding surface for $t > t_0$, then this system will become asymptotically stable as long as it satisfies the Liapunov condition. In the general case, a switching line might be a straight line, $\sigma = x_2 + \lambda x_3$ $(0 < \lambda < \infty)$, but must pass through the origin (i e $\sigma(0) = 0$).

D. SLIDING CONDITION

Some of the possible advantages offered by the idea of switching the structure of a control system were described in the last subsection. But we remarked that if the structure does not change at the precise instance when the trajectory crosses the switching line, due to the effect noise, then additional control action will be
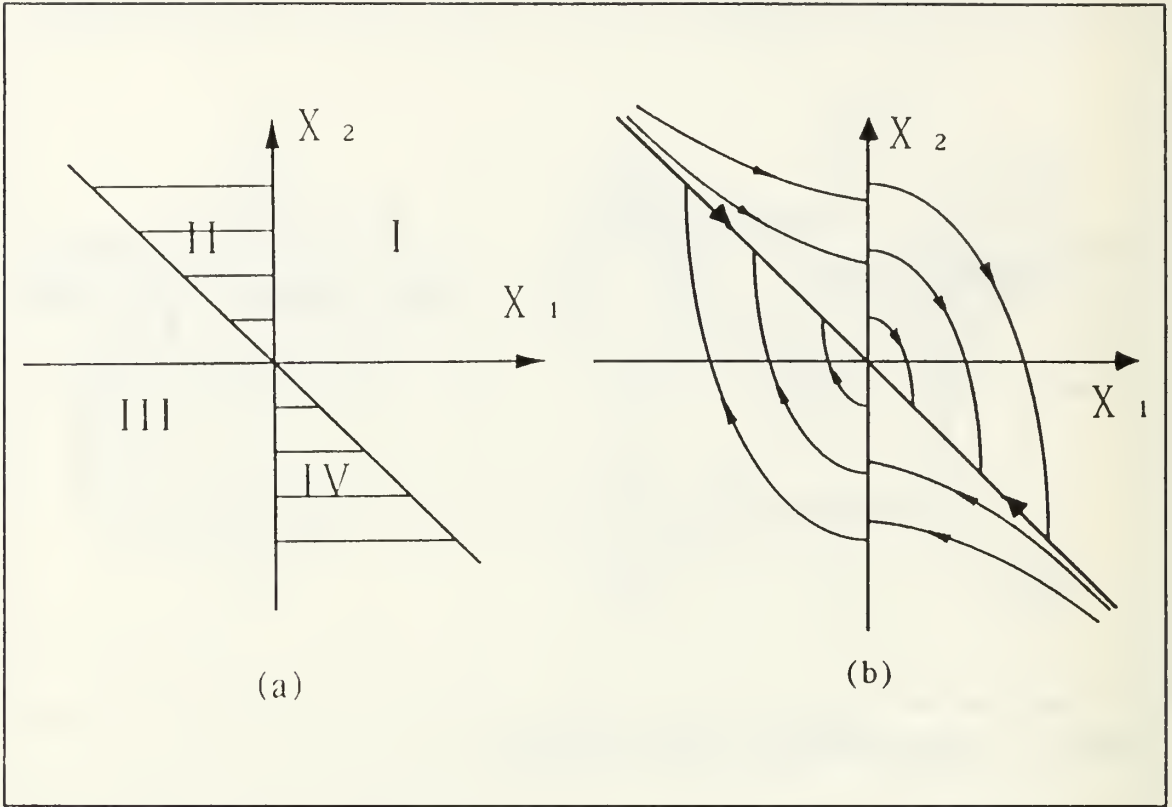
Figure 3.   Phase plane division and combined stable structure [Ref.5]

required to enforce the sliding condition. The motion of the system now depends on sliding surface parameters which are insensitive to the external disturbances and variations of the plant parameters within a wide range of the switching line. If the system trajectory of the subsection I crosses into the switching line and after passing the system trajectory of the subsection II crosses over the switching line repeatedly again, the system trajectory will be kept within some range of the switching line. Suppose such change occurs at infinitely high frequency, then the state of the system trajectory is maintained with an infinitesimal amplitude oscillation. It is an asymptotically stable system on this line as shown in Figure 4 on page 9.

The motion of the system on the switching line is described by the solution of the general differential equation (2.5) [Ref. 2] together with the equation of the general switching line given by

8
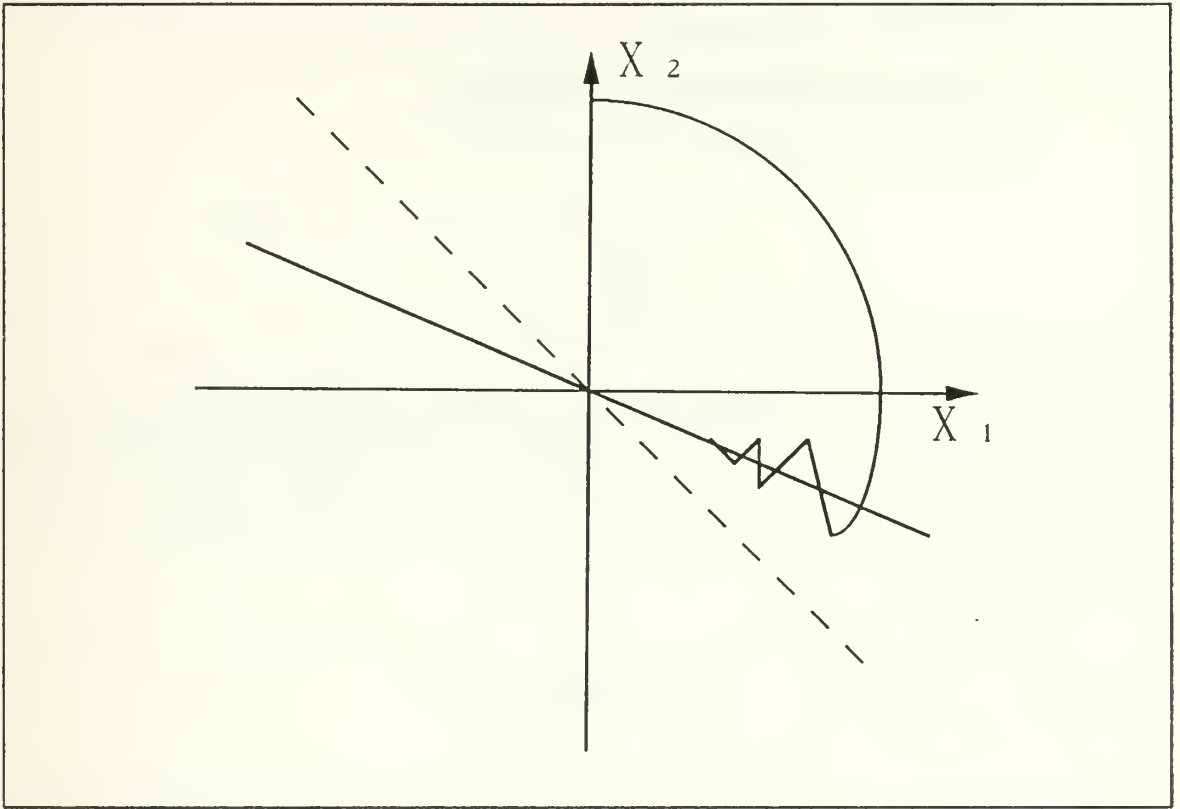
Figure 4. Switching line and asymptotic trajectory [Ref.5]

$$\sigma(x) = (\frac{d}{dt} + \lambda)^{n-1}\tilde{x} = 0 \tag{2.6}$$

where $\tilde{x} = x - x_d$, a single element of the state vector

$\lambda > 0$ (arbitrary constant)

n = order of system

The motion defined by the equation (2.6) describes the system dynamics in the sliding mode. A sliding mode has an important property that the corresponding motion of the system depends on the sliding surface (Switching Line) which is chosen by the designer only. In order to know the mathematical existence condi-

9

tion for the sliding mode, the theory of sliding mode has given a considerable attention to the methods guaranteeing the existence of the sliding mode.

1. Condition for Existence of a Sliding Mode

Considering the general dynamic system

$$\frac{dx}{dt} = f(x,t) \tag{2.7}$$

Let us assume that the right hand members of this equation are discontinuous on a certain sliding surface $\sigma(x) = 0$ in the phase space, where, as phase trajectory of the system approaches $\sigma(x) = 0$ from either side, the following limits are defined [Ref. 5]:

$$\lim_{\sigma \to 0^-} f(x,t) = f^-(x,t)$$

$$\lim_{\sigma \to 0^-} f(x,t) = f^+(x,t) \tag{2.8}$$

where $\quad f^-(x,t) \neq f^-(x,t)$

then the derivative of the sliding surface (σ) along the trajectories of the system is

$$\frac{d\sigma}{dt} = \frac{\partial\sigma}{\partial x}\frac{dx}{dt} = \frac{\partial\sigma}{\partial x}f = (f.grad\sigma) \tag{2.9}$$

where $\quad$ f = phase velocity vector, and

$$\lim_{\sigma \to 0^-} \frac{d\sigma}{dt} = (f^- grad\sigma)$$

$$\lim_{\sigma \to 0^-} \frac{d\sigma}{dt} = (f^+ grad\sigma) \qquad (2.10)$$

where $\quad \sigma, f$ is a smooth function.

At each point of $\sigma = 0$, the sign of the limit equation (2.8) has seven cases. There is a case which is most interesting as it corresponds to the existence of an ideal sliding mode on the sliding surface $\sigma = 0$, if

$$\lim_{\sigma \to 0^-} \frac{d\sigma}{dt} < 0$$

$$\lim_{\sigma \to 0^-} \frac{d\sigma}{dt} > 0 \qquad (2.11)$$

The equivalent inequality being the condition for existence of a sliding mode is

$$\lim_{\sigma \to 0} \sigma \frac{d\sigma}{dt} \leq 0$$

or

$$\lim_{\sigma \to 0} \frac{d(\sigma^2)}{dt} \leq 0 \qquad (2.12)$$

2. Proof of Stability

This inequality is also suggested by [Ref. 5] as a necessary condition for the system in equation (2.5) to have a degenerating Liapunov function in the following form:

$$V(x) = \frac{1}{2} [\sigma(x)]^2 \qquad (2.13)$$

11

The asymptotic stability of the system (2.5) is guaranteed provided that $V(x)$ is negative definite as discussed in the previous section. If $\sigma(x,t)$ is a sliding surface by the definition above, it follows that

$$\frac{1}{2} \frac{d}{dt} \sigma^2(x,t) \le -\eta^2 \, | \, \sigma(x,t) \, | \tag{2.14}$$

where η is the sliding control gain and
$\sigma(x,t)$ is the sliding surface.

It will guarantee stability of the sliding mode motion. The control law driving motion in the sliding mode can be obtained by using this condition [Ref. 2]. The next section will be devoted to a discussion for the development of the sliding mode control law.

E. SLIDING SURFACE DESIGN

The sliding surface has a very important property that is shown in the previous section. The sliding surface should be designed so that system response restricted to $\sigma(x)$ has a desired behavior, such as asymptotically stable state or tracking error.

Let us consider a linear time invariant system to design the sliding surface

$$\dot{x} = Ax + Bu \tag{2.15}$$

where $x \in R^n$, $u \in R^m$

Consider that the sliding surface of the equation (2.15) has the following form:

$$\sigma(x) = S^T x = 0 \tag{2.16}$$

where   S is the sliding surface coefficient $(m \times n)$

The existence of the sliding mode implies that $\sigma(x)\dot{\sigma}(x) \leq 0$ and $\sigma(x) = 0$ for all $t \geq t_0$. Using the method of equivalent control [Ref. 6]

$$\dot{\sigma}(x) = 0 = \frac{\partial \sigma}{\partial x}\frac{dx}{dt} = S^T\dot{x} = 0 \tag{2.17}$$

Substituting equation (2.15) for $\dot{x}$ of the above equation

$$S^T(Ax + Bu_{eq}) = 0$$

or

$$u_{eq} = -[S^TB]^{-1}S^TAx \tag{2.18}$$

Substituting equation (2.18) to Eq (2.15) and rearranging

$$\dot{x} = Ax - B[S^TB]^{-1}S^TAx$$

or

$$\dot{x} = [A - B(S^TB)^{-1}S^TA]x \tag{2.19}$$

Equation (2.19) gives the dynamics of the system on the sliding surface for $t \geq t_0$ given $\sigma(x) = 0$, but the S matrix is unknown. In order to determine S matrix, the equation (2.19) can be rearranged in the following form:

$$\dot{x} = [A - BK_c]x$$

$$\dot{x} = A_c x \tag{2.20}$$

where $\quad K_c = (S^TB)^{-1}S^TA$
$$A_c = A - BK_c$$

The K_c matrix can be obtained from the pole placement for which we can select specifically desired closed-loop poles of the system equation (2.20) on the sliding

surface. If we get the K_c matrix by using the standard pole placement method, the sliding surface matrix ($m \times n$) can be determined in the following procedure:

$$K_c = (S^T B)^{-1} S^T A$$

$$S^T A - S^T B K_c = 0$$

$$S^T(A - BK_c) = S^T A_c = 0 \tag{2.21}$$

It should be noted that A_c must be rank deficient by one and that the procedure must therefore place one pole of A_c at the origin. The left eigenvector of the A_c matrix of equation (2.21) corresponding to a pole placed at the origin are the sliding surface coefficients which give the desired behavior system on the sliding surface.

F. SLIDING MODE CONTROL LAW

Given the dynamic model, the sliding surface definition, and the stability criteria, a suitable control law can be obtained. We assume that a wide range of single input, single output dynamic systems, and sliding surfaces can be described by

$$\dot{x} = Ax + Bu \tag{2.22}$$

$$\sigma(x,t) = S^T \tilde{x}(t)$$

where S^T is a row vector of the form $[1, s_2, s_3, \dots s_{n-1}]$, a specific choice of S^T to achieve a stable tracking error and to enhance robustness as discussed in the previous section. If $u(t)$ could be chosen so as to keep the trajectory on $\sigma(x,t) = 0$, we would have the sliding control law from the sliding condition equation (2.14) and sliding surface equation (2.16) that

$$\dot{\sigma}(x) = S^T \dot{x} = -\eta^2 sign(\sigma)$$

$$S^T A + S^T B u = -\eta_0^2 sign(\sigma)$$

$$u = -(S^T B)^{-1} S^T A x - (S^T B)^{-1} \eta_0^2 sign(\sigma) \qquad (2.23)$$

where η_0^2 is a arbitrary nonlinear feedback gain

The control law has two parts.

$$u = \hat{u} + \bar{u}$$

where $\hat{u}$ is linear feedback control law

$\bar{u}$ is nonlinear feedback control law

Initially, $\hat{u}$ compensates directly for the known portions of the dynamics. Thus, $\bar{u}$ is discontinuous across the sliding surface. This nonlinear term is obtained directly from the time-varying bounds on parametric uncertainty and disturbances. As a result, control discontinuity across $\sigma=0$ grows as the model becomes less certain and increasingly disturbed. This insures that σ^2 is a Liapunov function of the closed-loop system, since it satisfies the sliding condition equation (2.14) and thus guarantees stability despite the uncertainty in the model and disturbances [Ref. 2]. This type of control law can guarantee stability and perfect tracking for a large class of nonlinear systems. The discontinuous form results in a chattering type of control action that would be very undesirable for most systems and this chattering behavior has been one of the main reasons sliding control techniques have not been more widely applied. This problem will be solved by smoothing out the control law in a thin boundary layer around the sliding surface as given in the next section.

G. CONSIDERING CHATTERING AND UNCERTAINTY

While sliding mode control provides a control law which is robust to parameter variations and disturbance inputs, it was a chattering problem for the input as shown in Figure 5 on page 17. In fact, imperfections such as delays in switching and hysteresis in switching, will cause the trajectory to chatter along the sliding surface. Although as such imperfections vanish, control activity remains as undesirable switching and high frequency signals on the sliding surface.

The basic idea of eliminating chattering is simple. This chattering problem caused by a discontinuous and nonlinear switching feedback control law can be eliminated by replacing it with a continuous feedback control law. But if the sliding mode control has a continuous feedback function, there are steady state errors due to variations in parameter and disturbance [Ref. 2]. Suppose the control law has a continuous feedback, whose terms are continuous function inside a small boundary layer thickness on the sliding surface, as shown in Figure 6 on page 18, then the steady state error can be calculated by a smooth function which eliminates chattering in the boundary layer thickness (ϕ). This boundary layer thickness can be determined directly from the desired sliding surface coefficient limit and estimates of the uncertainty dynamics of the system to be controller. If the specified bounds on disturbances and parameter uncertainty are not exceeded, the system is guaranteed to stay within the boundary layer once inside. If a disturbance temporarily exceeds the specified bounds, the state may go outside the boundary layer. However, the sliding condition equation(2.14) implies that the system will always move back inside the boundary layer once the disturbances return to their projected levels.

The dynamics of the state trajectory inside the boundary are only an approximation to the desired dynamics on the sliding surface. The advantage of the scheme is that the state trajectory does not chatter close to the sliding surface. To carry out the preceding program, we use the sliding surface considered in the previous section with $\sigma(x,t)$ of the form:

$$\sigma(x) = \lambda_i \tilde{x}(t) \tag{2.24}$$
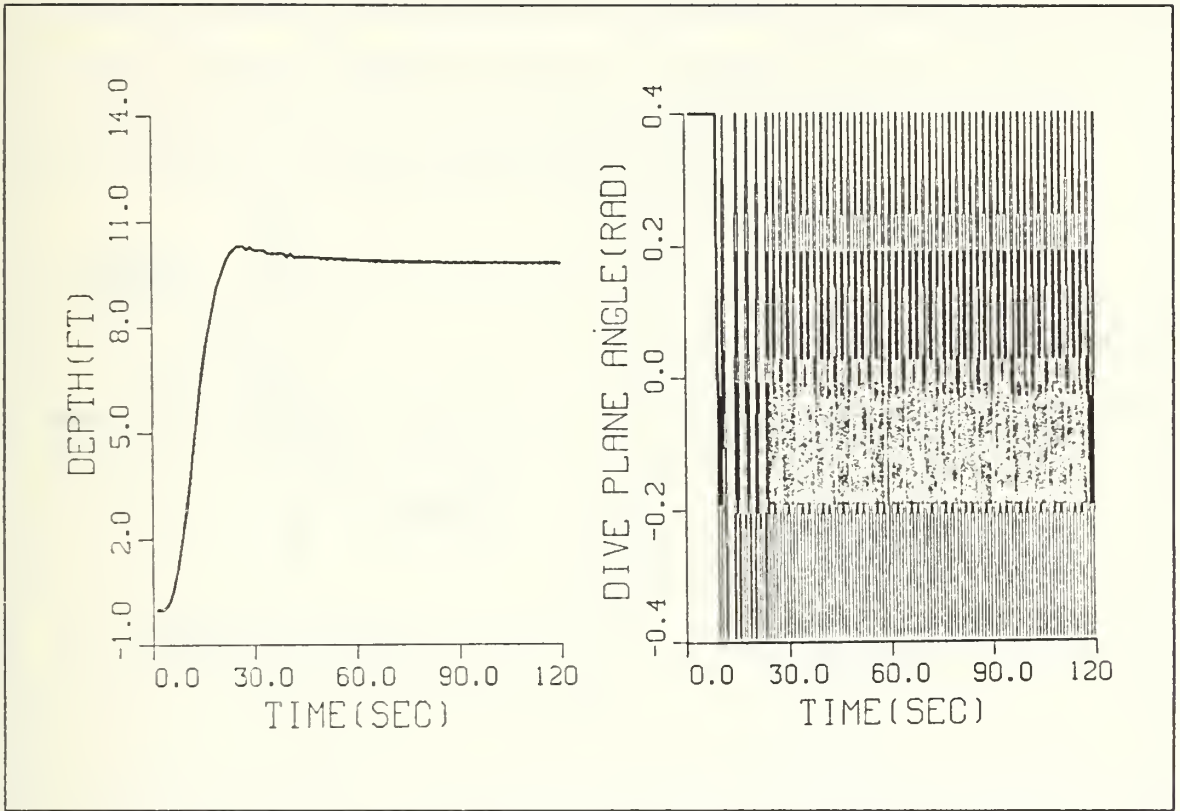
Figure 5. Chattering problem

where $\tilde{x}(t) = x(t) - x_d(t)$

$X_d(t)$ = desired state variable

To define the boundary layer thickness about the sliding surface of equation (2.14), define

$$\sigma^+(x) = \sigma(x) + \phi$$

$$\sigma^-(x) = \sigma(x) - \phi \qquad (2.25)$$

where ϕ is the boundary layer thickness

It is immediately from equation (2.25) that

17
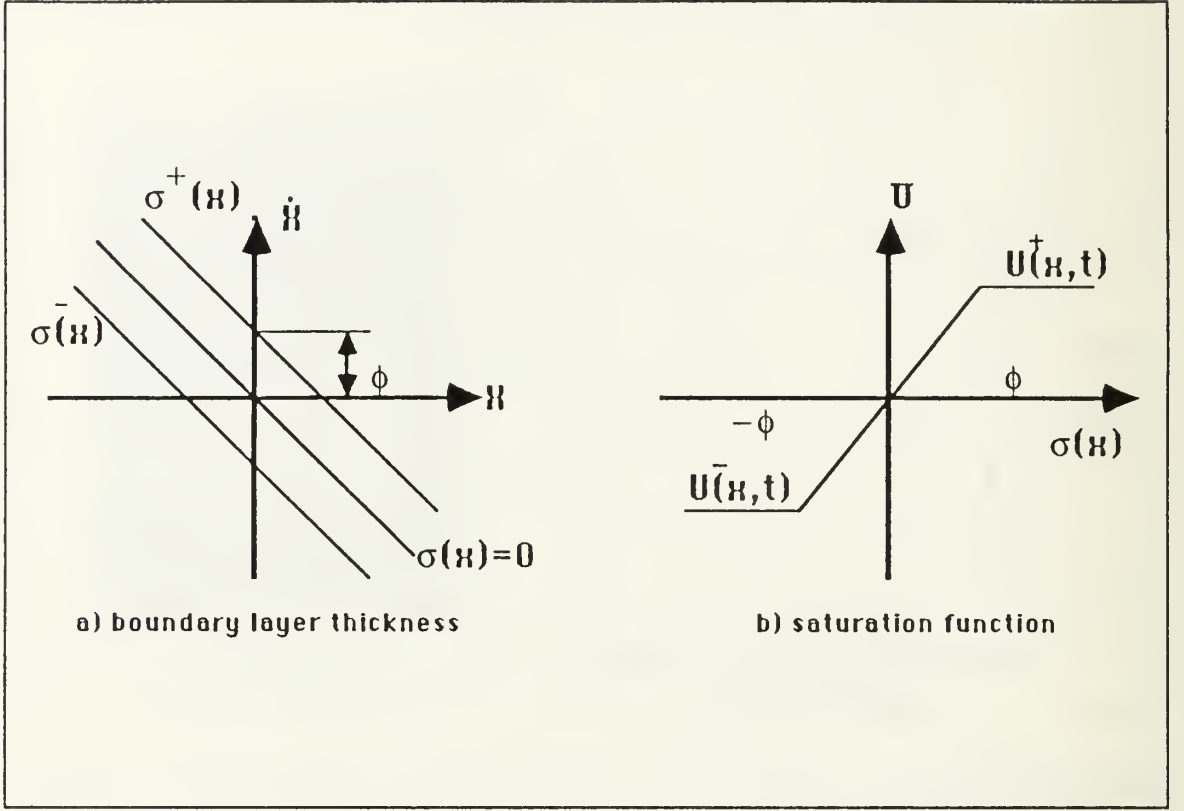
Figure 6.   Boundary layer thickness and saturation function

$$| \sigma(x) | \leq \phi \tag{2.26}$$

and

$$\frac{d}{dt} \sigma^-(x,t) = \frac{d}{dt} \sigma(x,t) = \frac{d}{dt} \sigma^+(x,t) \tag{2.27}$$

We choose the control law $u(t)$ as by equation (2.27) for $\sigma^-(x,t) < 0$ or $\sigma^-(x,t) > 0$. This guarantees that

$$\frac{d}{dt} \sigma^-(x,t) > 0 \tag{2.28}$$

$$\frac{d}{dt} \sigma^+(x,t) < 0 \tag{2.29}$$

18

Equation (2.28) and (2.29) establish that trajectories starting outside boundary layer tend towards boundary layer, and further trajectories starting inside boundary layer stay in it for $t_o \leq t$. It only remains to specify $u(x,t)$ to be a continuous function of x inside boundary layer thickness.

III. SLIDING MODE CONTROL FOR NONLINEAR A.U.V. IN DIVE PLANE

A. GENERAL

Underwater vehicles present difficult control system design problems due to their nonlinear dynamics, uncertain hydrodynamic coefficients and the presence of disturbances that are difficult to measure or estimate. This chapter describes the dynamics of a selected automonous underwater vehicle (AUV) and the design of a sliding mode controller which can handle these problems effectively.

Motions of underwater vehicles are expressed in a body fixed reference frame, because hydrodynamic forces and inertia properties are most readily computed in a ship reference frame. The nonlinear equations of motion in six degrees of freedom vehicles which are commonly known as the DTNSRDC 2510 equations of motion are used for verification of the sliding mode control design. These highly nonlinear equations of motion are linearized by a Taylor series expansion and modified to suit the needs of an AUV [Ref. 7]. First, these linearized and modified equations of the system are used to design the sliding surface, sliding mode control law and observer. These values of the linear system are, then, used to implement the sliding mode control law for the nonlinear system. This chapter shows how to design the sliding mode control for the highly nonlinear AUV.

B. NONLINEAR COMPUTER MODEL

The nonlinear model used for sliding mode control verification was derived from the original NSRDC 2510 document [Ref. 8]. The nonlinear model used in this thesis consists of 8 differential equations which describe the AUV dynamics. The six equations as derived from force and moment equalities account for the states u, v, w, p, q and r. The shape of AUV, which is 17.4 feet long, weighs 12000 pounds, and neutrally buoyant, is depicted in Figure 7 on page 21.
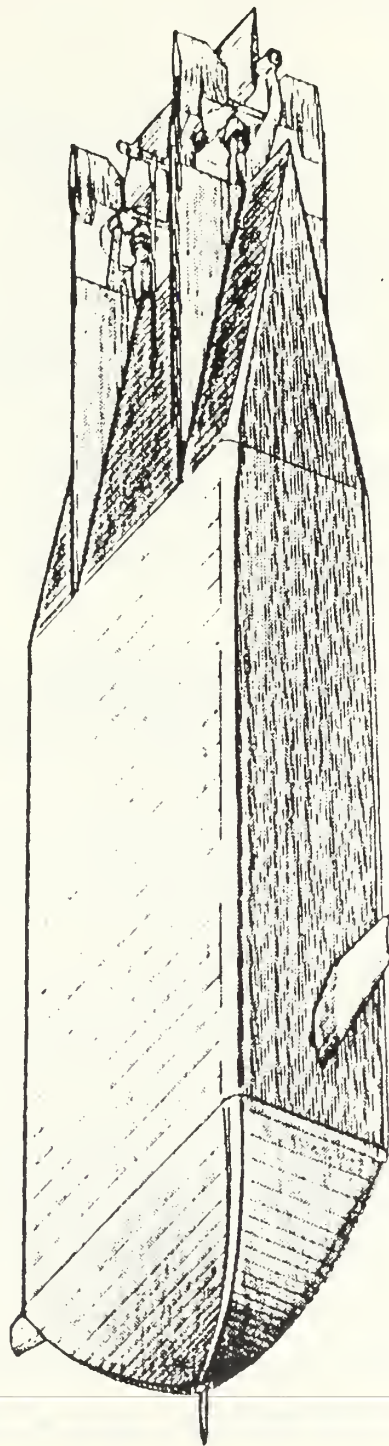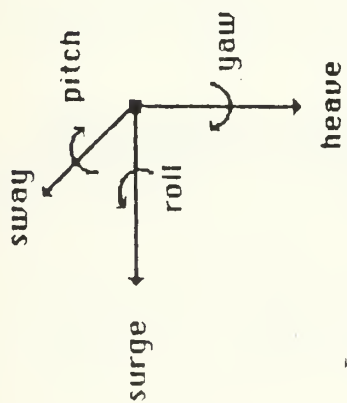
Figure 7.   Sketch of the autonomous underwater vehicle

General dynamical equations are derived from Newton's law in an inertial reference frame:

$$\left\{ \begin{matrix} \vec{F} \\ \vec{M} \end{matrix} \right\} = f(\ dynamical\ response\ terms\ ) \tag{3.1}$$

The general form of the force balance is

$$\vec{F} = \frac{d}{dt}\ (M\vec{x}) \tag{3.2}$$

where M = mass matrix

$$x = [\ u, v, w\ ]^T$$

and the moment balance is

$$\vec{M} = \frac{d}{dt}\ (\ I\vec{\Omega}\ ) \tag{3.3}$$

where I = moment of inertia matrix

$$\Omega = [\ p, q, r\ ]^T$$

Three dimensional motions of underwater vehicles are normally described using the body-fixed coordinate and inertial reference frame. Position of the body-fixed coordinate system is expressed in X, Y, and Z coordinates and orientation of the vehicle's coordinate system in expressed in Euler angles ϕ, θ, and ψ. The definitions of u, v, w, p, q, r and controls are listed in Table 1 and Table 2.

Table 1.   DEFINITION OF A U V STATES.

STATE	DEFINITION	UNITS
u	surge rate	(ft/s)
v	sway rate	(ft/s)
w	heave rate	(ft/s)
p	roll rate	(rad/s)
q	pitch rate	(rad/s)
r	yaw rate	(rad/s)
ϕ	spin	(radians)
θ	elevator	(radians)
ψ	azimuth	(radians)

Table 2.   DEFINITION OF A.U.V CONTROLS

CONTROL	DEFINITION
δ_r	rudder angle
δ_{bs}	starboard bow plane angle
δ_{bp}	port bow plane angle
δ_s	stern plane angle
δ_{rm}	delta form
δ_b	delta buoyancy

The dynamical response terms of the left hand side of equation (3.1) or equation (3.2) and (3.3) express the external forces and moments exerted on the vehicle by hydrodynamic, control surface, propulsion and other effects. The force and moment equalities of equation (3.2) and (3.3) describe motions in six degrees of freedom of the AUV. The three forces are in the axial, lateral and normal directions which give rise to motions in surge, sway and heave respectively. The three moment equations produce moments and motions in roll, pitch and yaw. Figure 8 on page 24 shows the positive directions of forces, moments, motions, and control surface deflections.
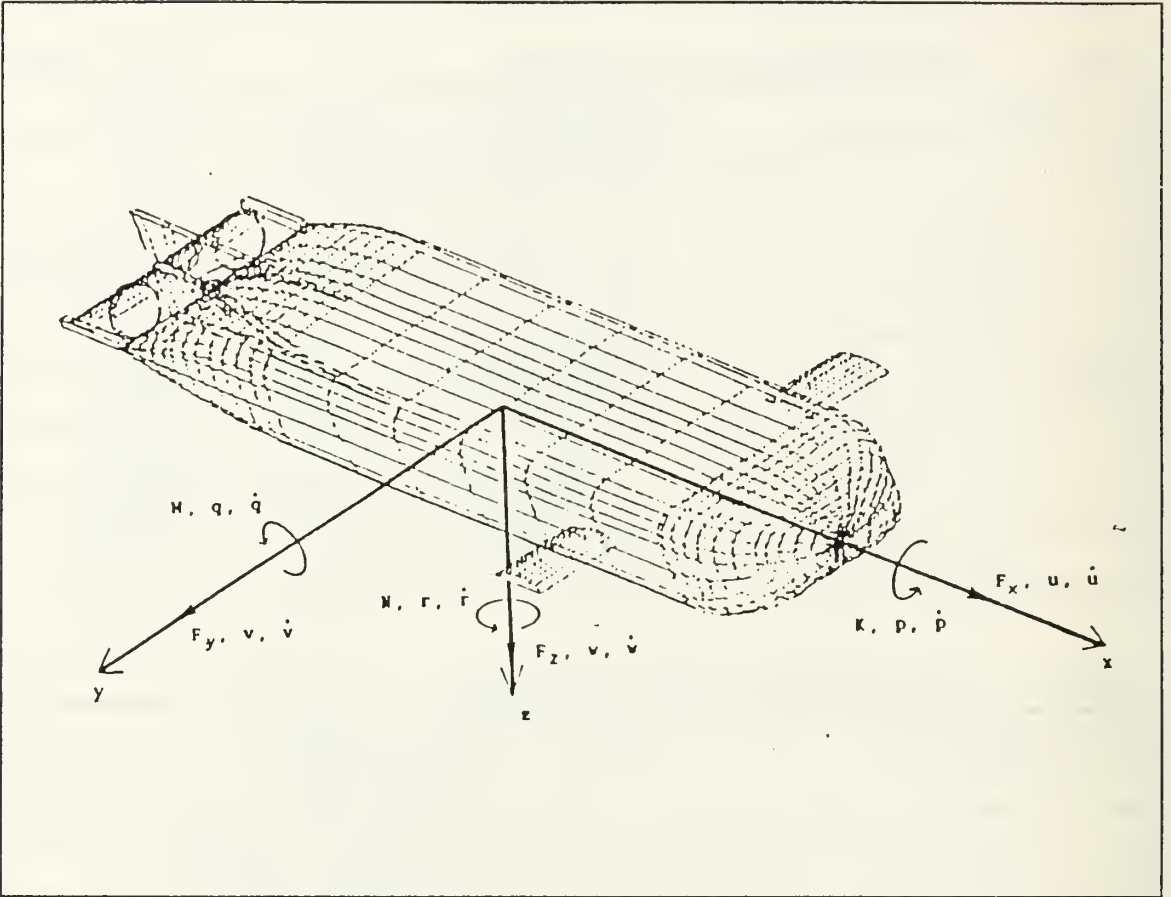
Figure 8.   Positive motion directions of the AUV

The equations of motion for the six degrees of freedom for the fully nonlinear model are listed in the following page. The hydrodynamics coefficient of those equation used for this thesis are those that were determind using an analytic approach [Ref. 7] and later simplified [Ref. 9]. The four nonlinear equations that are considered for designing sliding mode control of the AUV are written in the following form:

Normal Equation of Motion

$$m[\dot{w}-u_xq+vp+X_g(pr-\dot{q})+Y_g(qr+\dot{p})-Z_g(p^2+q^2)]=$$

24

$$\frac{\rho}{2}\, l^4 [Z'_q \dot{q} + Z'_{pp}p^2 + Z_{pr}pr + Z'_{rr}r^2]$$

$$+ \frac{\rho}{2}\, l^3 [Z'_w \dot{w} + Z'_q u_x q + Z'_{vp}vp + Z'_{vr}vr]$$

$$+ \frac{\rho}{2}\, l^2 [Z'_w u_x w + Z'_{vv}v^2 + u_x^2 (Z'_{\delta s}\delta_s + Z'_{\delta b}\delta_b)]$$

$$- \frac{\rho}{2} \int [C_{Dy}h(x)(v+xr)^2 + C_{Dz}b(x)(w-xq)^2]\frac{(w-xq)}{U_{cf}(x)}\,dx$$

$$+(W-B)\cos\theta\cos\phi$$

$$+ \frac{\rho}{2}\, l^3 Z'_{q\eta}u_x q\varepsilon(\eta) + \frac{\rho}{2}\, l^2 (Z'_{w\eta}u_x w + Z'_{\delta s\eta}u_x^2\delta_s)\varepsilon(\eta) \tag{3.4}$$

Pitch Equation of Motion

$$I_y\dot{q} + (I_x - I_z)pr - I_{yz}(pq-\dot{r}) + I_{xz}(p^2 - r^2) - m[X_g(\dot{w} - u_x q + vp) - Z_g(\dot{u} - vr + wq)] =$$

$$\frac{\rho}{2}\, l^5 [M'_q \dot{q} + M'_{pp}p^2 + M'_{pr}pr + M'_{rr}r^2]$$

$$+ \frac{\rho}{2}\, l^4 [M'_w \dot{w} + M'_q u_x q + M'_{vp}vp + M'_{vr}vr]$$

$$+ \frac{\rho}{2}\, l^3 [M'_w u_x w + M'_{vv}v^2 + u_x^2 (M'_{\delta s}\delta_s + M'_{\delta b}\delta_b)]$$

$$- \frac{\rho}{2} \int [C_{Dy}h(x)(v+xr)^2 + C_{Dz}b(x)(w-xq)^2]\frac{(w-xq)}{U_{cf}(x)}\,x\,dx$$

$$-(X_g W - X_B B) \cos \theta \cos \phi - (Z_g W - Z_B B) \sin \theta$$

$$+ \frac{\rho}{2} l^4 M'_{q\eta} u_x q \varepsilon(\eta) + \frac{\rho}{2} l^3 (M'_{w\eta} u_x w + M'_{\delta s \eta} u_x^2 \delta_s) \varepsilon(\eta) \qquad (3.5)$$

Kinematic Relations

$$\dot{\theta} = q \cos \phi - r \sin \phi \qquad (3.6)$$

$$\dot{Z} = -u_x \sin \theta + v \cos \theta \sin \phi + w \cos \theta \cos \phi \qquad (3.7)$$

The simulations for the dive plane control were performed by using the FORTRAN language code (Appendix. B) for the simulation of nonlinear system response as a function of time.

C. LINEAR MODELING

1. Equations of Motion

The sliding mode controller design procedure begins with the expression of the equations of motion in linear time invariant state space form. The highly nonlinear AUV system is

$$\frac{d}{dt} x(t) = M^{-1} f(x(t), u(t)) \qquad (3.8)$$

$$y(t) = g(x(t)) \qquad (3.9)$$

where   x is the state vector

           u is the control input vector

           y is the output vector

Although equations (3.8) can be significantly simplified as in Larsen [Ref. 9], they appear still very complex for this study. The nonlinear equations can be linearized through a Taylor series expansion in the vicinity of a nominal point (ideally where

$\frac{d}{dt}(t) = 0)$ for small deviations of u(t) and x(t) from the reference values. These equations of motion were linearized by Boncal [Ref. 7]. Alternatively, least squares techniques can be used for parameter identification in order to develop a linear model for the relationship between dive plane angle (δ), pitch rate (q), depth (z) and pitch angle (θ) [Ref. 10]. The linearized and very simplified equations for the dive plane motion

$$\dot{q} = -0.7q - 0.03\theta - 0.035\delta$$

$$\dot{\theta} = q$$

$$\dot{z} = -U_0\theta \qquad (3.10)$$

were found to provide a satisfactory approximation of the open loop dive plane dynamics of nonlinear equation (3.4) to (3.7) for the nominal speed of 6 ft/sec (or 500 rpm).

2. Sliding Surface Design

It is evident from the discussion of the sliding mode theory (Chapter 2) that description of AUV motion depends on the sliding surface regardless of disturbance and unmodel parameters, after it hit sliding surface. So it is very important to design sliding surface of the AUV with disturbance and unmodelled parameters. The sliding surface of the AUV will be designed based on the linear model. The state space form of the linear model is

$$\dot{x} = Ax + Bu$$

$$y = Cx \qquad (3.11)$$

where $\qquad x^T = [q. \theta. z]$

$$A = \begin{bmatrix} -0.7 & -0.03 & 0 \\ 1 & 0 & 0 \\ 0 & -U_0 & 0 \end{bmatrix}$$

27

$$B = \begin{bmatrix} -0.035 \\ 0 \\ 0 \end{bmatrix}$$

$$u = \delta$$

and

$$C = [0\ 0\ 1]$$

For a three dimensional system, the sliding surface is the Euclidean plane $\sigma(x) = S^T x = 0$

where $\quad S = \begin{bmatrix} 1 \\ s_2 \\ s_3 \end{bmatrix}$

Equation (2.6) can be expressed in terms of the state variables and sliding surface coefficients as following

$$\sigma(x) = q + s_2\theta + s_3 z \tag{3.12}$$

where the coefficient of q has been normalized to 1. S will determine the sliding surface plane uniquely. To compute the equivalent control (u_{eq}). we substitute A, B and S in to equation (3.11). and the closed-loop dynamics of the linear model are

$$\dot{x} = [A - B(S^T B)^{-1} S^T A] x$$

or

$$\dot{x} = (A - BK)x \tag{3.13}$$

where the gain vector K can be found from standard pole placement methods. The closed-loop dynamics matrix

$$A_c = A - BK \tag{3.14}$$

where $\quad K = (S^T B)^{-1} S^T A$

has eigenvalues specified for desirable response of the AUV. One of the eigenvalues of A_c must be specified as zero. With A_c specified and K computed from pole placement, S^T matrix can be determined as using the equation (3.13) and (3.14).

$$S^T(A - BK) = 0$$

or

$$S^T A_c = 0 \tag{3.15}$$

Therefore S^T is found as a left annihilator of A_c or S is a left eigenvector of A_c which corresponds to the zero value. This sliding surface of the AUV satisfy the sliding surface condition $S^T x = 0$. To find proper sliding surface of the AUV, Matrix-x program "SCM" in Appendix A is used. The response of the AUV according to different sliding surface is shown in Figure 9 on page 30, Figure 10 on page 31, and Figure 11 on page 32. The sliding surface of Figure 10 which has no overshot and fast response time is selected as the reference sliding surface of the AUV in order to design control law. The sliding surface of the AUV is

$$\sigma(x) = q + 0.52\theta - 0.0112z \tag{3.16}$$

This sliding surface has the desired dynamics of the closed-loop system. The perfect depth tracking of the selected AUV is then defined as remaining along the surface. The dynamic response of AUV is affected by the chosen sliding surface. The selected sliding surface is used to handle accurate depth control.
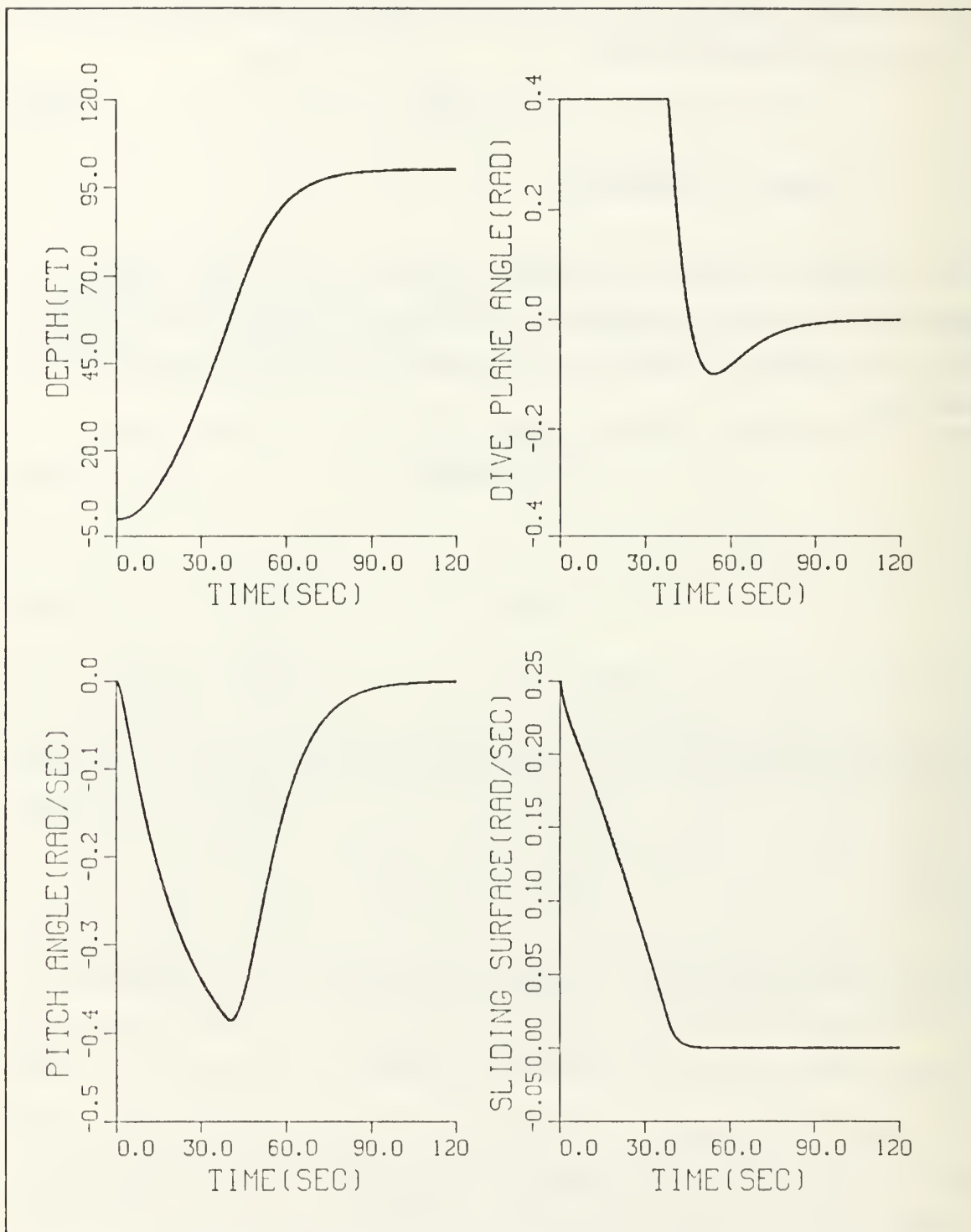
Figure 9.   The dynamic response for the closed-loop poles = 0, -0.1,-0.15

30
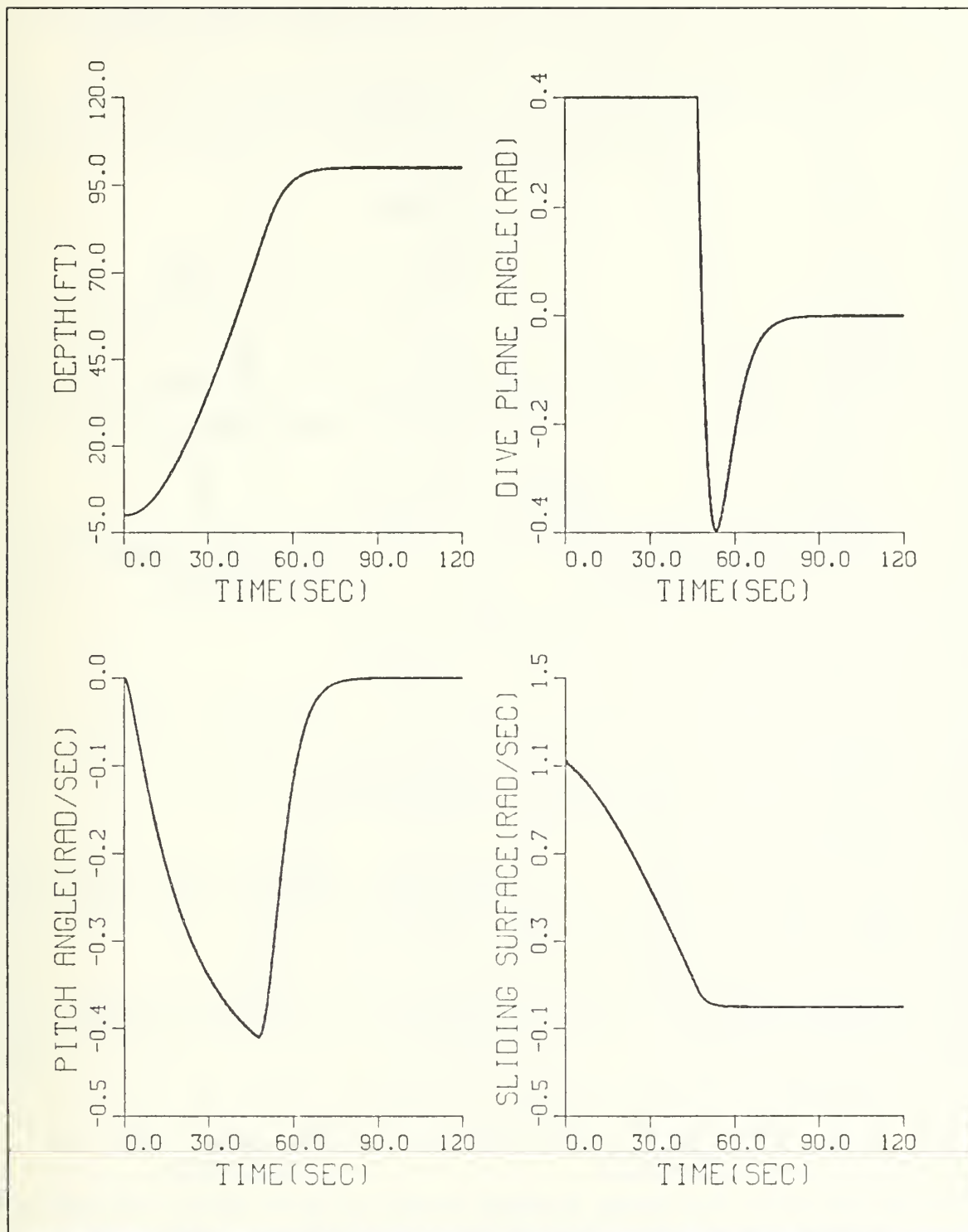
Figure 10.   The dynamic response for the closed-loop poles = 0,-0.25,-0.27
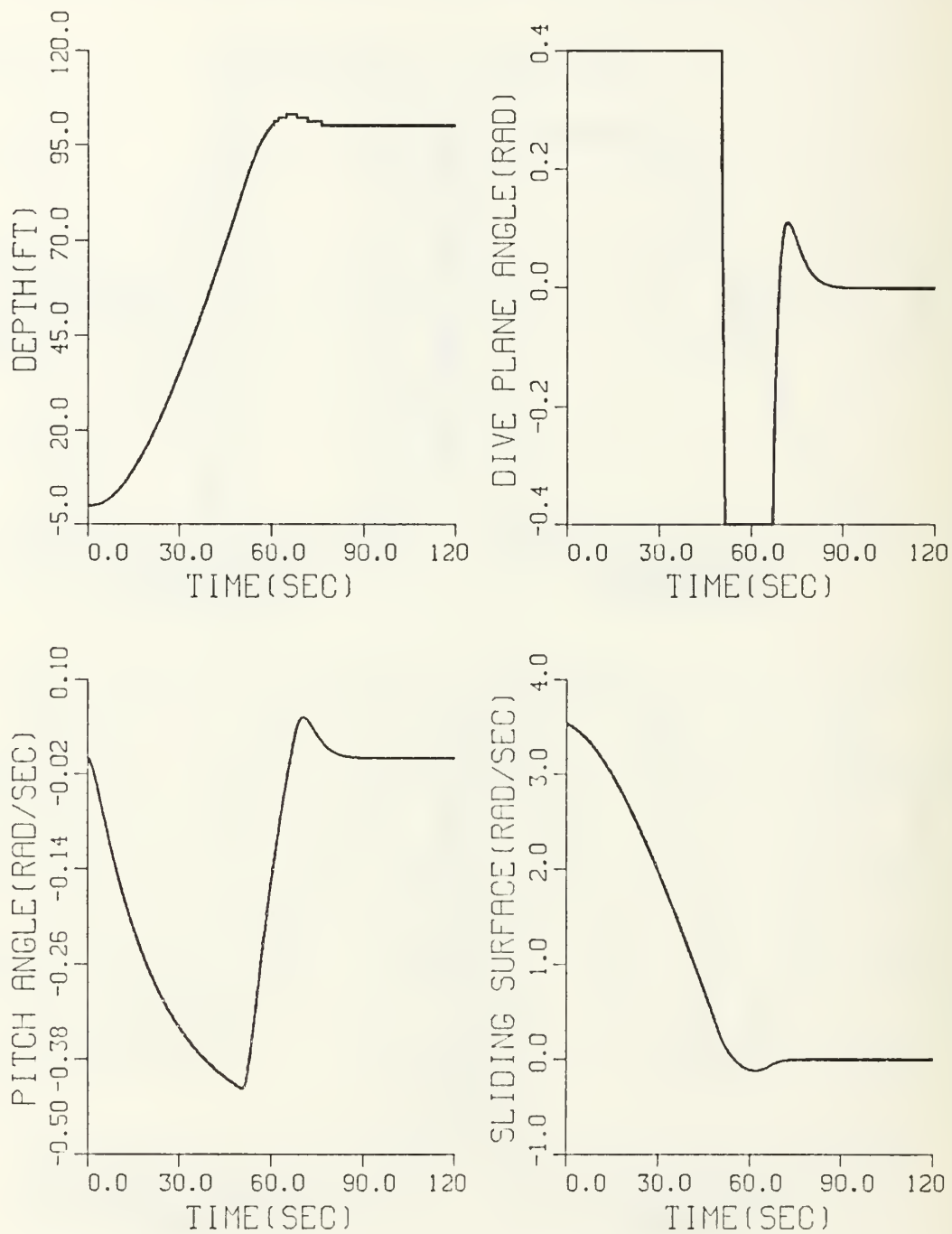
Figure 11. The dynamic response for the closed-loop poles = 0,-0.45,-0.47

3. Sliding Mode Control Law

Here the goal is to determine switched feedback gains which will drive the AUV state trajectory to the sliding surface and maintain sliding mode conditions. By defining the Liapunov function of the equation (2.13)

$$V(x) = \frac{1}{2} \left[\sigma(x) \right]^2 \tag{3.17}$$

where $\sigma(x) = q + 0.52\theta - 0.0112z$

asymptotic stability of the AUV on the sliding surface is guaranteed, that provided $V(x)$ is a negative definite function or

$$\sigma(x)\dot{\sigma}(x) = -\eta^2 \left| \sigma(x) \right|$$

or

$$\dot{\sigma}(x) = -\eta^2 sign(\sigma(x)) \tag{3.18}$$

Since $\sigma(x) = S^T x$, we have

$$S^T(Ax + Bu) = -\eta^2 sign(\sigma(x)) \tag{3.19}$$

and solving for the equivalent control input u

$$u = -(S^T B)^{-1} S^T A x - (S^T B)^{-1} \eta^2 sign(\sigma) \tag{3.20}$$

It is important to recognize that the feedback control law is composed of two parts,

$$u = \acute{u} + \bar{u}$$

The first $\acute{u} = -(S^T B)^{-1} S^T A x$ is a linear feedback control law, where the second $\bar{u} = -(S^T B)^{-1} \eta^2 sign(\sigma(x))$ is a nonlinear feedback with its sign toggling between plus and minus according to which side of the sliding plane the AUV is located in. Two comments are in order here: First, since $\bar{u}$ has to change its sign as the

AUV crosses $\sigma(x) = 0$, the sliding surface has to be a hyperplane (dimension of one less than the state variable). Second, it is $\bar{u}$ which is mainly responsible for driving and keeping the AUV onto the sliding plane $\sigma(x) = 0$ (where $\bar{u} = 0$ as well). The block diagram of the sliding mode control is illustrated in Figure 12 on page 34.
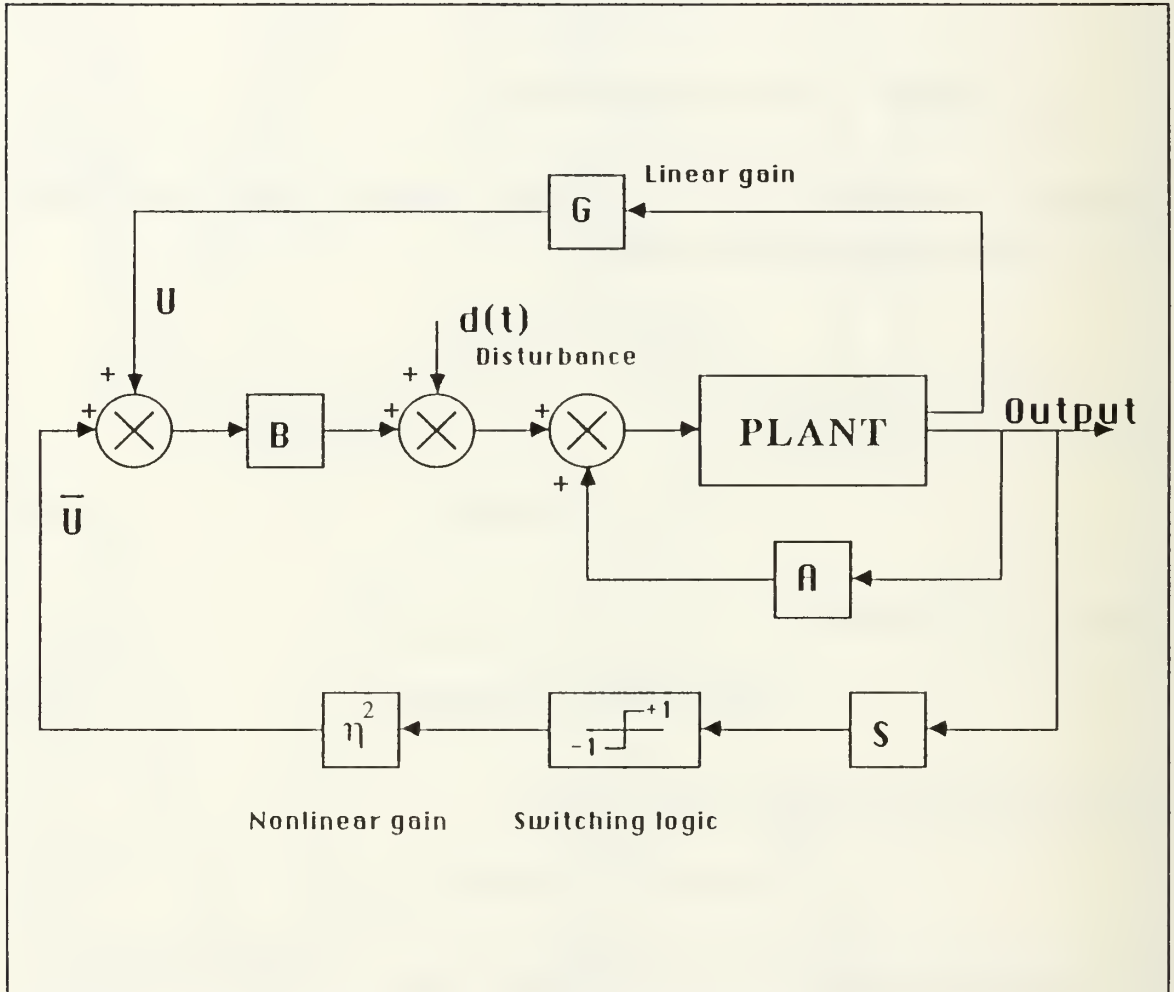
Figure 12.   The block diagram of the sliding mode control

Provided that the gain has been chosen large enough, $\bar{u}$ can provide the required robustness due to momentary disturbance and unmodeled AUV without any compromise in stability. The linear feedback law is designed such that the AUV has the desired dynamics on the sliding plane. Since $\sigma(x) = 0$ in this case

$$u = \hat{u} = -(S^T B)^{-1} S^T A x \qquad (3.21)$$

Large enough gain (ETA $= \eta^2 (S^T B)^{-1} = 4.0$) could be used in the computer simulation by using Matrix-x and FORTRAN program "SMC" in Appendix A. The dynamic response of the AUV according to several values of gain is shown in Figure 13 on page 37, Figure 14 on page 38, and Figure 15 on page 39. Choosing properly large enough nonlinear feedback gain, although the response time of the AUV is fast, the AUV overshoots on the sliding surface as shown in Figure 15 on page 39. The dive plane angle of the AUV presents chattering due to sign switching of the nonlinear part of the control law. Several varieties of nonlinear feedback gain (η^2) and boundary layer (ϕ) are evaluated through a series of numerical experiments in order to analysia dynamic response of AUV which are dependant on it. The characteristic of dynamic response according to the nonlinear feedback gain, boundary layer, and closed-loop poles are shown in Table 3.

Table 3.   THE DYNAMIC CHARACTERISTIC OF THE AUV ACCORDING TO DESIGN PARAMETER s

Parameters	Depth response	Dive plane angle	Pitch angle (radians)	Sliding surface
C.P = 0,-0.1.-0.15	slow, no overshoot	no saturated	maxi angle = 0.4	no overshoot
C.P = 0.-0.25.-0.27	fast, no overshoot	no saturated	maxi angle = 0.41	no overshoot
C.P = 0.-0.45.-0.47	fast, overshoot	saturated	maxi angle = 0.42	overshoot
ETA = 3. PHI = 0.2	slow, overshoot	no saturated	maxi angle = 0.4	overshoot
ETA = 4. PHI = 0.4	fast, no overshoot	no saturated	maxi angle = 0.41	no overshoot
ETA = 8. PHI = 0.4	fast, no overshoot	saturated	maxi angle = 0.42	overshoot

We already knew that system behavior is dependent on the sliding surface which is designed based on closed-loop poles. The closed-loop poles (0,-0.25,-0.27), nonlinear feedback gain (ETA = 4), and the boundary layer ($\phi = 0.4$) are selected in order to satisfy the necessary motions of the AUV.
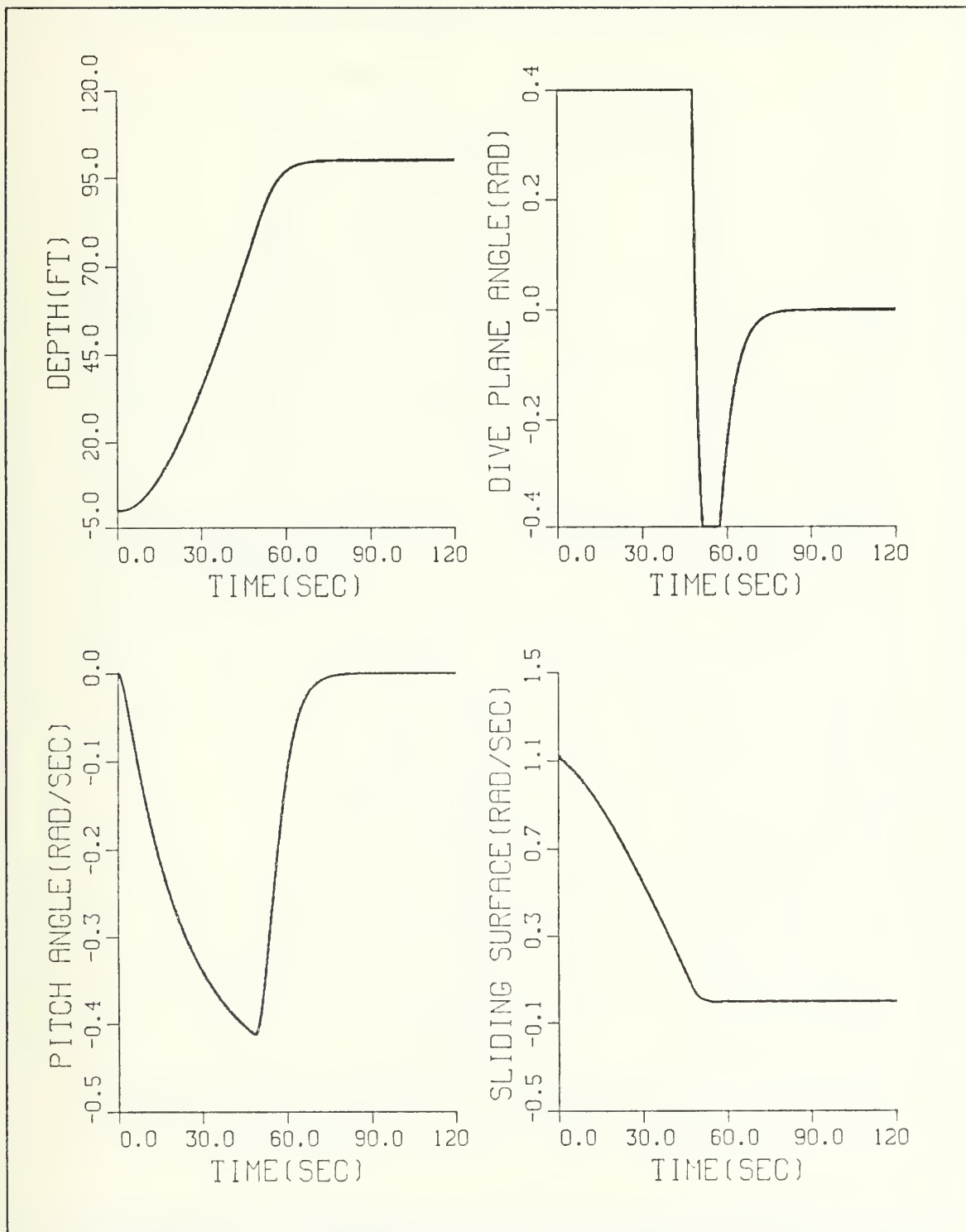
Figure 13.   The dynamic response for ETA(3) and PHI(0.2)

37
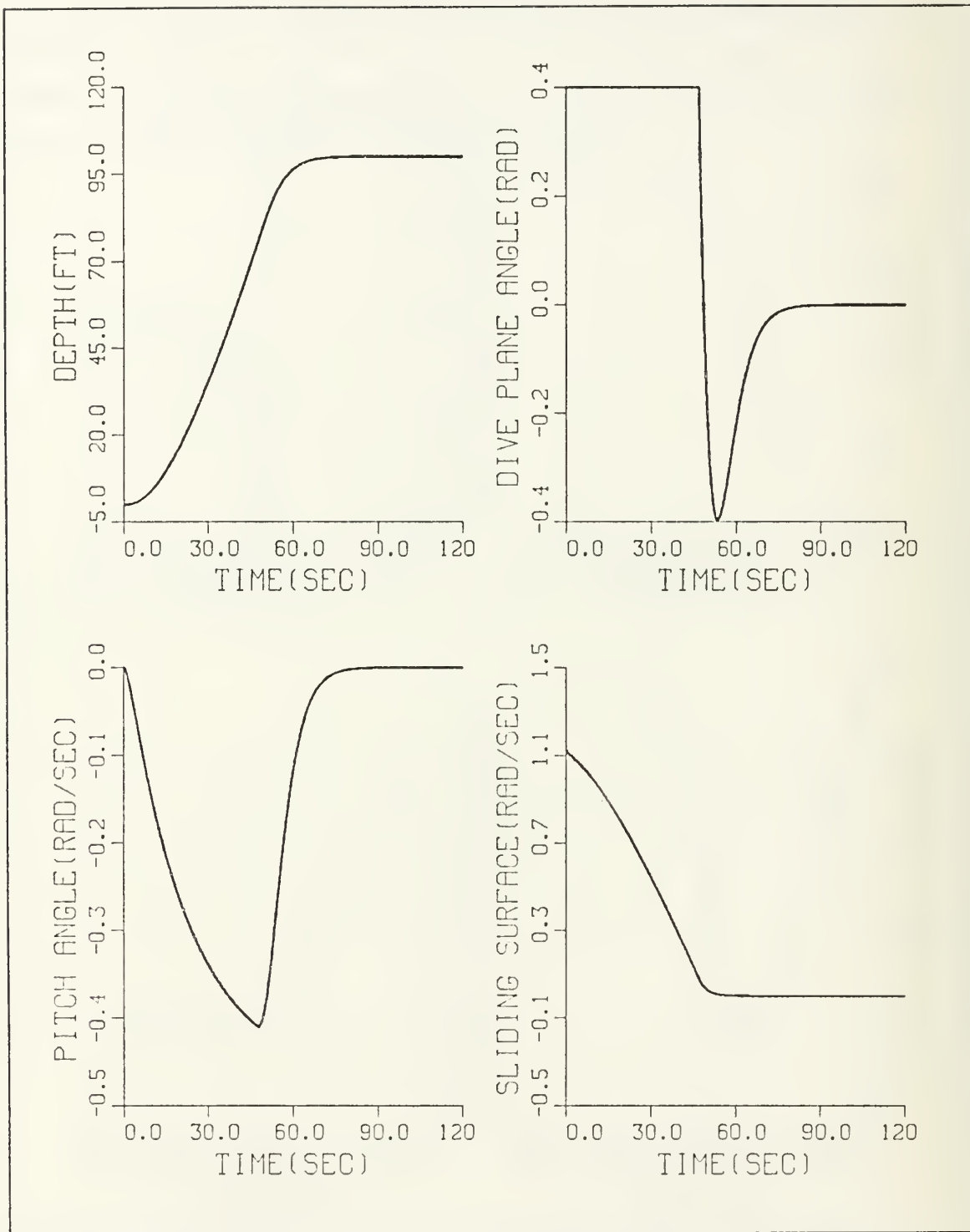
Figure 14.   The dynamic response for ETA(4) and PHI(0.4)

38
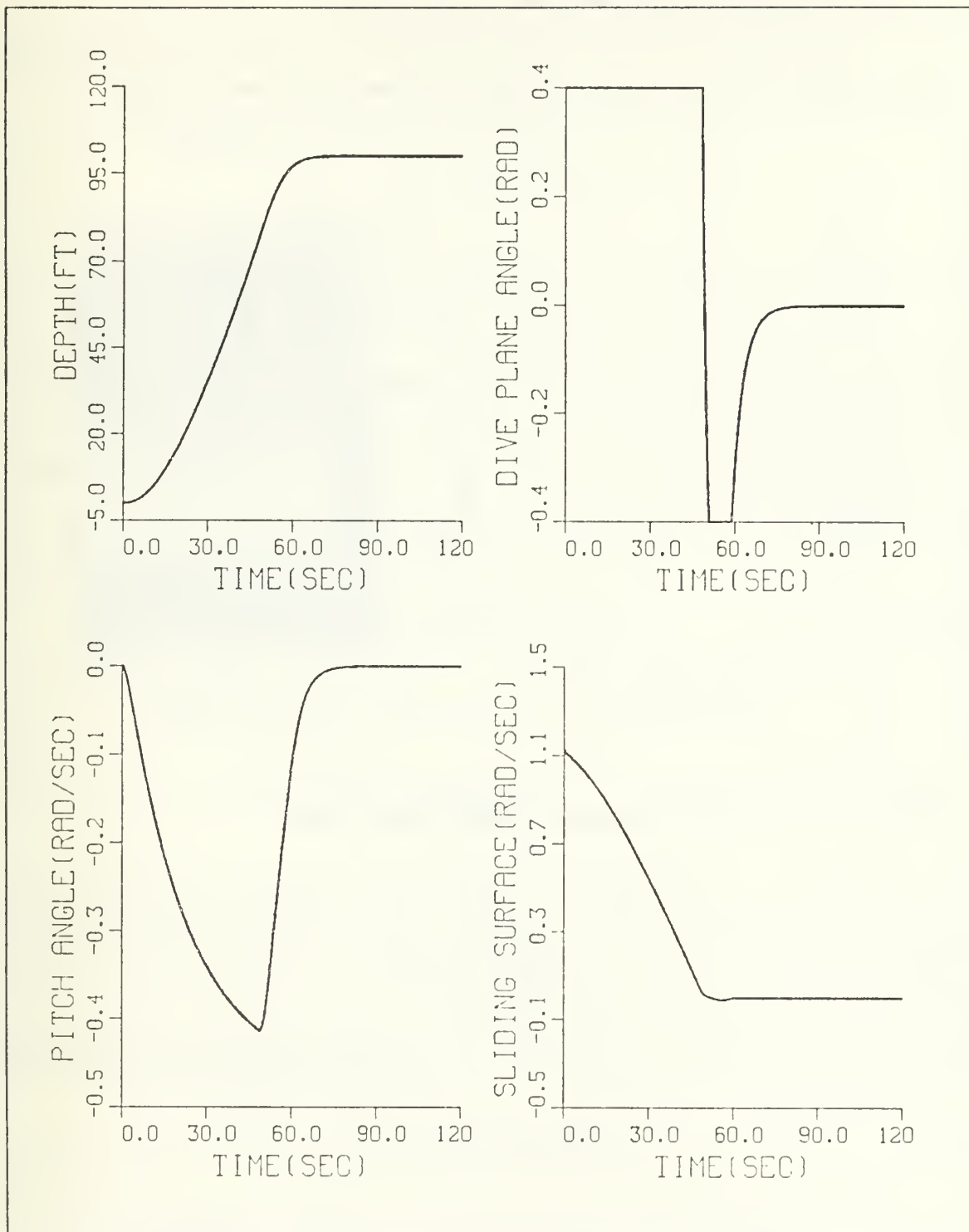
Figure 15. The dynamic response for ETA(8) and PHI(0.4)

4. Chattering Problem and Steady State Error

The nonlinear part of the sliding mode control may give rise to chattering where constant or random disturbances are present, as shown in Figure 16.
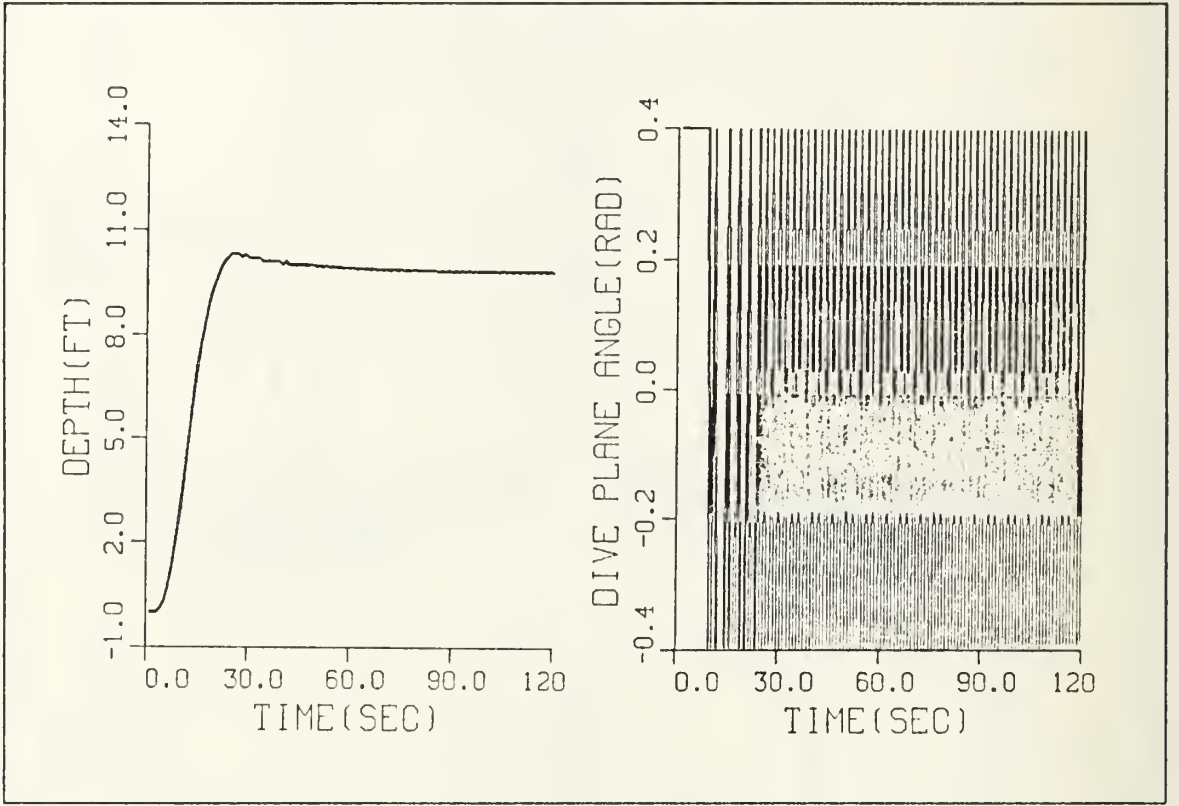
Figure 16. The chattering problem of sliding mode control

A choice of a saturation function (satsgn(σ)) instead of the pure switch (sign(σ)) for the nonlinear control law is prefered in order to avoid chattering problems. Since the boundary layer thickness is related to the characteristic of dynamic response, it can be selected according to the manuvering conditions of underwater vehicles. Therefore the control law for the AUV is modified to

$$u = -5.1429q + 1.07140 + K_n satsgn(\sigma) \tag{3.22}$$

where $\quad K_n = \eta^2 (S^T B)^{-1}$

and

$$
satsgn(\sigma) = \begin{array}{ll} +1 & if \quad \sigma \geq \phi \\ -1 & if \quad \sigma \leq -\phi \\ \dfrac{\sigma}{\phi} & if \quad -\phi < \sigma < \phi \end{array}
$$

This provides a linear interpolation across the boundary layer as illustrated in Figure 17 on page 42.

A boundary layer thickness (ϕ) essentially assigns a lowpass filter structure to the dynamics of the sliding surface (σ). If a specific bound on disturbance is not exceeded, the system is guaranteed to stay within the boundary layer once inside.

The steady state error of the sliding mode control of the AUV with a disturbance can be computed as following. From the equation (3.11)

$$
\dot{q} = -0.7q - 0.03\theta - 0.035u + d \tag{3.24}
$$

where   d is disturbance

$q = q = 0$

$\theta = 0$ in steady state

The steady state control input for the given disturbance is

$$
u\,|_{ss} = \frac{d}{0.035} \tag{3.25}
$$

The control law in steady state is

$$
u\,|_{ss} = \hat{u} + \bar{u} = \eta^2 satsgn(\frac{\sigma}{\phi}) \tag{3.26}
$$

where $\sigma(x) = -0.0112e_z$

$e_z = z - z_c$
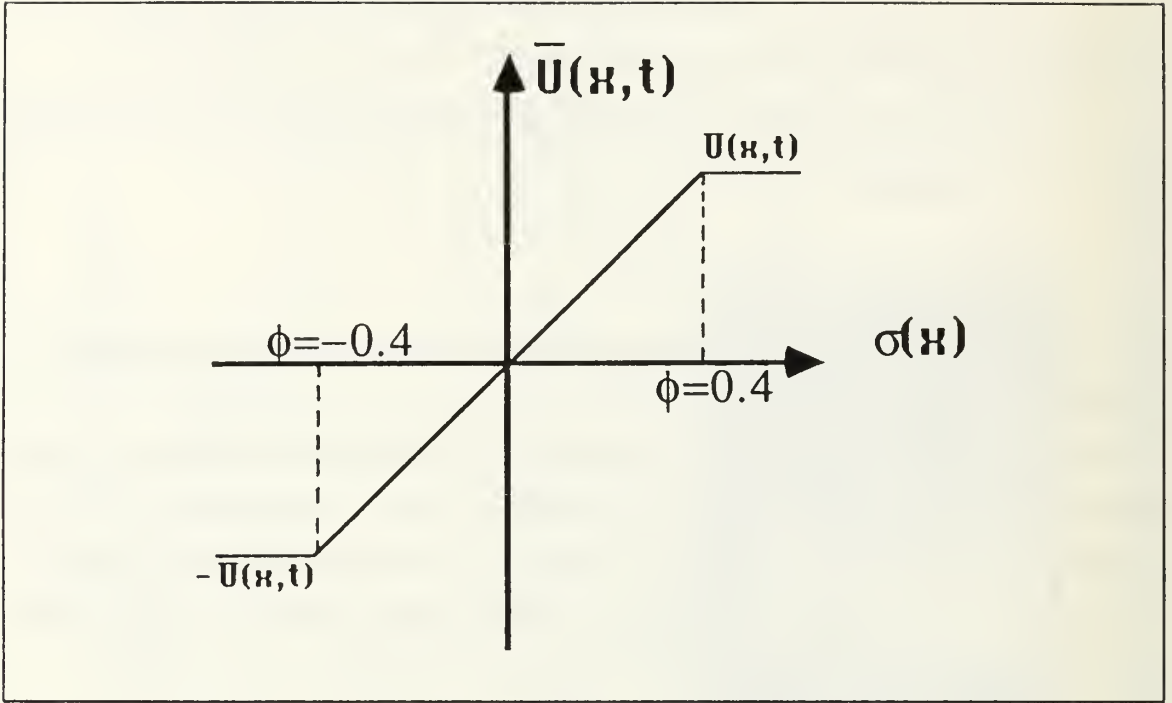
Figure 17. The saturation function for the nonlinear control law.

$$u\mid_{ss} = \eta^2 \left(\frac{-0.0112 \times e_z}{\phi} \right) \qquad (3.27)$$

$$e_z = - \frac{u\mid_{ss} \times \phi}{0.0112 \times \eta^2}$$

or

$$e_z = - \frac{d \times \phi}{0.0112 \times \eta^2 \times 0.035} \qquad (3.28)$$

The steady state error can be minimized by increasing the nonlinear control gain (η^2) and decreasing boundary layer (ϕ) as shown in Figure 18 on page 44. However, it can never be completely eliminated. The depth response of the Figure 18 (a) show the steady state error for the constant disturbance ($d = 0.005$) when using the nonlinear feedback gain (ETA = 4). Large nonlinear feedback gain is used

42

in order to decrease the steady state error as shown in Figure 18 (b). The steady state error for the command depth is decreased down to 10% approximately using large gain. However, dive plane is kept the same angle regardless nonlinear feedback gain. If we use large gain and small boundary layer, the depth response of the AUV may overshoot and the dive plane input may have numerical chattering. This is different from the chattering due to disturbance and unmodeled dynamics as shown in Figure 19 on page 45. This numerical chattering problem is an artifact of the numerical integration method (a fixed step Kutta-Merson and fixed Euler's method were used in the simulation) and, in principle, it can be reduced by choosing a more accurate method with smaller time step.
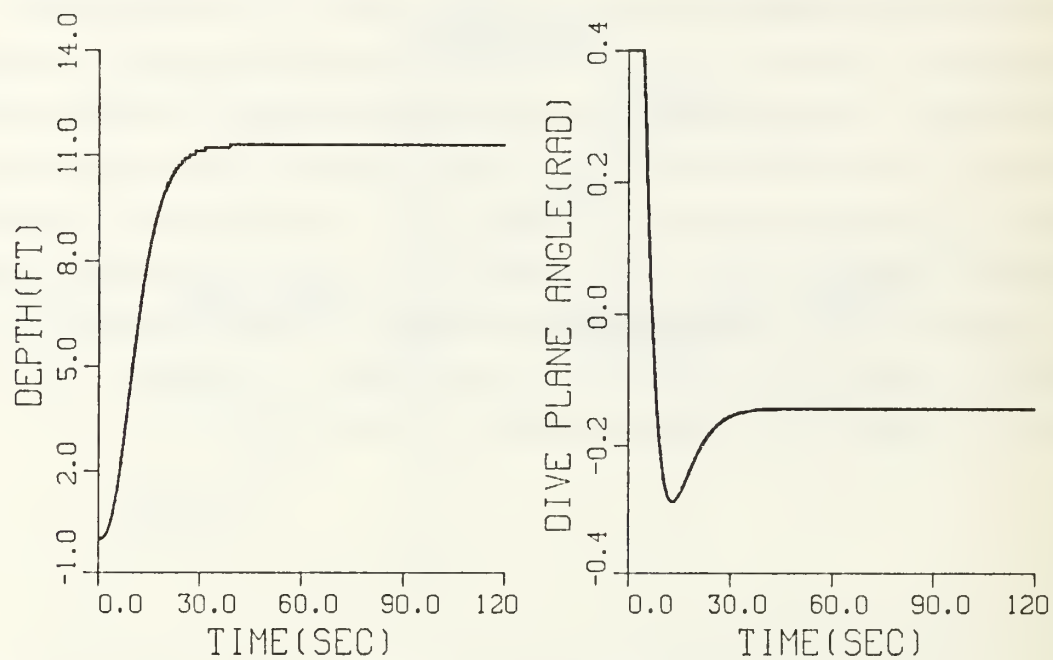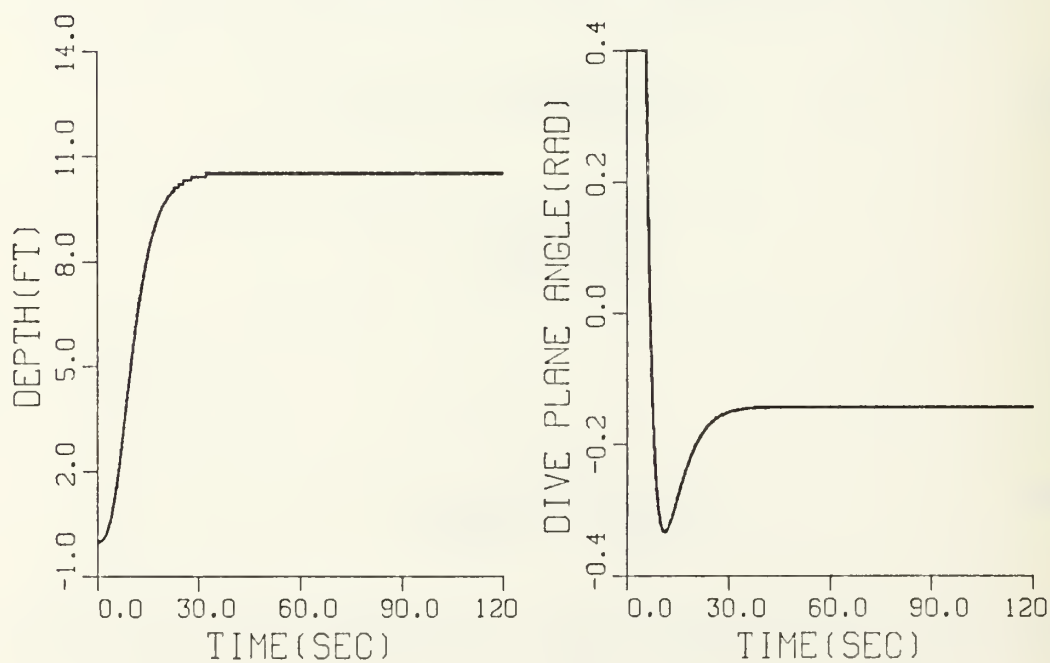
Figure 18.   The steady state error for increasing nonlinear feedback gain

44
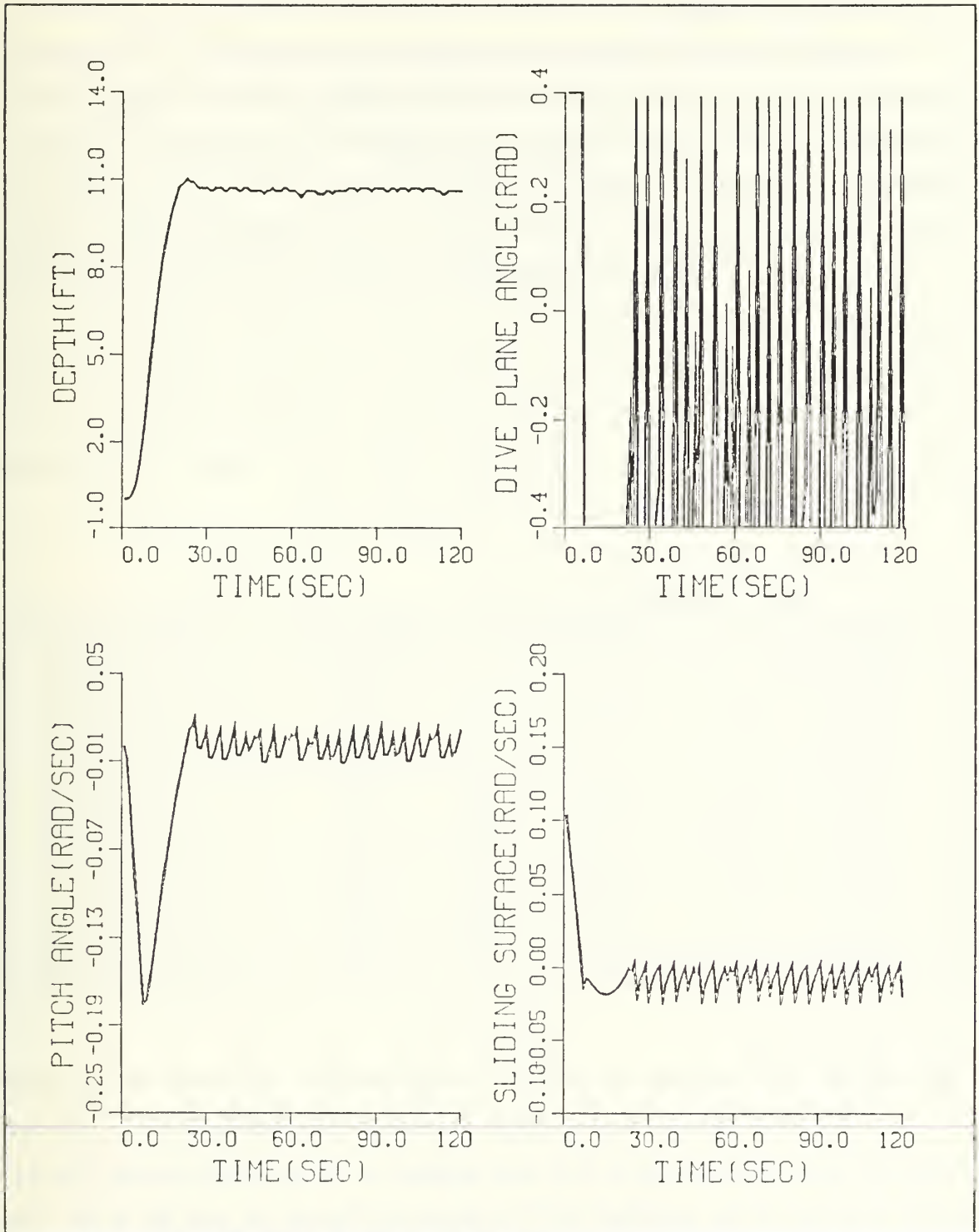
Figure 19.   The numerical chattering problem

5. Robustness tests

Another important aspect of the sliding mode control is its robustness to parameter variations and unmodeled dynamics. Sliding mode controllers are expected to outperform more conventional linear state feedback with respect to robustness. This is true for the following two reasons: First, choosing η^2 sufficiently large will guarantee that the system approaches the sliding surface asymptotically even for the off-design case. Second, since at the final stage the system evolves in a lower dimension state space (the sliding surface), it is naturally more robust than the original higher dimensionality system. To verify these expectations, we changed the hydrodynamic coefficient of the AUV, AUV rpm and dive plane strength as in Table 4. The standard design AUV equation are designated by A, B matrices at 6 ft/sec (rpm = 500).

Table 4. ROBUSTNESS TEST CASES

TEST. NO	A MATRIX	B MATRIX	SPEED(RPM)
Nominal test	A	B	6 ft/sec (500)
Test 1	2*A	B	6 ft/sec (500)
Test 2	A	2*B	6ft/sec (500)
Test 3	A 2	B	6 ft/sec (500)
Test 4	A	B 2	6 ft/sec (500)
Test 5	2*A	2*B	6 ft/sec (500)
Test 6	A 2	B 2	6 ft/sec (500)
Test 7	A	B	12 ft/sec (1000)

The sliding mode control for the AUV was designed based on the nominal case as in the previous section. The nominal nonlinear feedback gain ($\eta^2 = 2.4$) and boundary layer thickness ($\phi = 0.4$) were applied to the modified system. The dynamic response of the modified AUV is shown in Figures 14, and 20, to 26. The A matrix of test 1 model, which is related to the rotary damping coefficient, was doubled in magnitude in order to test the sliding mode control. Only the response time of test 1 model was longer. The test 3 model, which has a matrix equal to

46

one-half of the A matrix, presents fast response and overshoot due to decrease in the the rotary damping moment as shown in Figure 22. The hydrodynamic coefficient for the dive plane, which in proportional to dynamic response time, was changed in order to test performance of variable structure system for the AUV. In general, it is evident from the simulation results, that even under a 200% change in the coefficient of the A, B and RPM, the vehicle response remains stable, 7 ~ 8 % overshoot, faster or slower as expected.
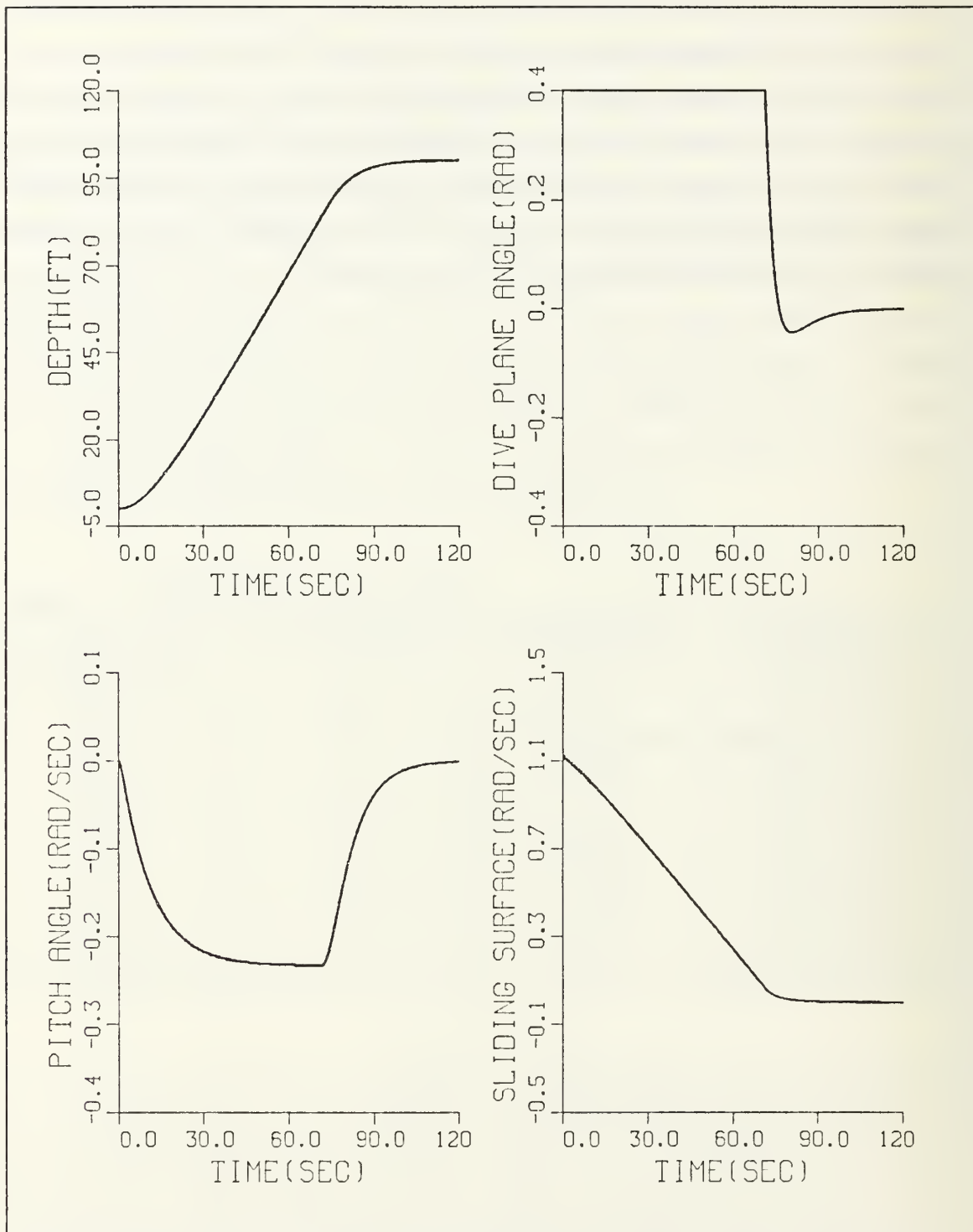
Figure 20. The response of 2*A, B and 500 rpm

48
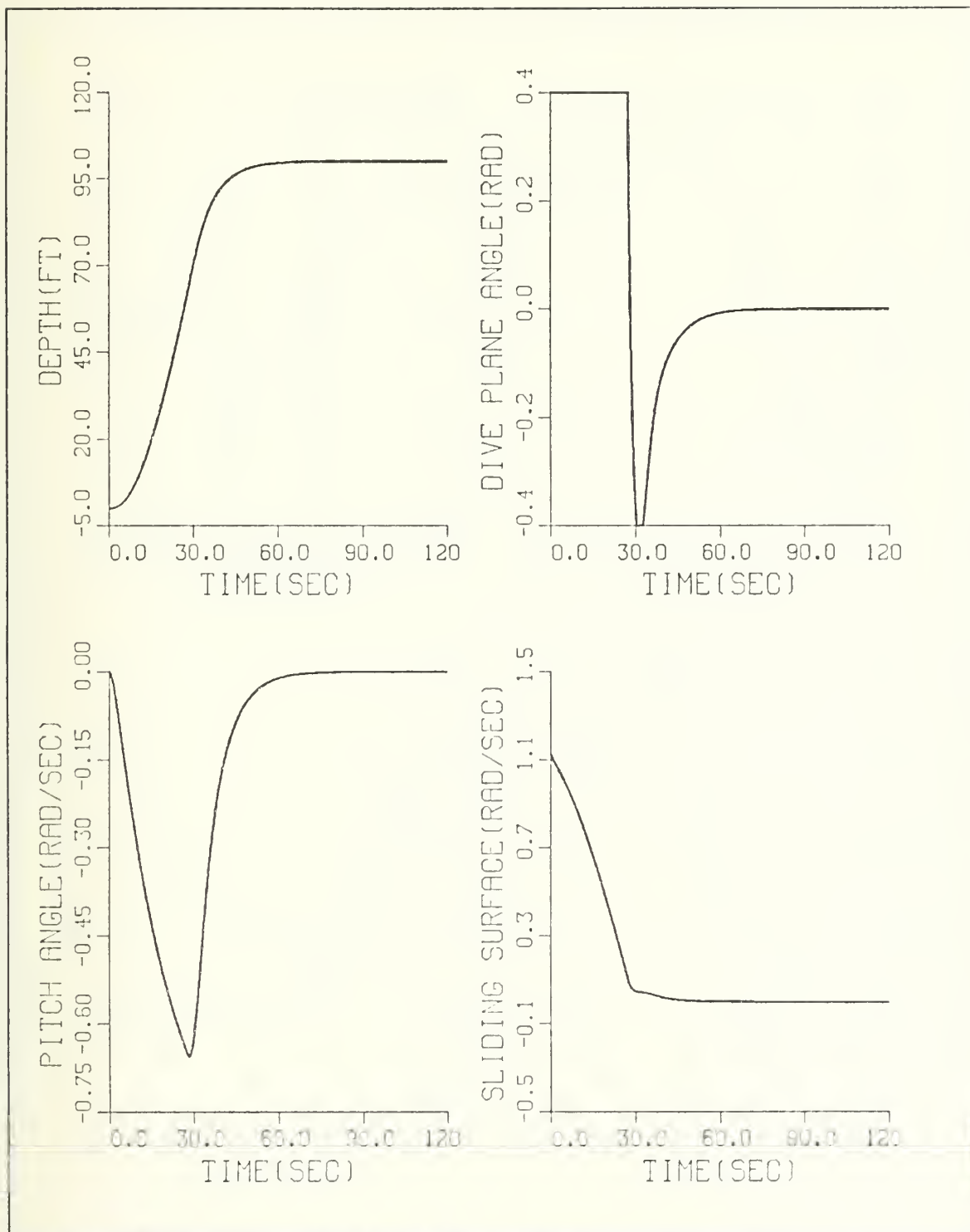
Figure 21.   The response of A, 2*B and 500 rpm

49
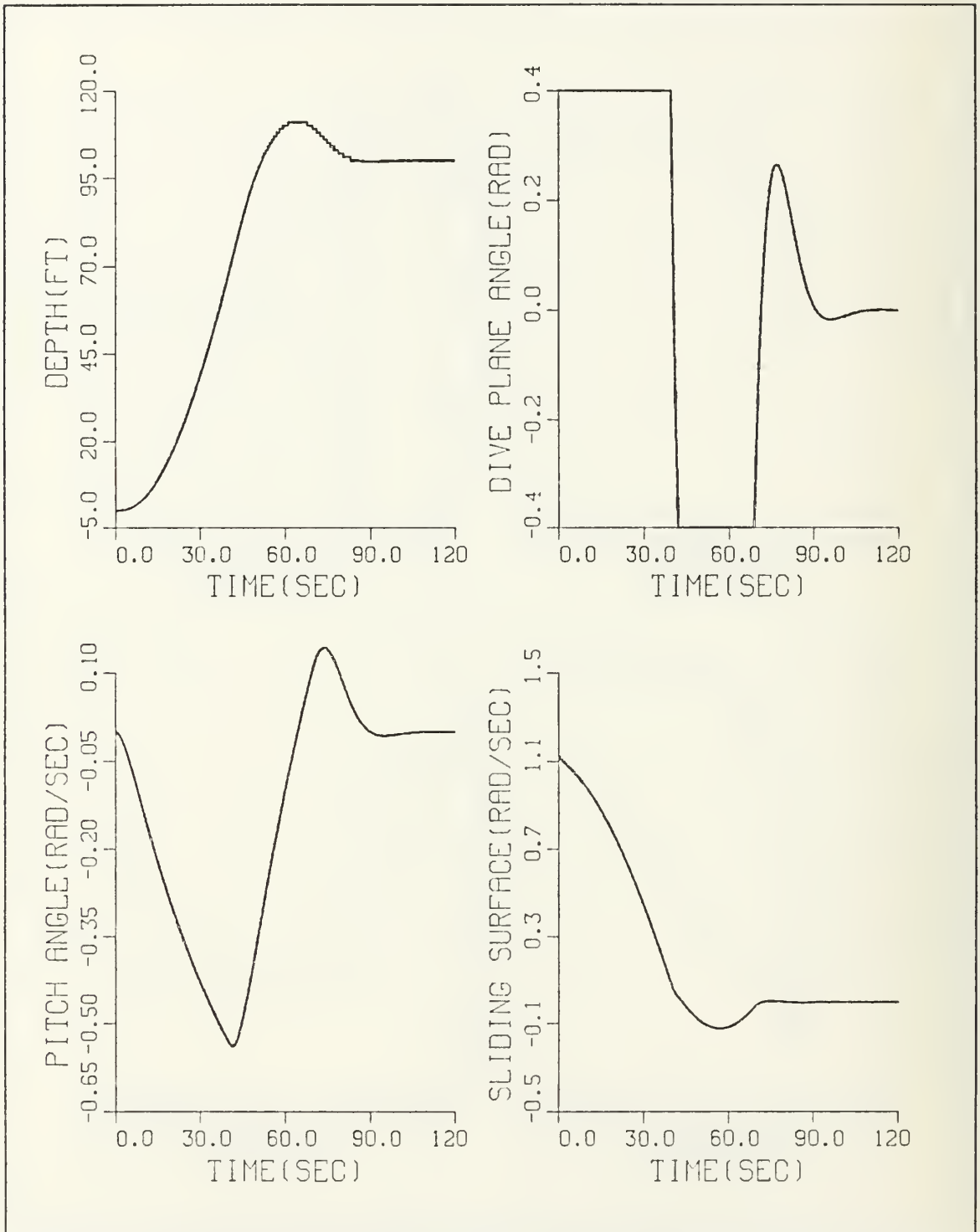
Figure 22. The response of A/2, B and 500 rpm

50
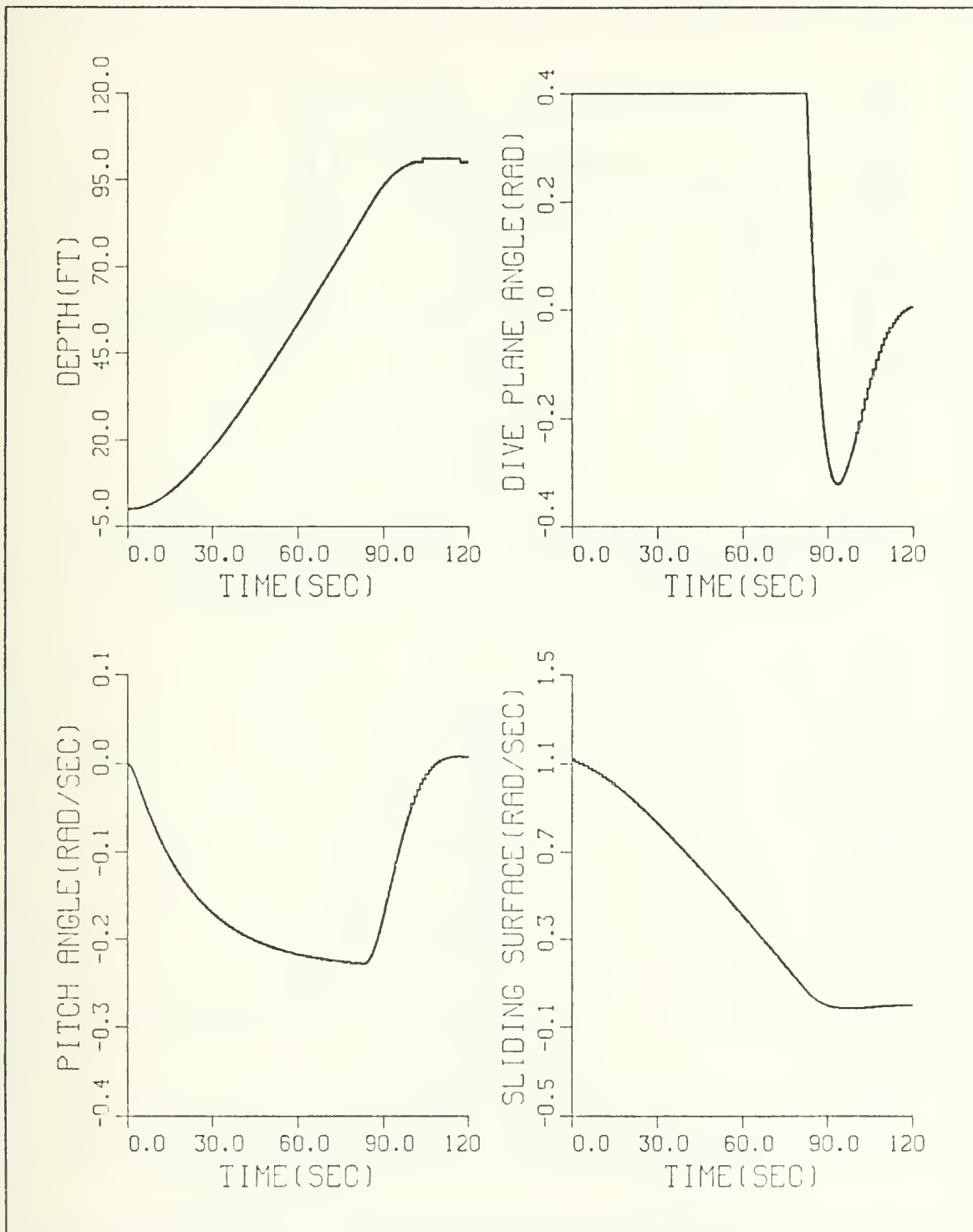
Figure 23.   The response of A, B/2 and 500 rpm

51
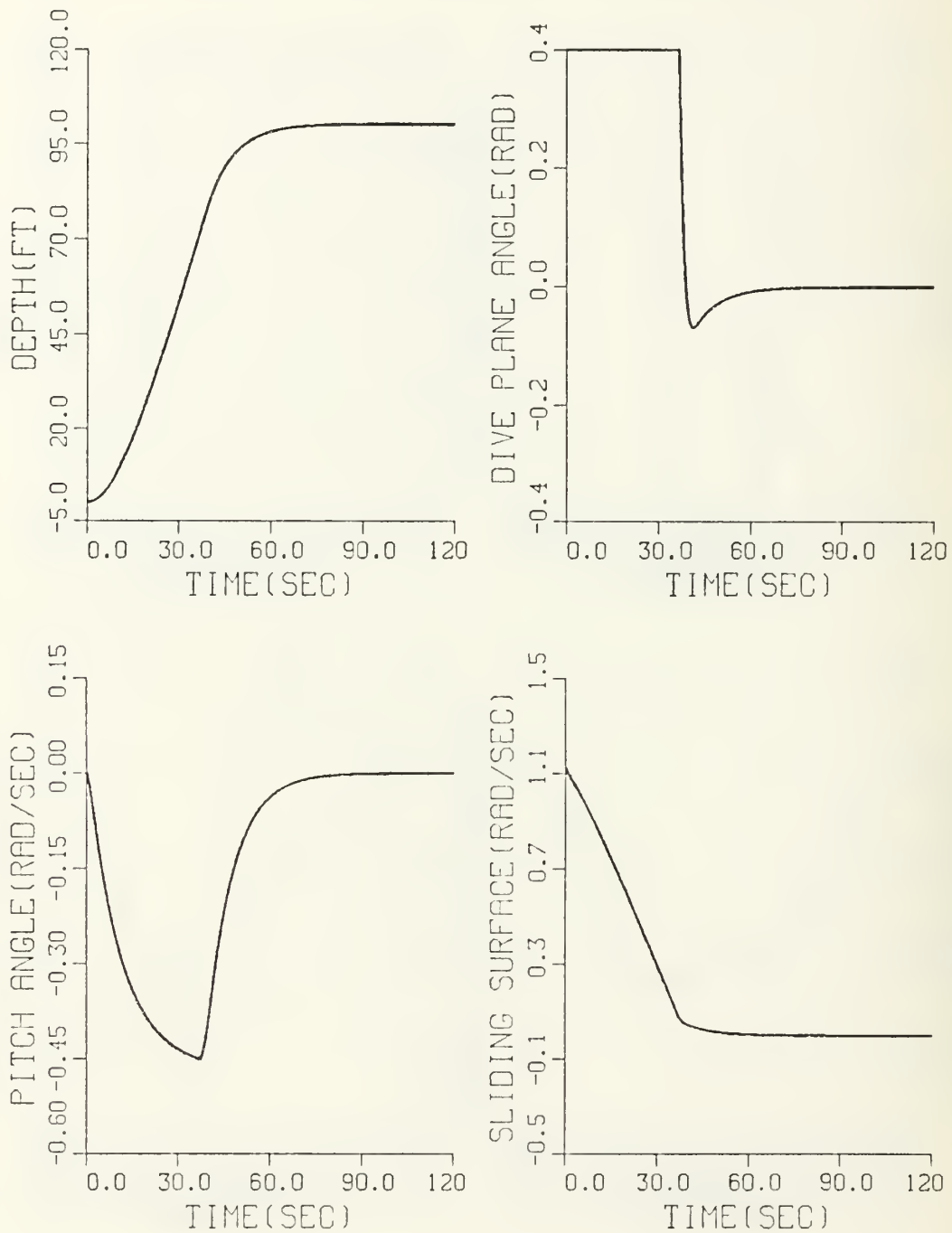
Figure 24. The response of 2*A, 2*B and 500 rpm
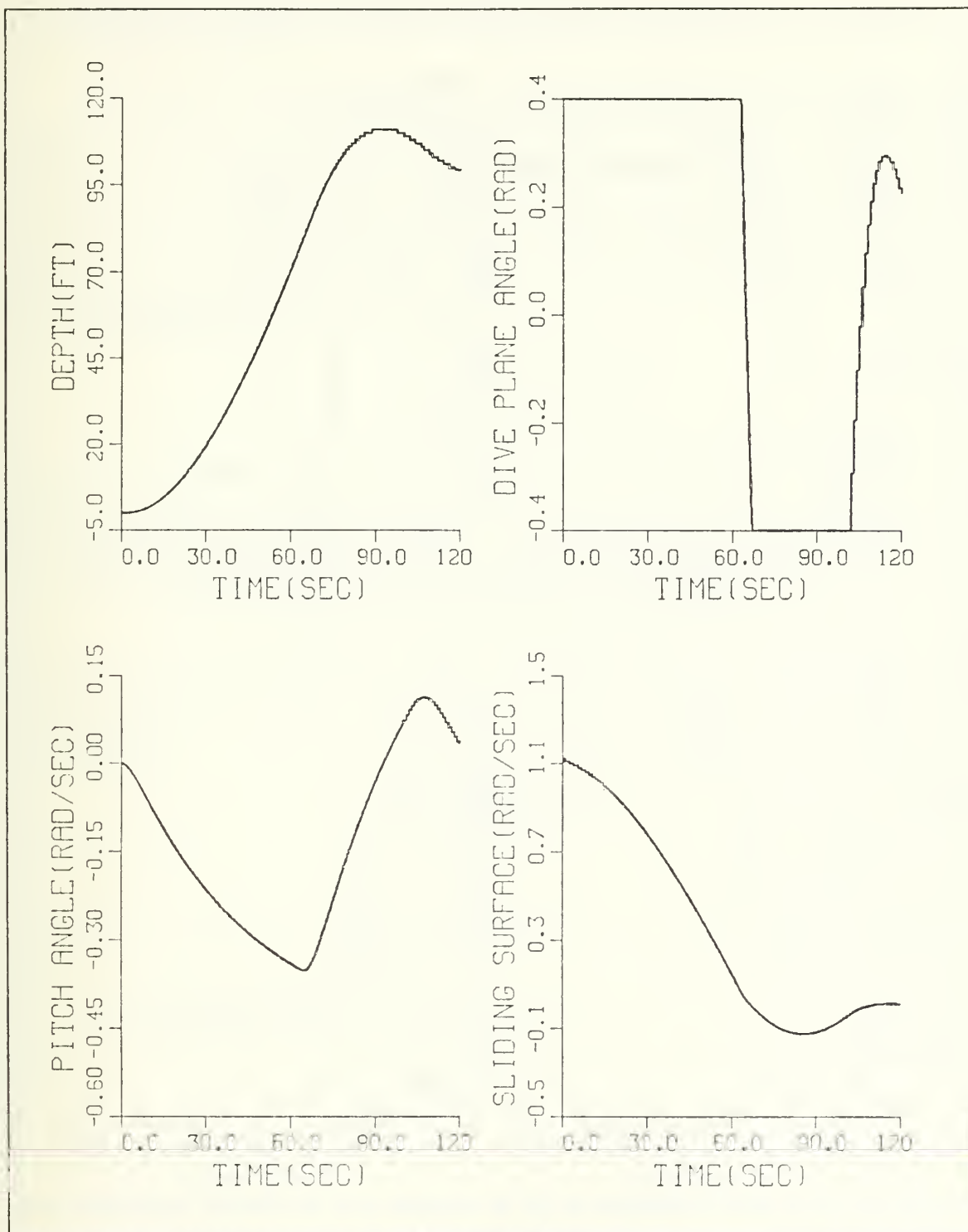
Figure 25.   The response of A/2, B/2 and 500 rpm

53
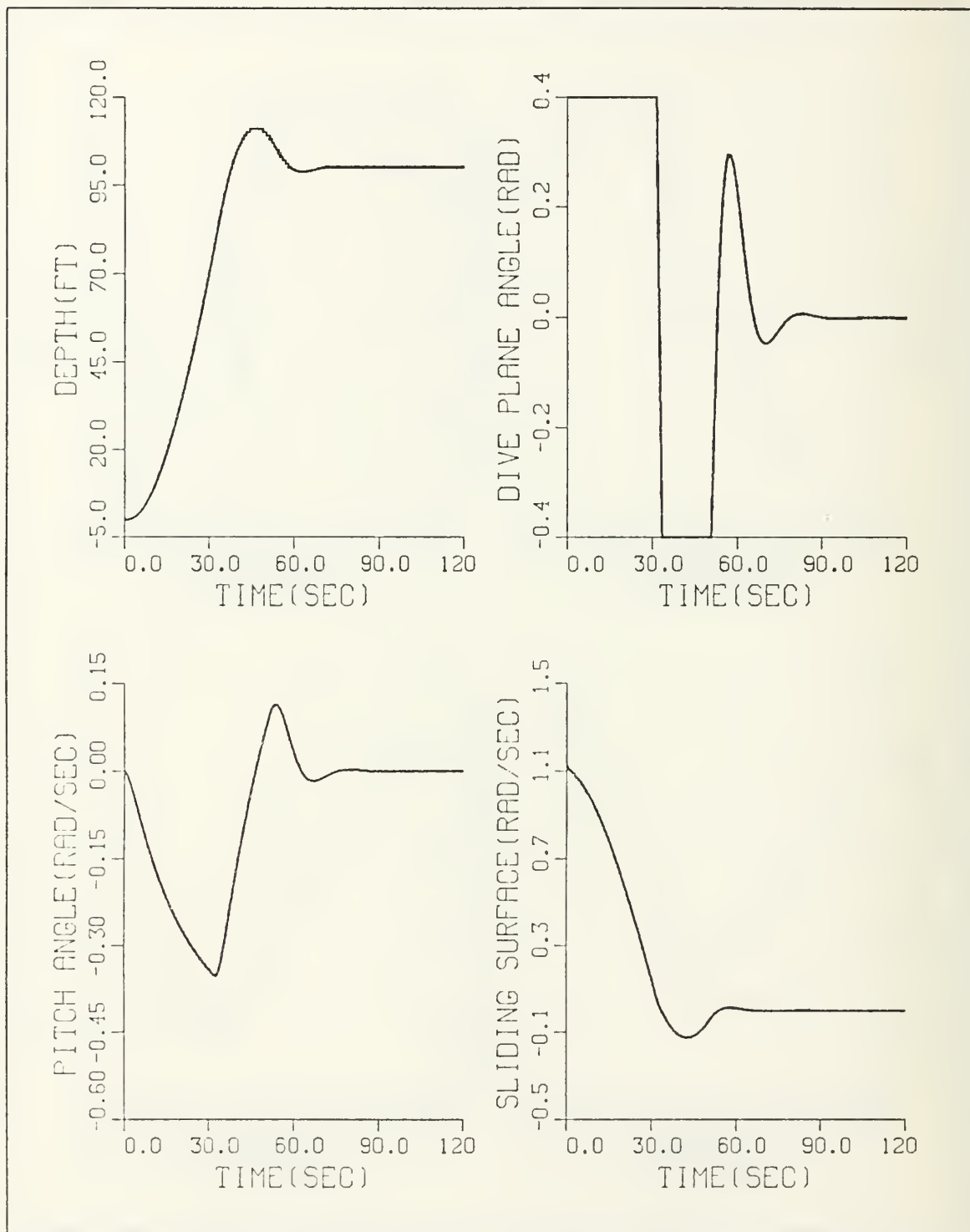
Figure 26.   The response of A, B and 1000 rpm

54

D.   DESIGN OF SLIDING MODE CONTROL FOR THE NONLINEAR MODEL

The sliding mode appeal is based on its ability to treat nonlinear, time varying and unmodelled systems in a straightforward manner [Ref. 3]. It is the purpose of this section to apply the linear sliding mode controller to the nonlinear model of the actual AUV. The sliding surface and control law gain for the actual AUV are based on the linearized nominal model. The mathematical form of the nonlinear model for the actual AUV is

$$\frac{dx}{dt} = Ax + \Delta f(x) + B(x)u + d(x, t) \tag{3.29}$$

where $B(x)$ is the nonlinear function associated with the control surface and actuator system

   $\Delta f(x)$ is the uncertainty of the nonlinear function f(x).

   $d(x, t)$ is the uncertainty disturbance.

The system matrix A is the estimate of f(x) and the magnitude of the uncertainty is bounded as

$$F \geq | S^T \Delta f(x) | \tag{3.30}$$

where $F = \begin{bmatrix} F_1 \\ F_2 \\ . \\ . \\ F_n \end{bmatrix}$

The individual bounds on any element of Δf as estimated from some knowledge of the extremes of possibility of $\Delta f(x)$. Also, let B(x) be approximated by B, a constant, where the varying gain β is defined by $B = \beta B(x)$, and β is taken to be scalars, but bounded within the limits of $\beta_{min} < \beta < \beta_{max}$, and $\beta_{nominal} = 1$. Then it

follows that $\beta = 1$, and $\Delta f = 0$, and $d(x,t) = 0$ will yield the nominal sliding mode control law (3.20). Disturbance $d(x,t)$ is unknown but is upper bounded by a known continuous function such that:

$$D \geq |S^T d(x, t)| \tag{3.31}$$

The dynamics of the system with bounded uncertainty of the actual AUV is

$$\frac{dx}{dt} = Ax + \Delta f(x) + \beta Bu + d(x, t) \tag{3.32}$$

This equations is used to simulate the uncertain nonlinear terms after the linearization process. We have designed the sliding surface $\sigma(x) = S^T x$ by using the nominal linearized model in the previous section. Using the sliding condition theory for the actual AUV, the sliding mode control law for the nonlinear model can be chosen from equations (3.17) and (3.18) such that if

$$\sigma(x)\dot{\sigma}(x) = -\eta^2 |\sigma(x)|$$

and the system will reach the surface $(\sigma(x) = 0)$ within a finite time t_r defined by

$$t_r \leq \frac{|\sigma(0)|}{\eta^2} \tag{3.33}$$

The true dynamics of the sliding surface with uncertainty are, however, given by

$$\dot{\sigma}(x) = S^T \dot{x}$$

$$= S^T[Ax + \Delta f(x) + \beta Bu + d(x, t)] \tag{3.34}$$

Substituting equation (3.20) to the above equation for u, then the derivatives of σ,

$$\dot{\sigma} = (1 - \beta^{-1})S^T Ax + S^T \Delta f(x) + S^T d(x, t)$$

$$-\beta^{-1}\eta^2 sign(\sigma) \tag{3.35}$$

56

From the above, stability is guaranteed, if and only if

$$\dot{\sigma}(x) \leq -\eta_0^2 sign(\sigma), \tag{3.36}$$

where η_0^2 is the nonlinear feedback gain without an uncertainty

If the control matrix B is exactly known ($\beta = 1$), then control law

$$u_b = -[S^T B]^{-1} S^T A x - [S^T B]^{-1} \eta^2 sign(\sigma(x)) \tag{3.37}$$

where $\eta^2 \geq |\eta_0^2 + F(x) + D(x, t)|$

can guarantee stability and perfect tracking for the nonlinear system with constant control matrix of the AUV. In case where the control system B(x) is uncertain, the following change (η^2) must be made:

$$u = -[S^T B]^{-1} S^T A x - [S^T B]^{-1} \eta^2 sign \sigma(x) \tag{3.38}$$

$$u = \hat{u} + \bar{u}$$

where $\acute{u} = -[S^T B]^{-1} S^T A x$

$\bar{u} = -[S^T B]^{-1} \eta^2 sign(\sigma)$

$\eta^2 \geq \beta_{max} |\eta_0^2 + F(x) + D(x, t)| + |(\beta_{max} - 1)| |S^T A x|$

Since the nonlinear term of the B(x) and $\Delta f(x)$ is uncertain in most cases, it is assumed to be zero equation (3.29) and η^2 is increased depending on their assumed bonuds to guarantee stable sliding mode control [Ref. 2]. The actual control law used in subsequent simulation was in fact equation (3.38) with sufficiently large η^2 to accomodate the uncertainty in $\Delta f(x)$ and B(x). The sliding mode switching control law equation (3.38) guarantees that equation (3.18) is satisfied even in the presence of parameter variations and unmodeled dynamics provided η^2 is large enough. The dive plane angle chattering due to modeling errors and disturbances can be eliminated by defining a boundary layer thickness

ϕ about $\sigma = 0$ as illustrated in the previous subsection. The smooth sliding mode control law of the actual AUV is then

$$u = -[S^T B]^{-1}\left(S^T Ax + \eta^2 satsign(\frac{\sigma}{\phi})\right) \tag{3.39}$$

where $\quad \eta^2 \geq \beta_{max} \mid \eta_0^2 + F(x) + D(x, t) \mid + \mid (\beta_{max} - 1) \mid \mid S^T Ax \mid$

The dynamic response, dive plane angle, and sliding surface obtained from nonlinear model simulation at 500 rpm are shown in Figure 27 on page 59. Although the sliding surface and control law gain based on the nominal linear system were applied to the nonlinear system, the response of the system is satisfactory as expected. The designed variable structure system based on the nominal linear equations dealt with the full nonlinear dynamics of the AUV as shown in Figure 27. The technique of sliding mode control can handle the nonlinear system directly without linearization, if sliding surface coefficients are properly chosen. This is especially important for highly maneuverable underwater vehicles that can move in all directions.
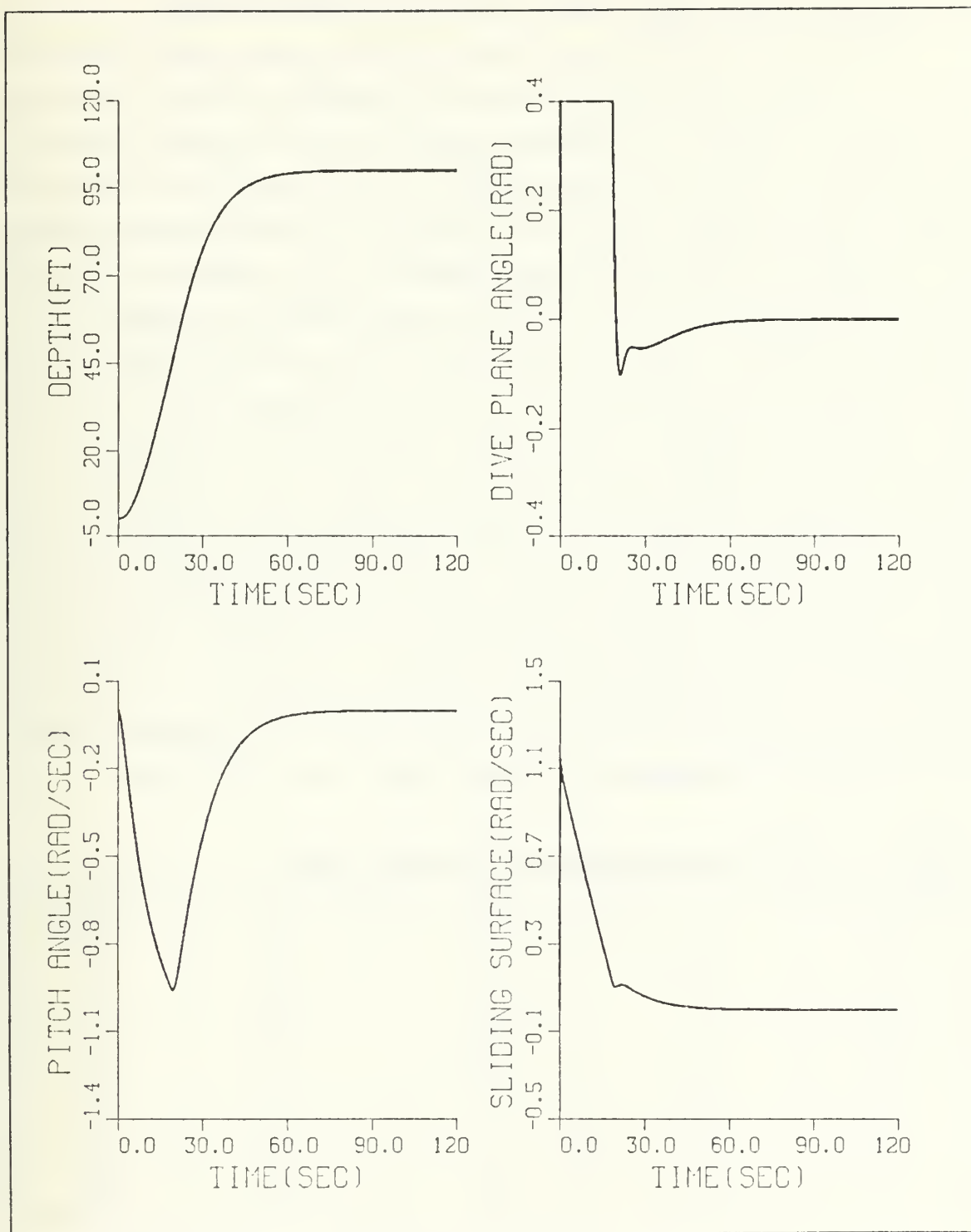
Figure 27.   The response of the actual AUV

E. ROBUSTNESS TESTS USING THE NONLINEAR MODEL

The variable structure systems have an important property which is much less sensitive to nonlinearities, disturbances, and unmodeled dynamics as illustrated in the previous chapter. The nonlinear model of the AUV is used to demonstrate the properties of this control methodology. Accurate models are normally required in order to achieve good control. However, since hydrodynamic modeling is a key element in the design of control system for AUV, we have to rely on approximate expressions for the hydrodynamic forces which can introduce large errors into the control process. We have already seen the results of simulation for control performance using an accurate linear model, modified linear model and accurate nonlinear model. In this section, a simulation study is performed to illustrate the effectiveness of the sliding control under large modifications in the nonlinear model parameters. The modified hydrodynamic coefficients in Table 4 are closely related to system stability. The rotary damping coefficient (M_q) affects the hydrodynamic moment of the AUV in the vertical plane. The center of gravity center of buoyancy separation is directly proportional to restoring moment. Hydrodynamic coefficient ($M_{\delta s}$) directly affects the pitch moment generated by the dive planes. Speed was changed from 500 rpm to 1000 rpm.

Table 5.   TEST CASES FOR THE NONLINEAR MODEL

TEST NO	M_q	Z_g	M_{ds}	RPM
Test 1	$2*M_q$	Z_g	M_{ds}	500
Test 2	$2*M_q$	$Z_g/2$	$2*M_{ds}$	500
Test 3	M_q	Z_g	$2*M_{ds}$	500
Test 4	$M_q/2$	$Z_g/2$	$M_{ds}/2$	500
Test 5	M_q	Z_g	$M_{ds}/2$	500
Test 6	M_q	$Z_g/4$	M_{ds}	500
Test 7	M_q	Z_g	M_{ds}	1000

The controller used was based on the nominal linear model, while some vehicle coefficients differed by 200% and nonlinear terms were added. The FORTRAN

program in Appendix B was used for this purpose. Time plots of depth, pitch rate, sliding surface, and pitch angle response along with the depth commanded values are shown from Figure 28 on page 62 to Figure 33 on page 67.

The sliding mode controller is shown to provide stable response and performs consistently at different parameter values and speed. In every case, the system remains inside the boundary layer ($\sigma = 0$). It is felt that the sliding mode method can produce extremely robust controllers that perform predictably despite the use of simplified or unmodeled dynamics. The center of gravity of the AUV is the most sensitive parameter in the vehicle dynamic response. The depth response of the AUV did not overshoot, although the center of gravity was close to the center of buoyancy. In general, the rpm affected the dynamic response of the nonlinear vehicle. In this case, although the rpm was doubled in magnitude, the overshoot was not present and the response time reduced to 35 seconds. When variation of parameters and modeling error of the AUV were increased, the robustness of the sliding control was improved by increasing the nonlinear feedback gain (η^2). Of course, if the uncertain values exceed the limited boundary, the sliding mode control will not handle these variations effectively. The chosen nonlinear feedback gain ($\eta^2 = 2.4$) for the selected AUV was enough to handle the nonlinear terms and the modified hydodynamic coefficients. The modeling errors, variations of parameters, and nonlinear terms, which were difficult problems of robust using other control technique, were easily dealt with using the sliding mode control as shown from the results of simulations.
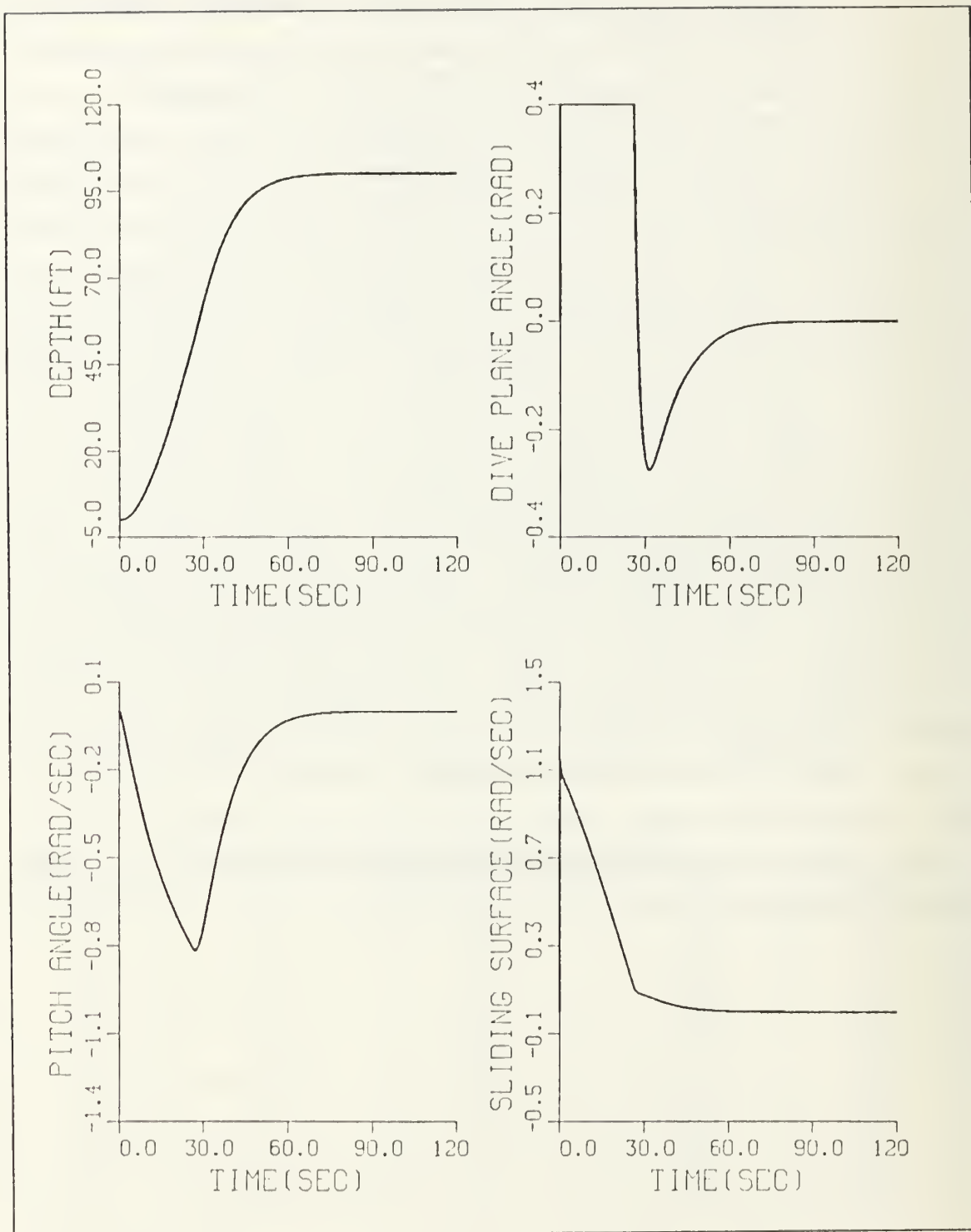
Figure 28.   The dynamic response of test 1 AUV (depth command = 100 ft)
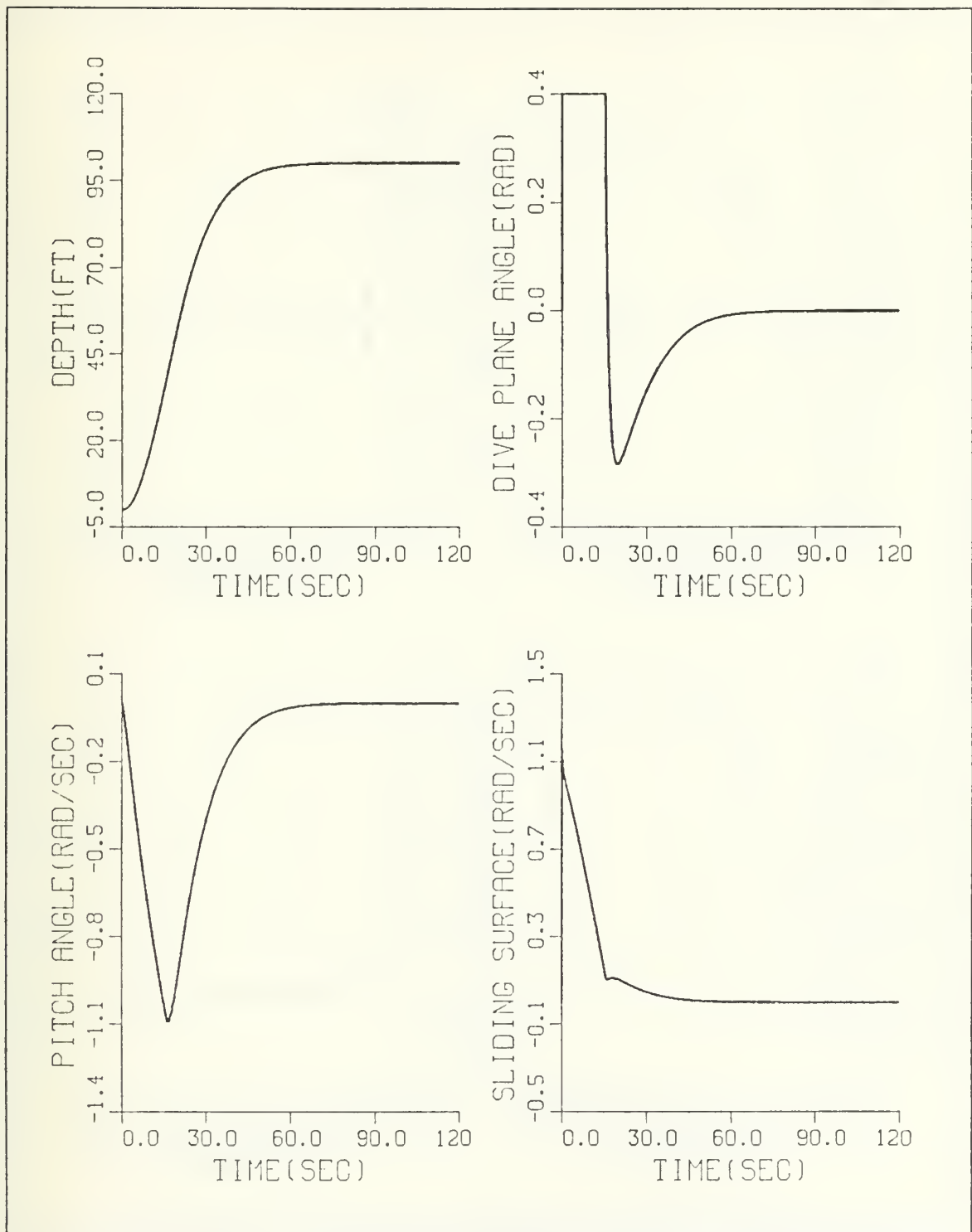
Figure 29. The dynamic response of test 2 AUV (depth command = 100 ft)
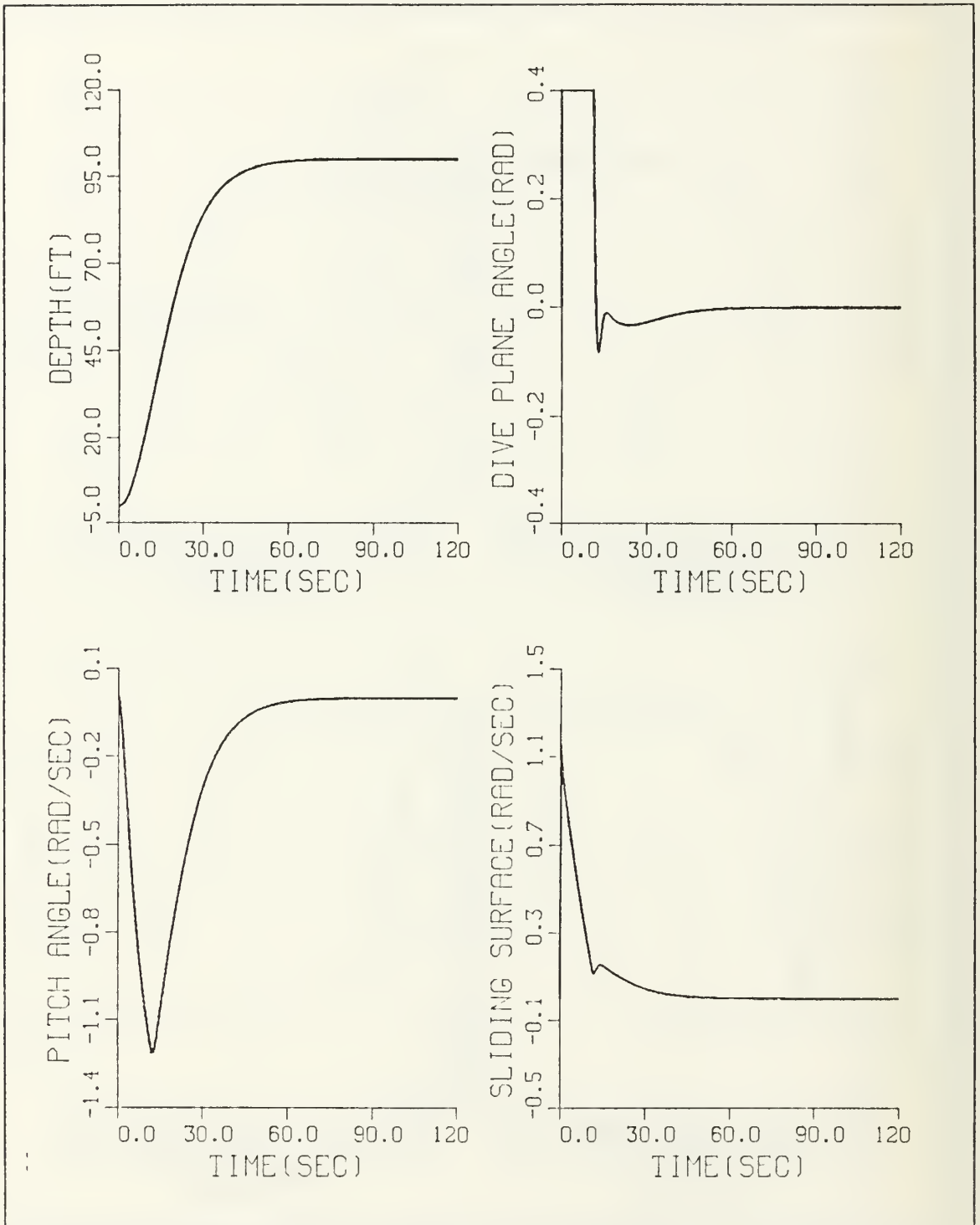
Figure 30.   The dynamic response of test 3 AUV (depth command = 100 ft)
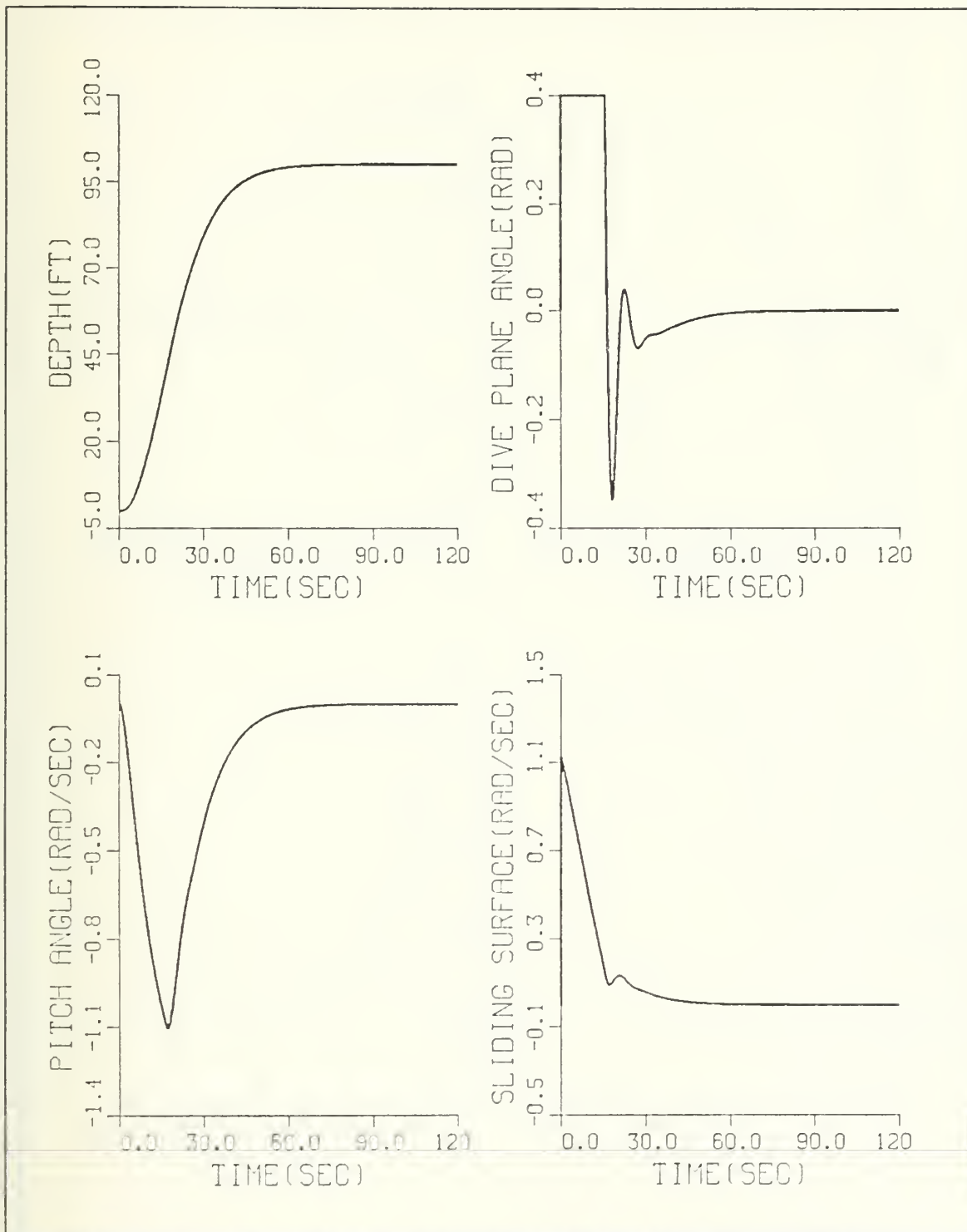
Figure 31. The dynamic response of test 4 AUV (depth command = 100 ft)

65
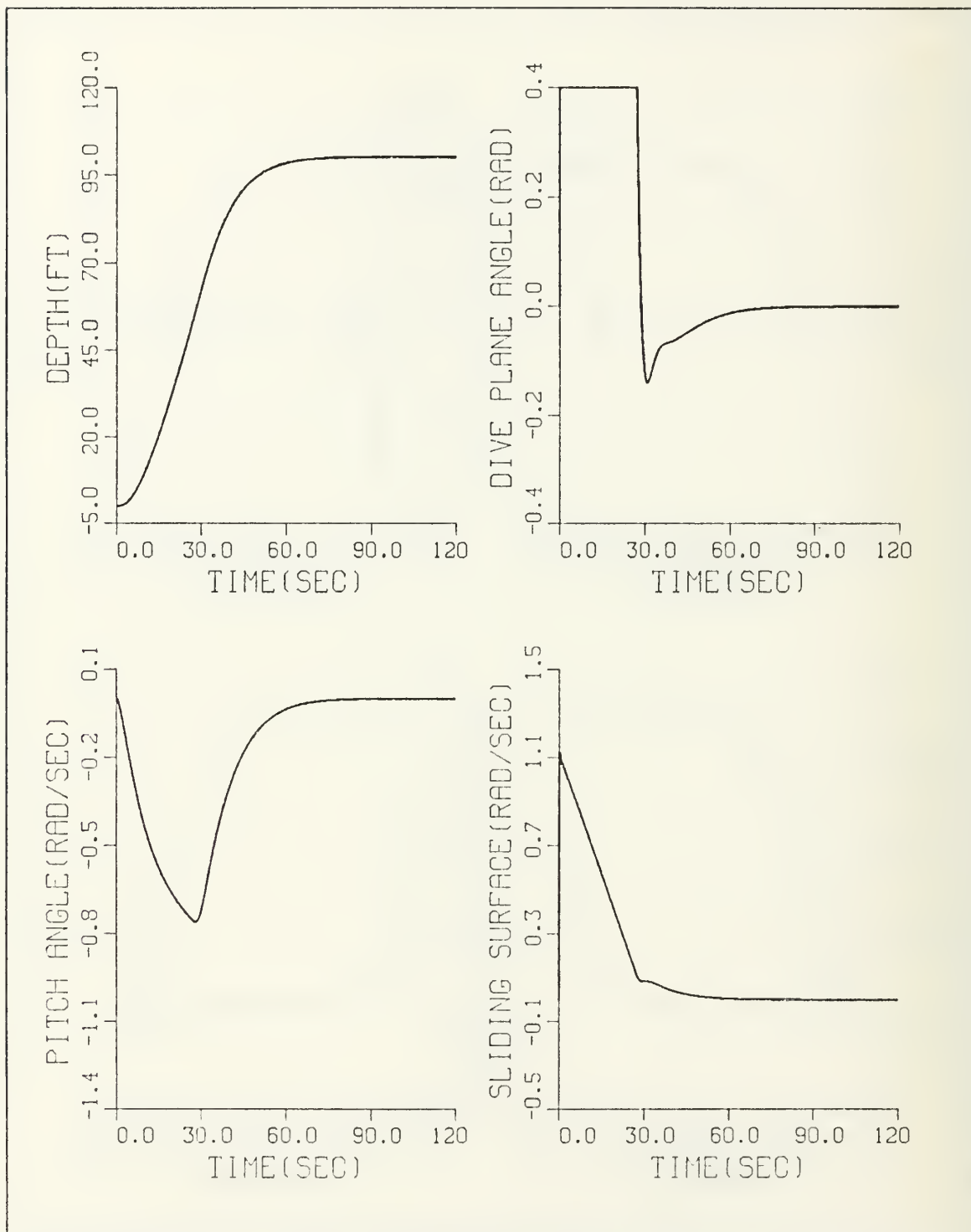
Figure 32.   The dynamic response of test 5 AUV (depth command = 100 ft)

66
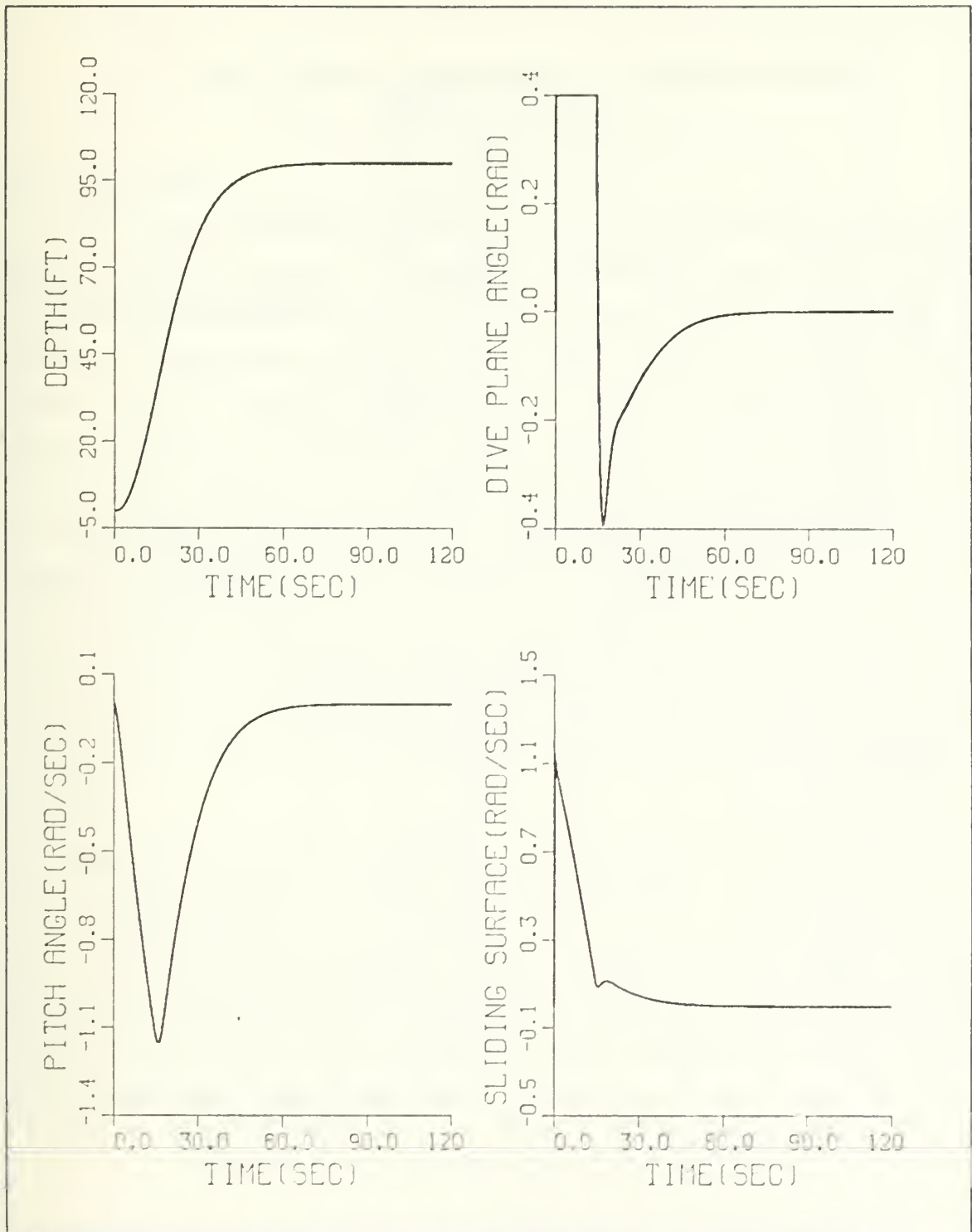
Figure 33.   The dynamic response of test 6 AUV (depth command = 100 ft)

67
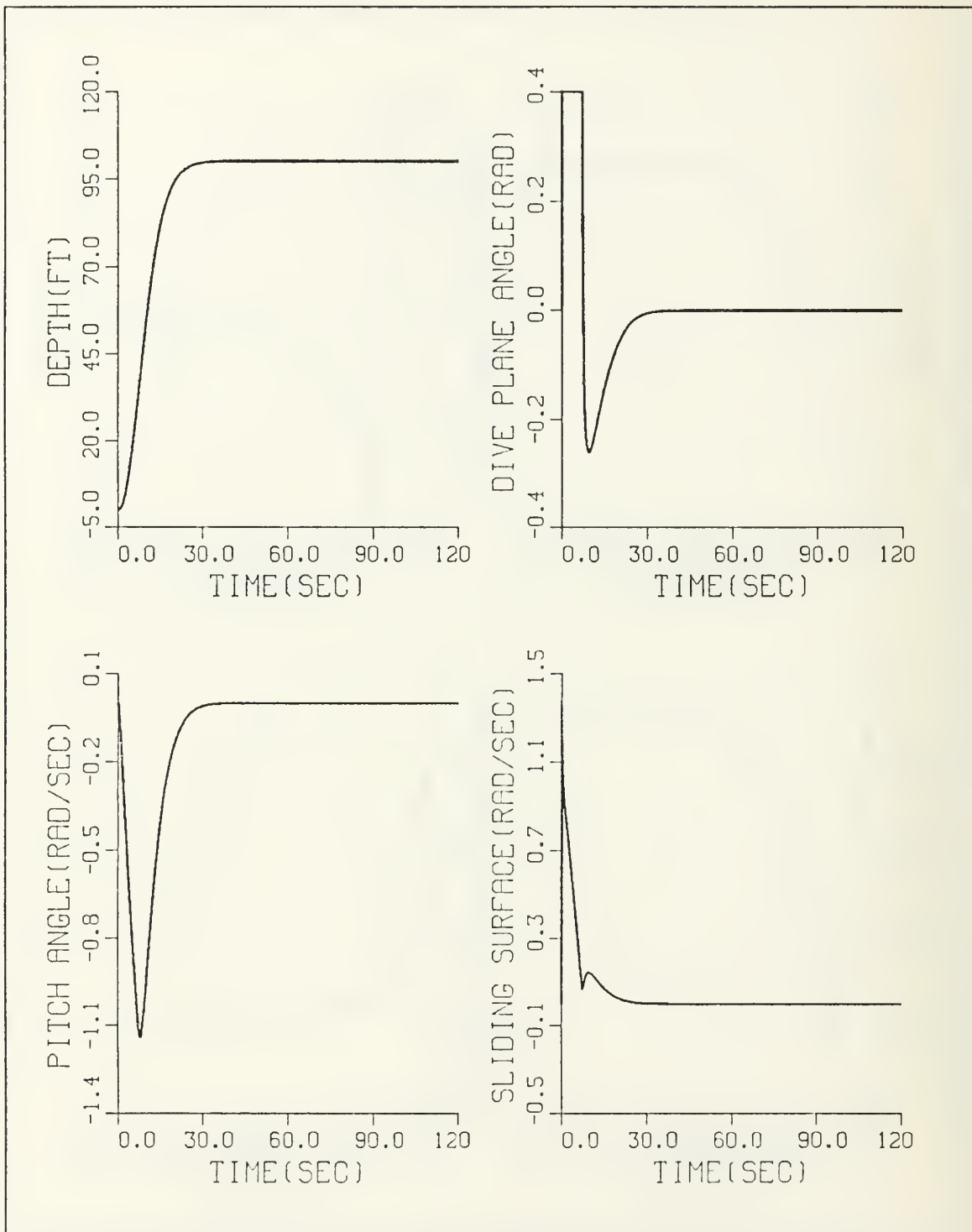
Figure 34. The dynamic response of test 7 AUV (rpm = 1000)

IV.   DESIGN AND EVALUATION OF A SLIDING MODE COMPENSATOR

A.   GENERAL

An autonomous underwater vehicle (AUV) must operate under its own power and be capable of navigation and guidance with sufficient accuracy to be easily recoverable. A navigation system for an underwater vehicle is subject to vehicle size or cost restrictions and this limits the ability to install the highly accurate sensors needed to produce reliable pitch rate data. The vehicle depth can be measured directly by a pressure cell sensor aboard the vehicle. Using the depth of the vehicle as the only external input, state observers can provide all remaining controller data. It is desirable to investigate the performance of a sliding mode compensator designed for a linear model and applicable to a nonlinear model with unmodeled vehicle dynamics. It is the purpose of this chapter to design such a sliding mode compensator and assess its robustness. This work involves numerical simulation of the performance of a sliding mode compensator scheme using a linear and a full 12 state nonlinear model of the equation of motion for the AUV.

B.   DESIGN OF SLIDING MODE COMPENSATOR

1.   Linear Model

A state observer is designed which uses measured depth only in order to estimate the vehicle pitch rate and pitch angle. The block diagram of the basic sliding mode compensator is illustrated in Figure 35 on page 71. The state observer design is based on the equation [Ref. 11].

$$\dot{\hat{x}} = A\hat{x} + Bu + K_0(y - C\hat{x}) \tag{4.1}$$

where $\hat{x}$ is the state variable estimated by the observer, and K_0 is the observer feedback which is required for the observer to be able to follow and duplicate control system operation.

A, B, and C are the original open-loop control matrices of equation (3.11).

u is the sliding mode control law based on the observer.

Note that in the sliding mode compensator, disturbance, nonlinear terms, and variation of parameters are ignored. Equation (4.1) is schematically depicted in Appendix A. Collecting terms and rearranging

$$\dot{\hat{x}} = (A - K_0 C)\hat{x} + Bu + K_0 y \qquad (4.2)$$

which is then rearranged into the familiar state space form:

$$\dot{\hat{x}} = \hat{A}\hat{x} + \hat{B}u$$

$$y = \hat{C}\hat{x} + \hat{D}U \qquad (4.3)$$

where $\hat{A}$ is the observer A matrix $(A - K_0 C)$
$\hat{B}$ is the observer B matrix
$\hat{C}$ is the observer C matrix

The values for observer feedback gain (K_0) are calculated using the Matrix-x program "OBSERVER" in Appendix A. This provids three values of gain for the one state (depth) that is used by the observer in order to estimate the remaining two (pitch rate and pitch angle). The poles chosen for the observer are -4.5, -4.75, and -4.95. These values are selected because they create a faster response in the observer than in the controller itself. This condition is necessary to ensure that the observer will not slow down the overall simulation speed of the controller. The sliding surface of the sliding mode compensator has the same form as the sliding surface of a controller $\sigma(x) = S^T x$.

The state observer provides necessary information to the sliding mode controller. The control input of the sliding mode compensator can be described in the following process. From the sliding condition we have

Figure 35.   The block diagram of the sliding mode compensator.

$$\dot{\sigma}(\hat{x}) = -\eta^2 sign(\sigma) \tag{4.4}$$

Substituting equation (4.3) to equation (4.4) and rearranging

$$S^T\hat{x} = -\eta^2 sign(\sigma)$$

$$S^T(\hat{A}\hat{x} + \hat{B}u) = -\eta^2 sign(\sigma) \tag{4.5}$$

Finally, the sliding mode control law can be expressed in terms of the estimated state variables in the following form:

$$u = -(S^T\hat{B})^{-1}S^T\hat{A}\hat{x} - (S^T\hat{B})^{-1}\eta^2 sign(\sigma) \tag{4.6}$$

or

$$u = \hat{u} + \bar{u}$$

where $\quad \hat{u} = -(S^T\hat{B})^{-1}S^T\hat{A}\hat{x}$

$\qquad\quad \bar{u} = -(S^T\hat{B})^{-1}\eta^2 sign(\sigma)$

The Figure 36 shows the dynamic response of the vehicle with the sliding mode compensator. The nonlinear feedback gain (η^2) in the compensator is the same as the gain in the controller without the observer. It can be seen that since the observer poles are fast, the performance of the current compensator resemble that of the controller alone of Chapter 3. A sliding mode compensator is easier to design and implement than conventional compensators.
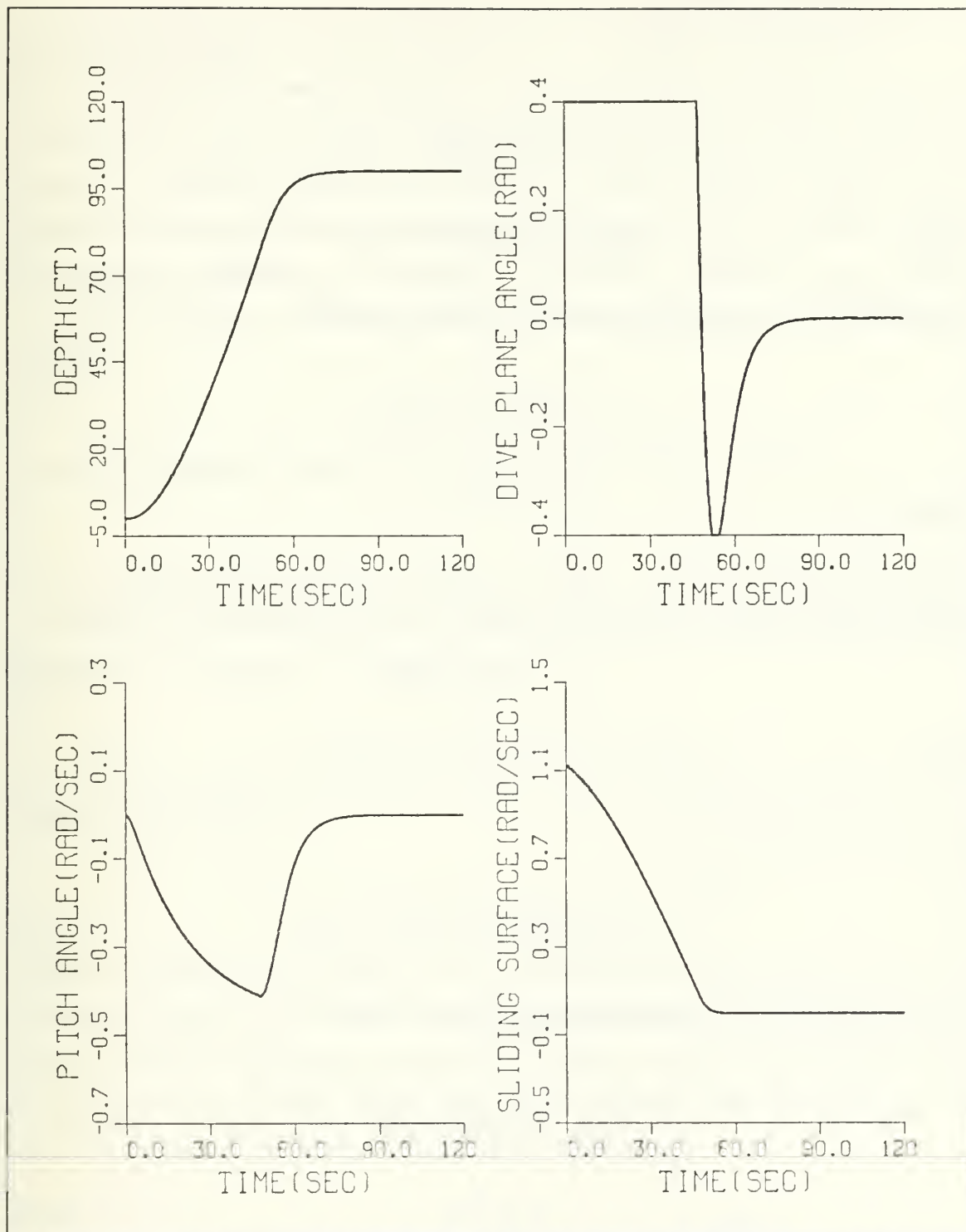
Figure 36.   The dynamic response of the vehicle with sliding mode compensator.

73

2. Nonlinear Model

The designed nonlinear control feedback gain (η^2), sliding surface ($\sigma(x)$), and observer feedback gain (K_0), which are based on the nominal linear model, are used to design a sliding mode compensator in order to handle a full nonlinear model. Since a nonlinear model can never be as easily predictable as a linear model, there exists certain degree of uncertainty in the nonlinear terms. A similar process as in Chapter 3 provides a design of a nonlinear sliding mode compensator. The AUV nonlinear dynamics is given by

$$\dot{x} = Ax + \Delta f(x) + B(x)u \tag{4.7}$$

where $\Delta f(x)$, $B(x)$ are the model errors of nonlinear terms and uncertainty.

Equation (4.7) can be rearranged by using the same procedure in Chapter 3.

$$\dot{x} = Ax + \Delta f(x) + \beta Bu \tag{4.8}$$

The procedure for obtaining $\hat{x}(t)$ of $x(t)$ is to compute the estimate to be the output of the dynamic system.

$$\dot{\hat{x}} = A\hat{x} + \Delta f(\hat{x}) + \beta Bu + K_0(y - C\hat{x}) \tag{4.9}$$

We can rewrite (4.9) in the following state space form

$$\dot{\hat{x}} = \hat{A}\hat{x} + \Delta f(\hat{x}) + \beta \hat{B}u$$

$$y = \hat{C}\hat{x}u \tag{4.10}$$

where $F(\dot{x}) \geq |S^T \Delta f(\hat{x})|$

The closed-loop dynamics of the state observer on the sliding surface with uncertainty is given by

$$\dot{\sigma}(\hat{x}) = S^T \dot{\hat{x}}$$

$$= S^T[\hat{A}\hat{x} + \Delta f(\hat{x}) + \beta \hat{B}u] \tag{4.11}$$

Substituting equation (4.6) to the above (4.11) for u, then we obtain the following equation

$$\dot{\sigma} = (1 - \beta^{-1})S^T \hat{A}\hat{x} + S^T \Delta f(\hat{x})$$

$$- \beta^{-1}\eta^2 sign\sigma(\hat{x}) \tag{4.12}$$

If $\sigma \leq -\eta_0^2 sign\sigma(\hat{x})$ is enforced, stability will result. We can establish conditions on the use of η^2 in equation (4.6) that will guarantee that sliding condition, given the bounds of uncertainty. It follows that

$$\eta^2 \geq \beta(\eta_0^2 + S^T \Delta f(\hat{x}) + (1 - \beta^{-1})S^T \hat{A}\hat{x}) \tag{4.13}$$

which can be achieved by

$$\eta^2 \geq \beta_{\max} \mid \eta_0^2 + F(\hat{x}) \mid + \mid (\beta_{\max} - 1) \mid \mid S^T \hat{A}\hat{x} \mid \tag{4.14}$$

These uncertainties in equation (4.10) are eliminated by using equation (4.6) but with large enough gain (η^2) in order to guarantee stability. The boundary layer used in numerical simulation was selected in order to have the interpretation of smoothing out the discontinuity in the nominal control law at the switching surface. The nominal control law considered in this section,

$$u = -[S^T B]^{-1}S^T \hat{A}\hat{x} - [S^T B]^{-1}\eta^2 satsign\left(\frac{\sigma(\hat{x})}{\phi}\right) \tag{4.15}$$

where $\quad \eta^2 \geq \beta_{\max} \mid \eta_0^2 + F(\hat{x}) \mid + \mid (\beta_{\max} - 1) \mid \mid S^T \hat{A}\hat{x} \mid$

guarantees asymptotic stability for the nonlinear model which have state observer as shown in Figure 37. The nonlinear feedback gain (η^2) was chosen according to the assumed bounding nonlinear terms. The selected gain (η^2) in the previous chapter is large enough to handle any unknown bounded uncertainty. The Figure 37 depicts the expected robustness of the dynamic response using sliding mode compensator. This method produces an extremely robust sliding mode compensator that performs predictably despite the use of the sliding surface, gain (η^2), control law, and observer feedback gain (K_0) which are based on the nominal nlinear model. The FORTRAN program "OBSERVER" in Appendix B has been written to implement the sliding mode compensator. The results of Figure 37 on page 77 were obtained by using the standard hydrodynamic coefficients of the nonlinear model at 500 rpm.
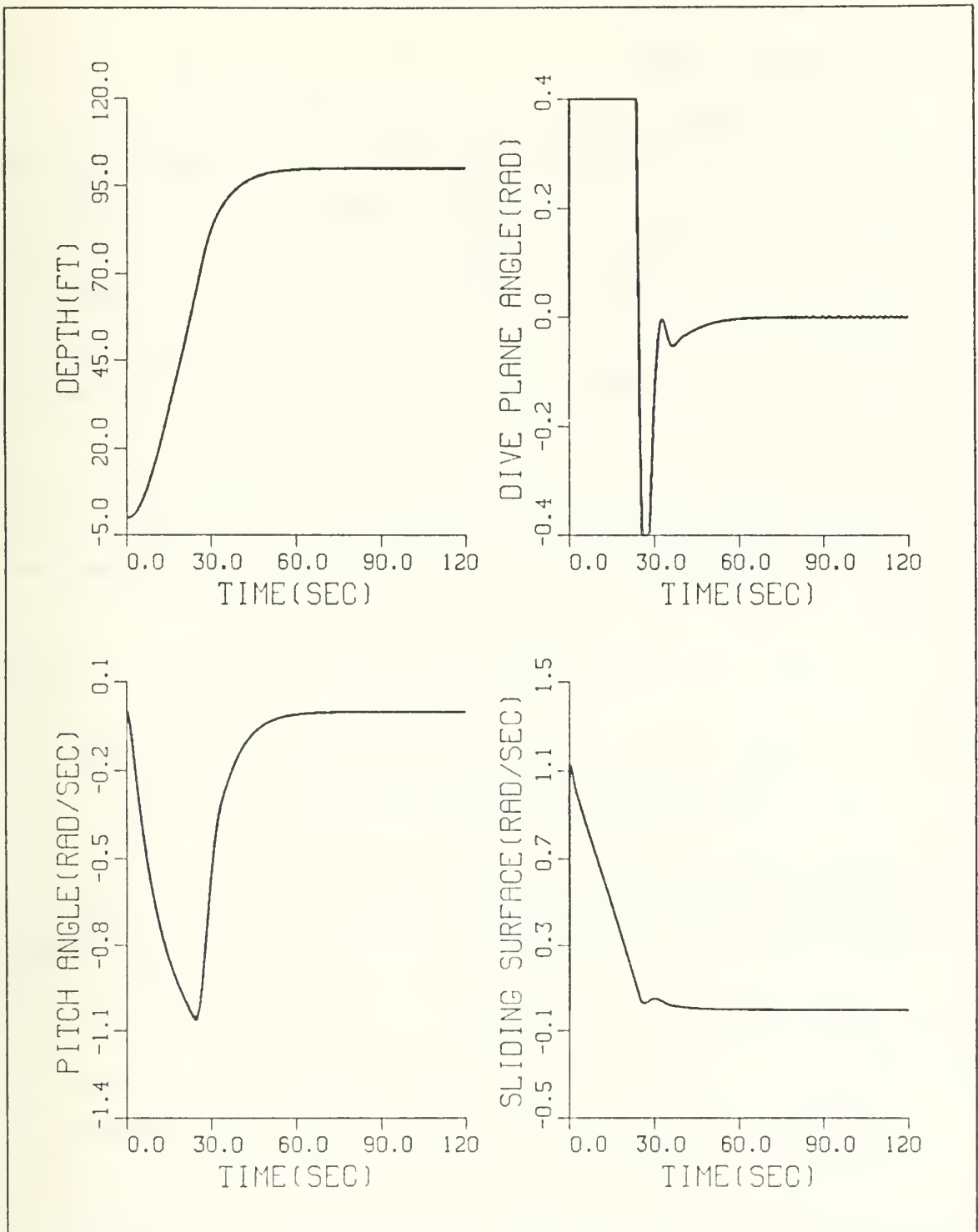
Figure 37.   The dynamic response of the sliding mode compensator for the standard
           AUV

C. ROBUSTNESS TESTS
1. Linear Model

In the previous numerical analysis we saw that sliding mode compensator could deal with unknown nonlinear terms by using nonlinear feedback control law $\bar{u}$. A modified system matrix A, and control matrix B is used to estimate robustness performance of the sliding mode compensator in this section. The effects of modeling error in a linear model can be compensated by considering the size of modeling error as in the classical state space methods [Ref. 11]. The variations in control matrix B can be handled using a similar method. This technique is easy to analyze for a single input system. The effects of modeling error can be considered for any system using sliding mode compensator. Consider the effect of a variation in the system matrix A and control matrix B. The system dynamics are given by

$$\dot{x} = (A+\delta A)x+(B+\delta B)u \qquad (4.16)$$

where δA is the unknown bounded changing system matrix
δB is the unknown bounded changing control matrix

The unknown changed system matrix (δA) and control (δB) matrix can be accommodated by using a large nonlinear (η^2) and boundary layer (ϕ). The large gain will guarantee stability and the boundary layer obtained in the previous chapter will eliminate the chattering which is intrinsically linked to the use of a switching surface. The FORTRAN program "OBSERVER" in Appendx A is used to estimate unmeasurable state and perform sliding mode compensator to the modified system. The same boundary layer (ϕ), nonlinear feedback gain (η^2), control law (4.6), and observer gain(K_0) as in the nominal system are applied to the modified system to estimate the performance of a sliding mode compensator designed on a nominal linear model. The system matrix A and control matrix B are modified as in the following Table 6.

Table 6. ROBUSTNESS TESTS CASE OF THE SLIDING MODE COMPENSATOR

Test No	System matrix A	Control matrix B	Speed
Test 1	2*A	B	6 ft/sec
Test 2	A/2	B	6 ft/sec
Test 3	A	2*B	6 ft/sec
Test 4	A	B/2	6 ft/sec
Test 5	2*A	2*B	6 ft/sec
Test 6	A/2	B/2	6 ft/sec

The dynamic response for each test is shown in Figure 38 on page 80 through Figure 43 on page 85. Although the system matrix A and control matrix B are modified by 200%, there is only 10 ~ 11% overshoot to the test 5. The expected robustness of the dynamic response is presented by using sliding mode compensator based on nominal linear model. Sliding mode compensator performance is verified for a linear vehicle with uncertain A and B matrix without considering additional design.

The sliding mode compensator developed in this section was stable and insensitive to change in hydrodynamic coefficients of the AUV. It therefore appears that variable structure systems will provide the most robust design for a sliding mode compensator that needs to maintain an accurate prediction of vehicle response under varying conditions.
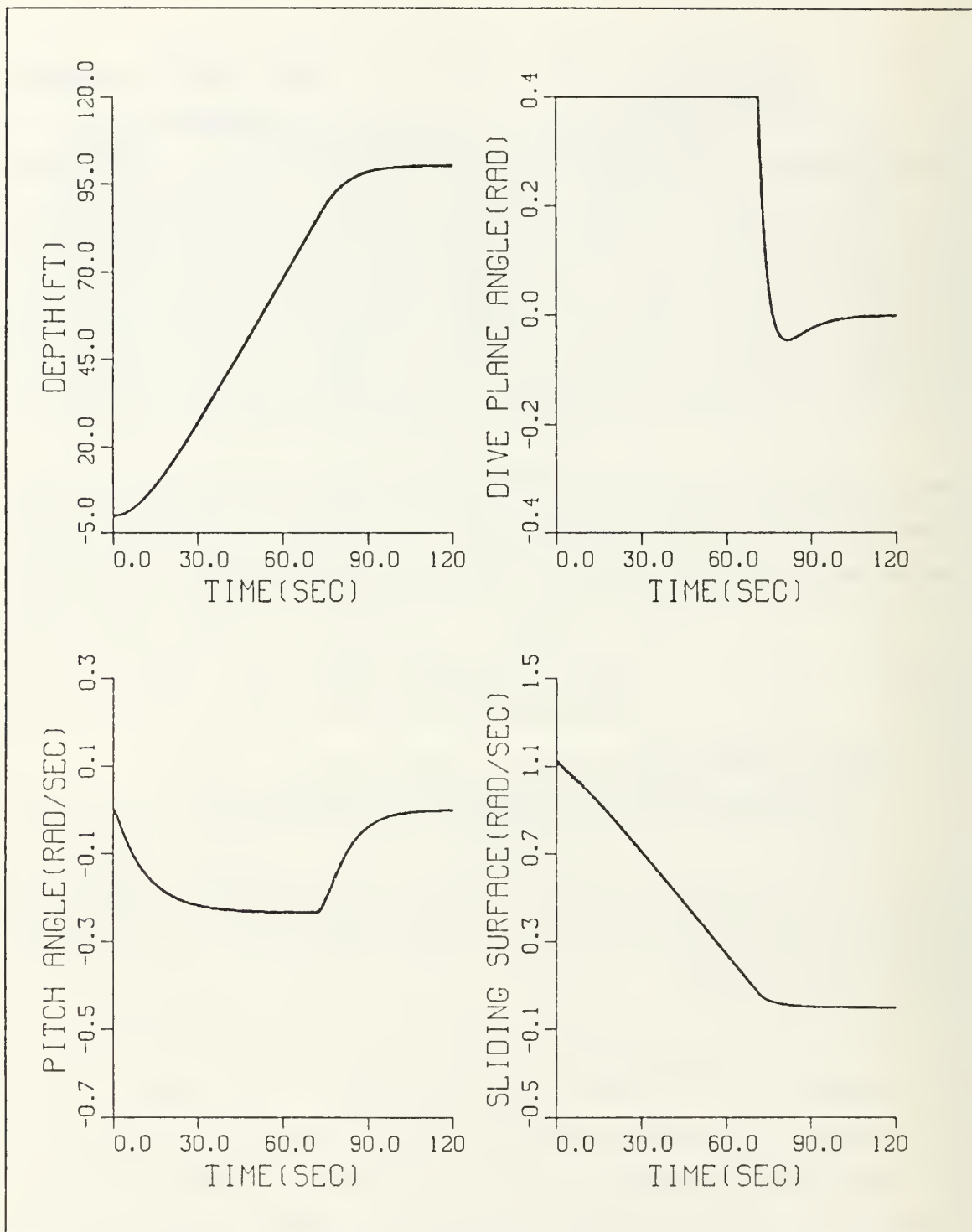
Figure 38.   The dynamic response of test 1 AUV (depth command = 100 ft)
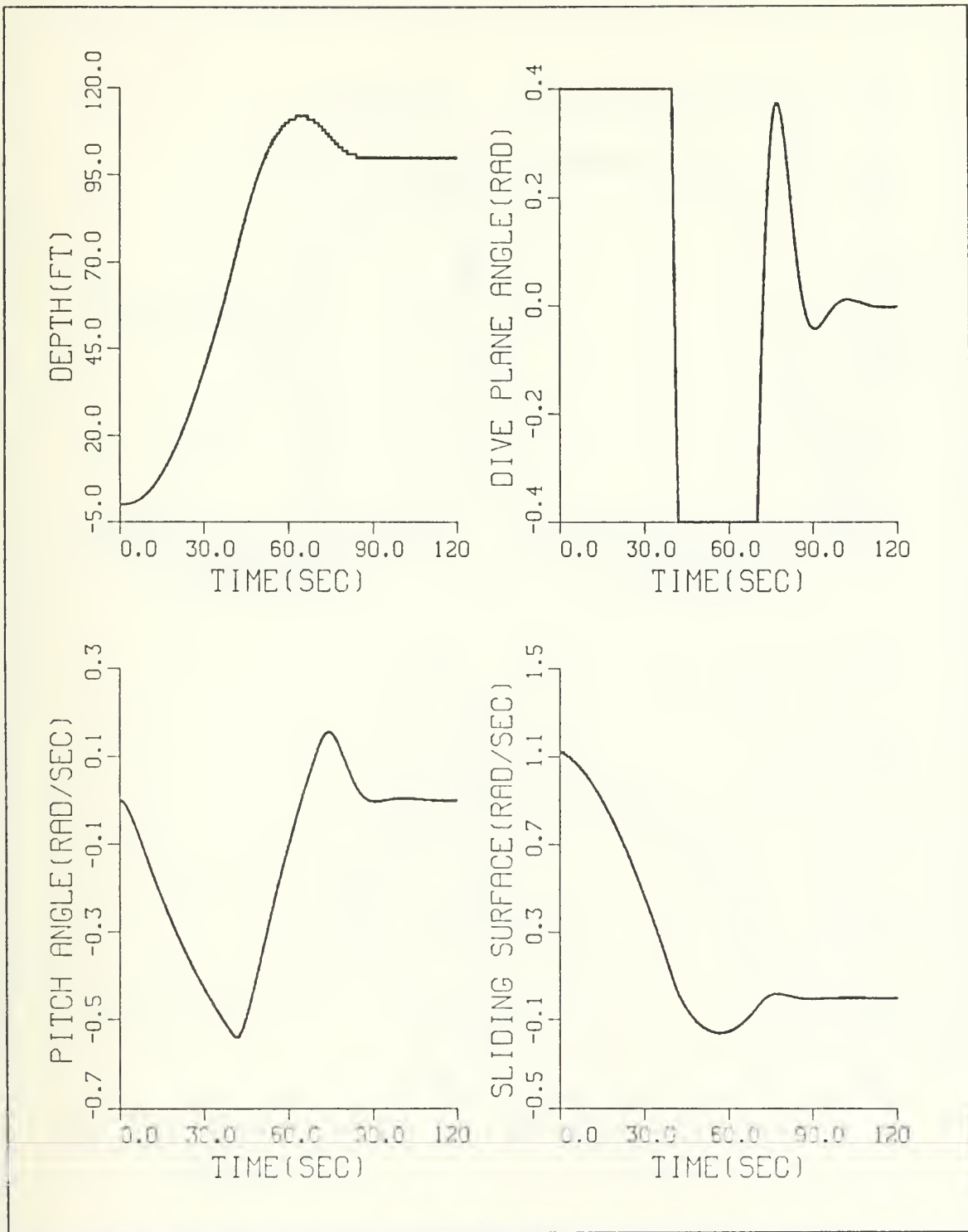
Figure 39.   The dynamic response of test 2 AUV (depth command = 100 ft)
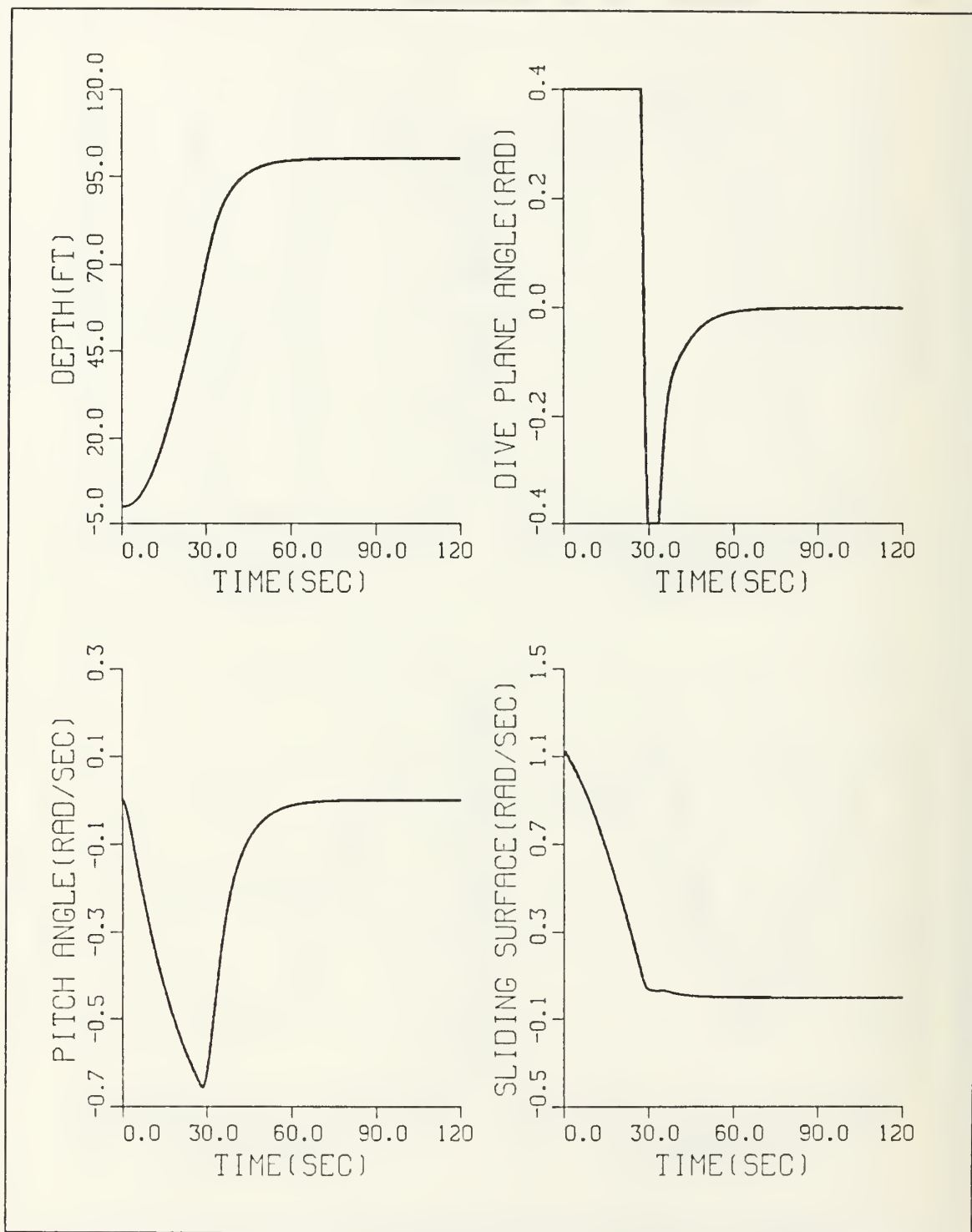
Figure 40. The dynamic response of test 3 AUV (depth command = 100 ft)
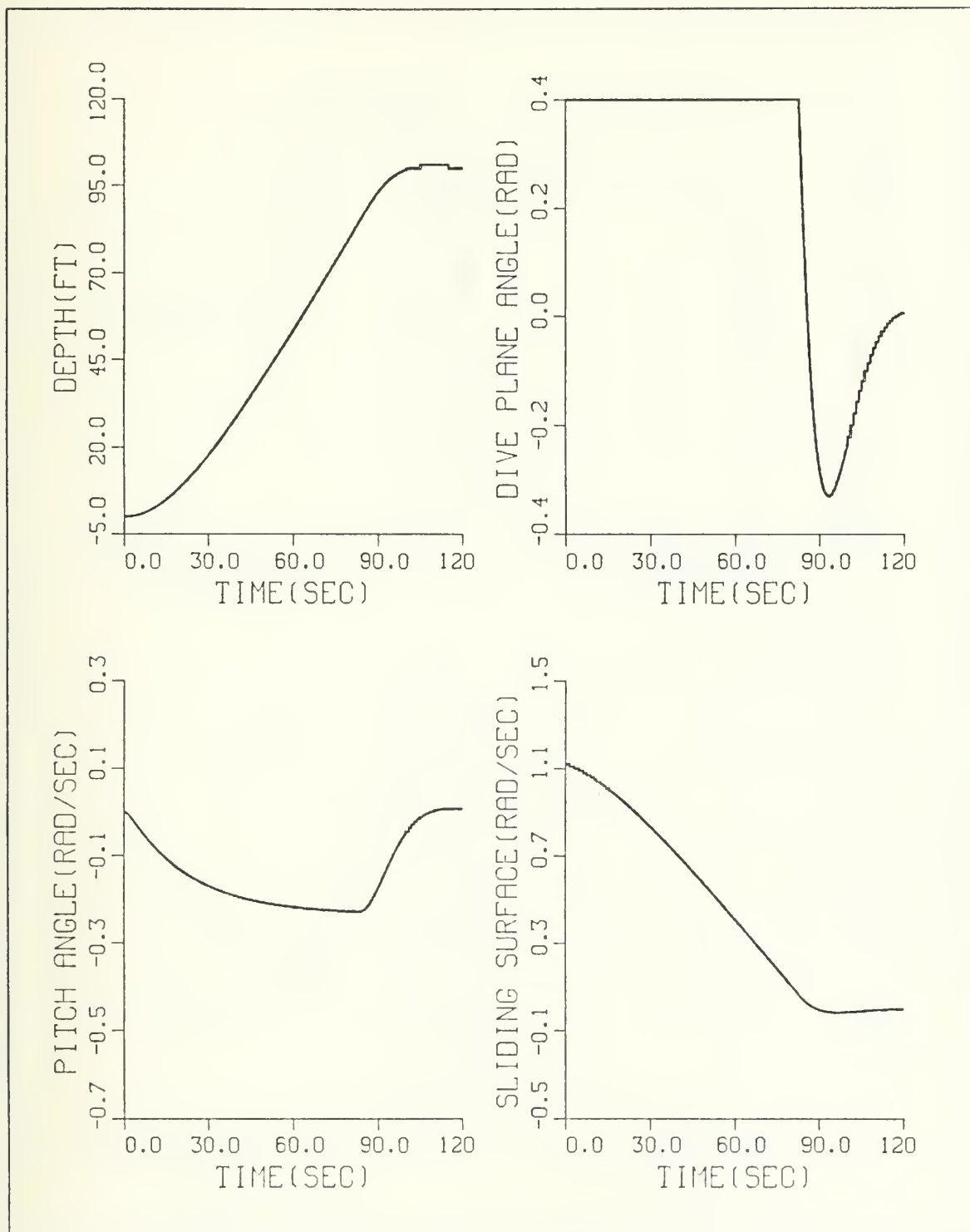
Figure 41. The dynamic response of test 4 AUV (depth command = 100 ft)
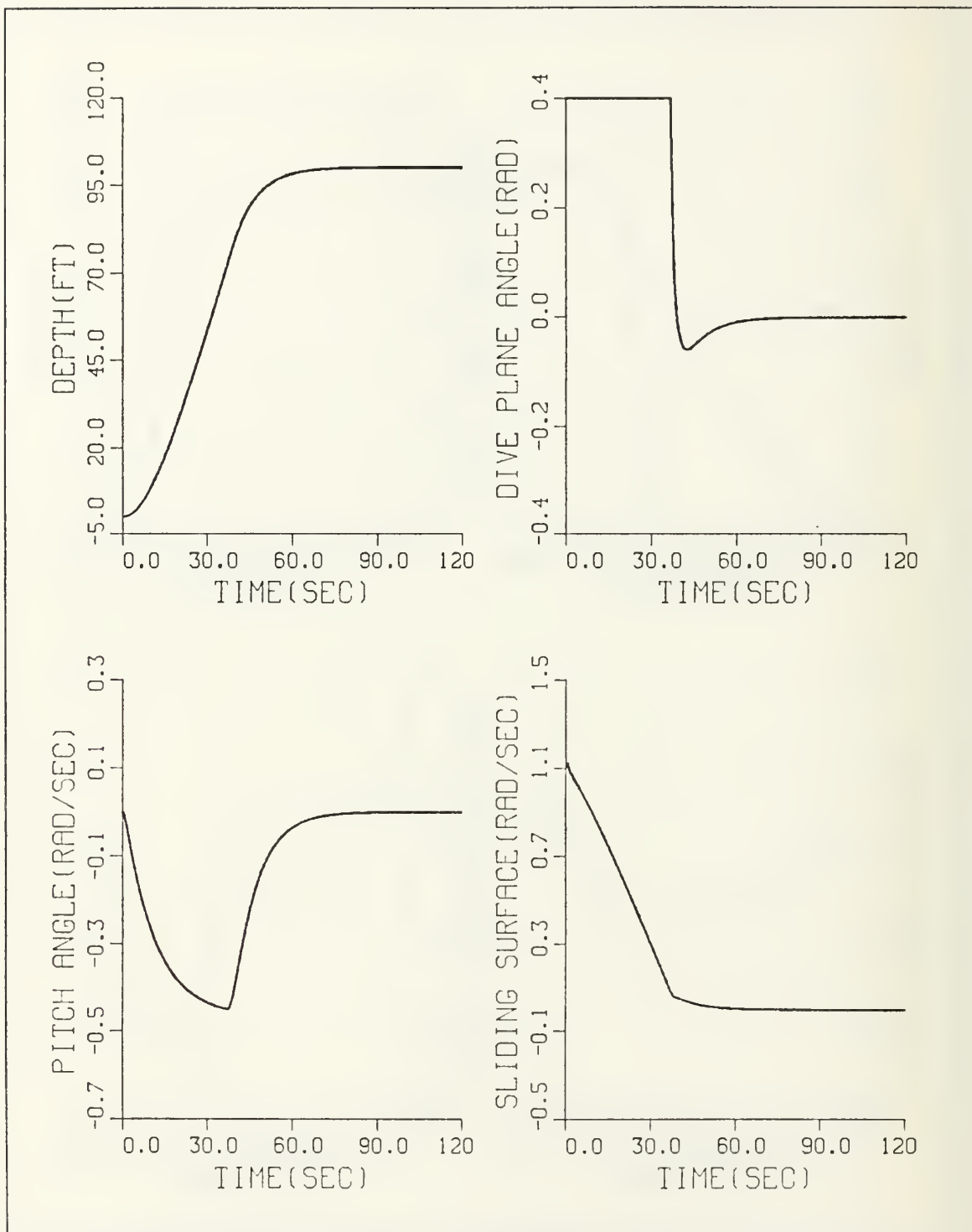
Figure 42.   The dynamic response of test 5 AUV (depth command = 100 ft)

84
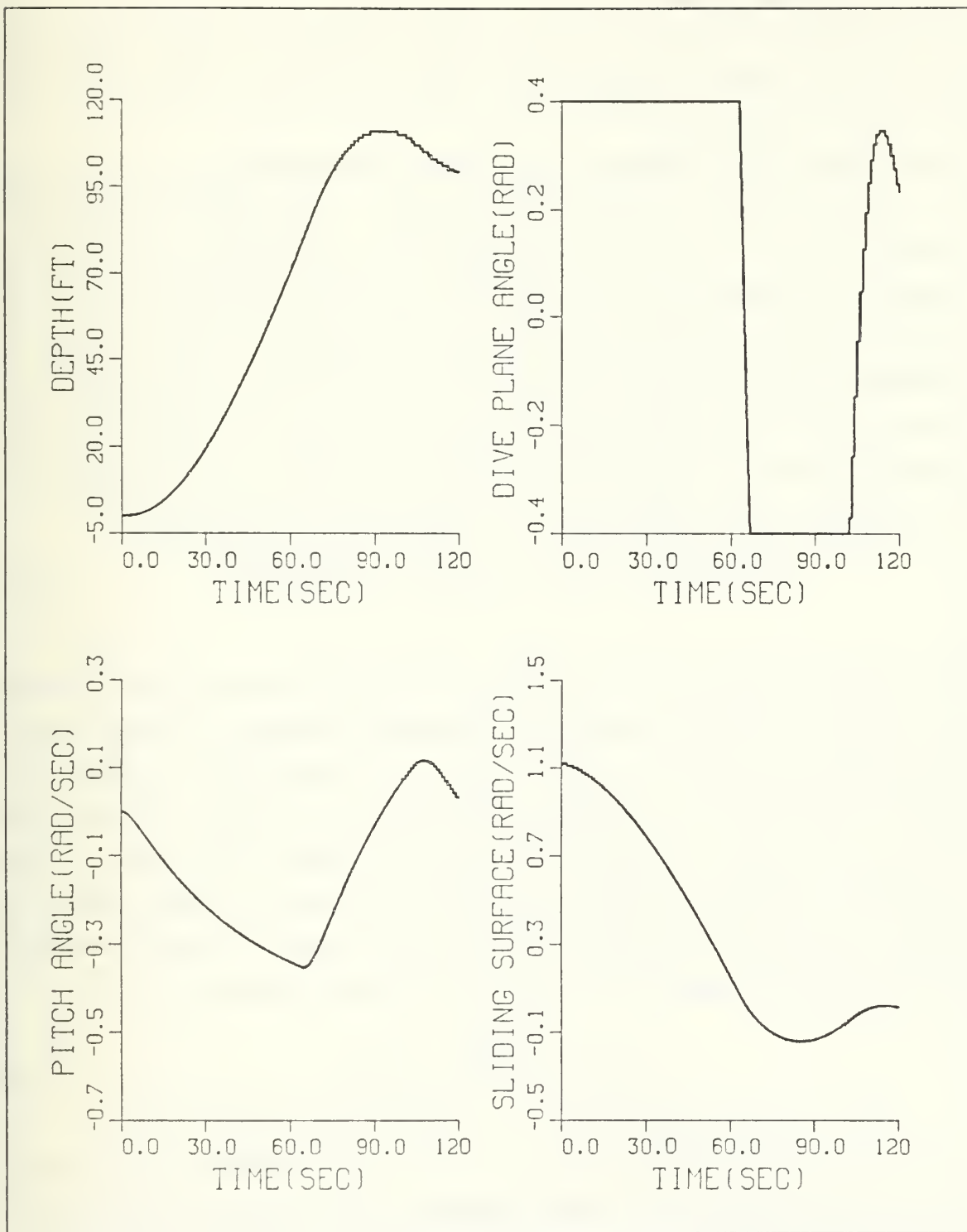
Figure 43.   The dynamic response of test 6 AUV (depth command = 100 ft)

2. Nonlinear Model

The siding mode compensator based on the nominal linear model is here applied to the highly nonlinear vehicle with modified hydrodynamic coefficients in order to estimate its robustness.

The hydrodynamic coefficients, which affect in the depth change maneuvering, are modified as Table 5 in the previous chapter. Although an unmodeled disturbance could be made up for using model based compensator, parameter mismatch was determined to be sensitive to the used method [Ref. 12]. This would reduce the robustness of the controller when confronted with the varying, uncontrolled condition found in the ocean enviroment. In this section, sliding mode compensator is used to investigate robustness for control of depth change maneuvering in the face of unmodeled nonlinear terms and parameter uncertainty. The nonlinear system dynamics for this purpose were described by

$$\dot{x} = Ax + \delta Ax + f(x) + [B + \delta B + g(x)]u \tag{4.17}$$

Since δA, δB, $f(x)$, and $g(x)$ are unknown values in the present system equation described above, they are assumed to be zero and η^2 is increased through numerical simulation in order to guarantee sliding mode control [Ref. 2]. The nominal control law (4.6) is used to simulate the response of all values (q, u, z, and s) both actual and estimated. The FORTRAN program "NSMC" was written in order to simulate numerical experiments provided in Appendix B. Note that in this section, a soft saturation function might be used to handle the highly nonlinear model within the boundary layer. The soft saturation function is

$$SAT = (\frac{\sigma(\hat{x})}{\phi}) \times abs\sigma(\hat{x}) \tag{4.18}$$

This saturation function produces soft inputs at approximately zero $\sigma(\hat{x})$ values. The dynamic response of the highly nonlinear AUV is shown in Figure 44 on page 87 through Figure 49 on page 92.
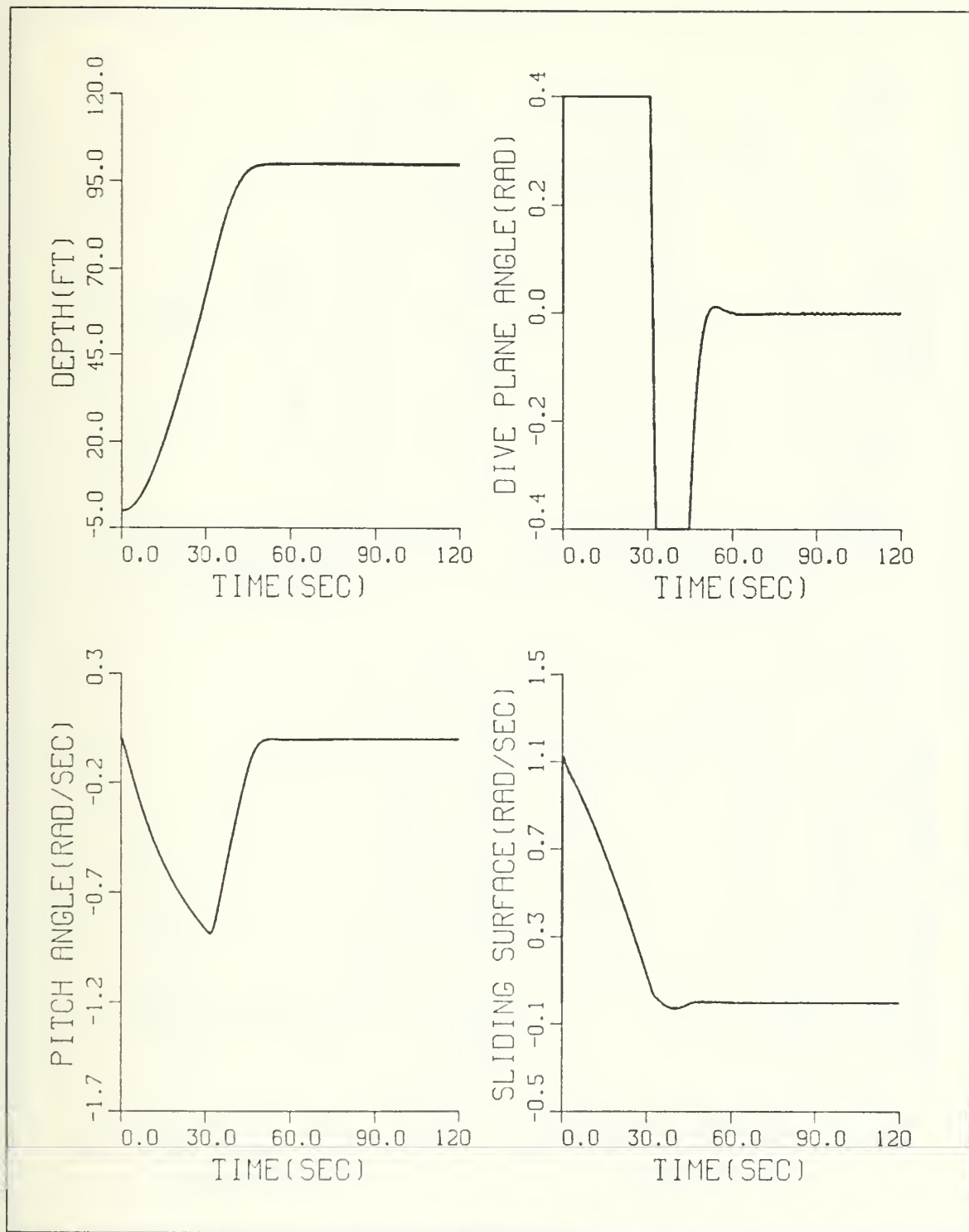
Figure 44. The dynamic response of nonlinear test 1 AUV
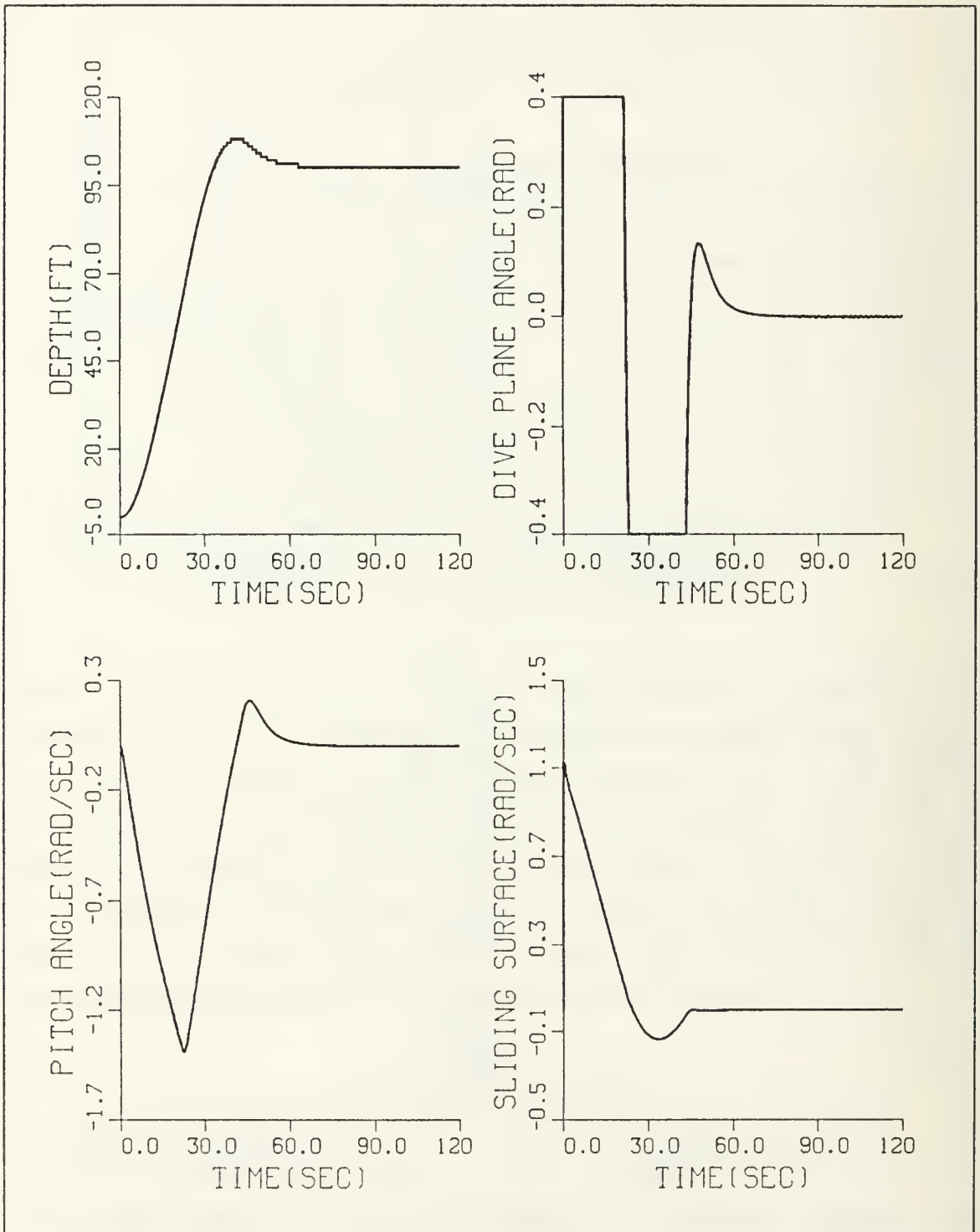
Figure 45.   The dynamic response of nonlinear test 2 AUV

88
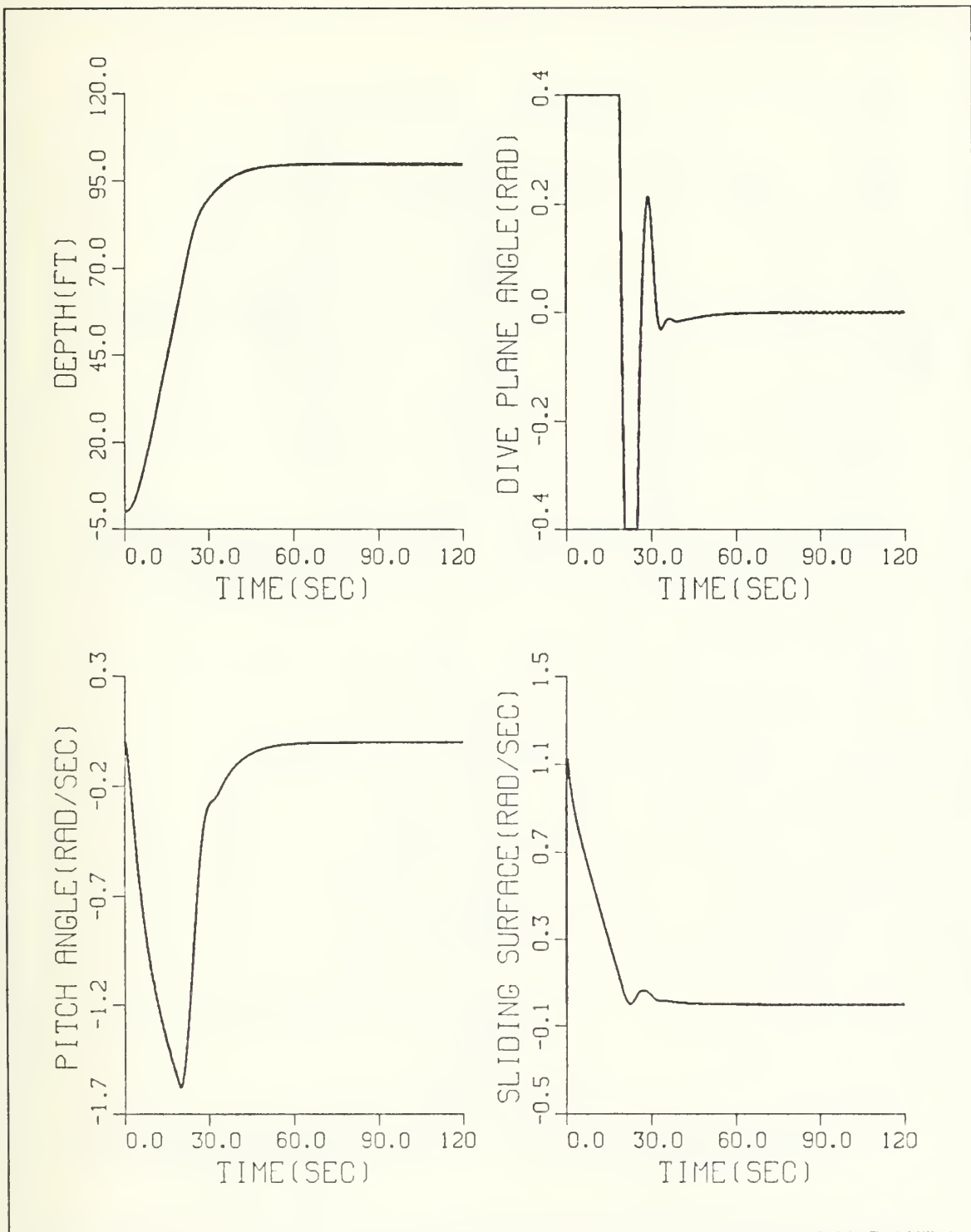
Figure 46. The dynamic response of nonlinear test 3 AUV
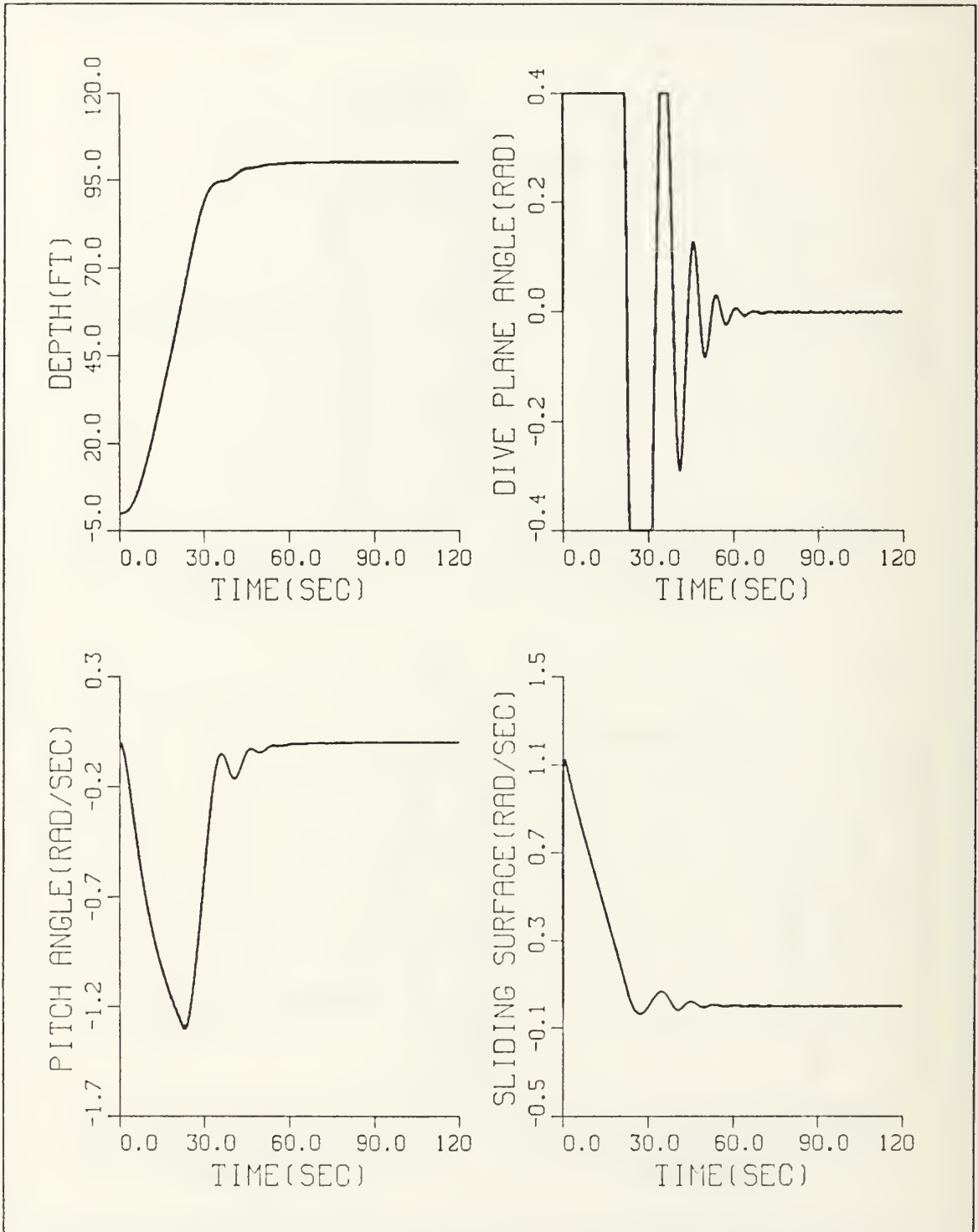
Figure 47.   The dynamic response of nonlinear test 4 AUV

90
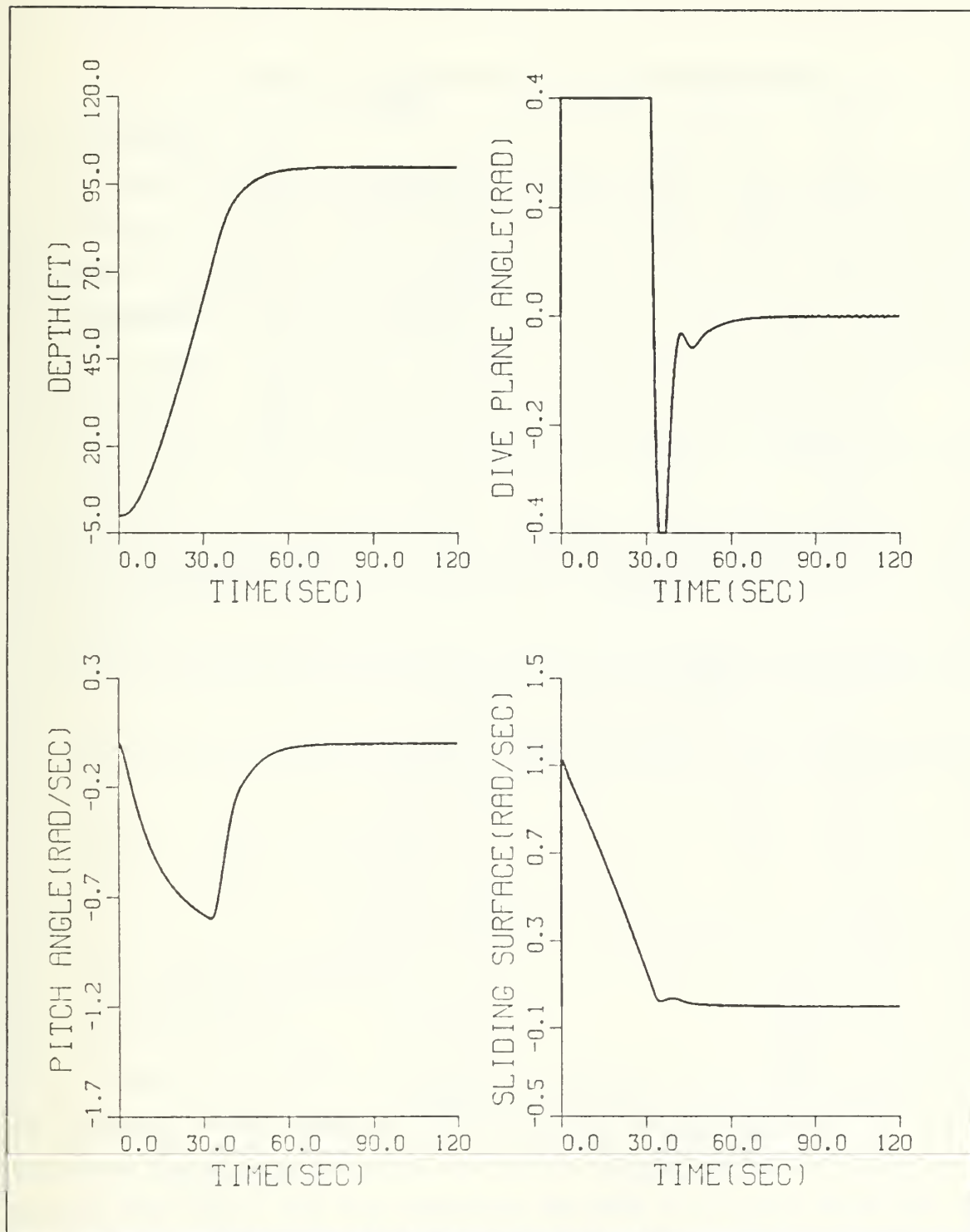
Figure 48. The dynamic response of nonlinear test 5 AUV
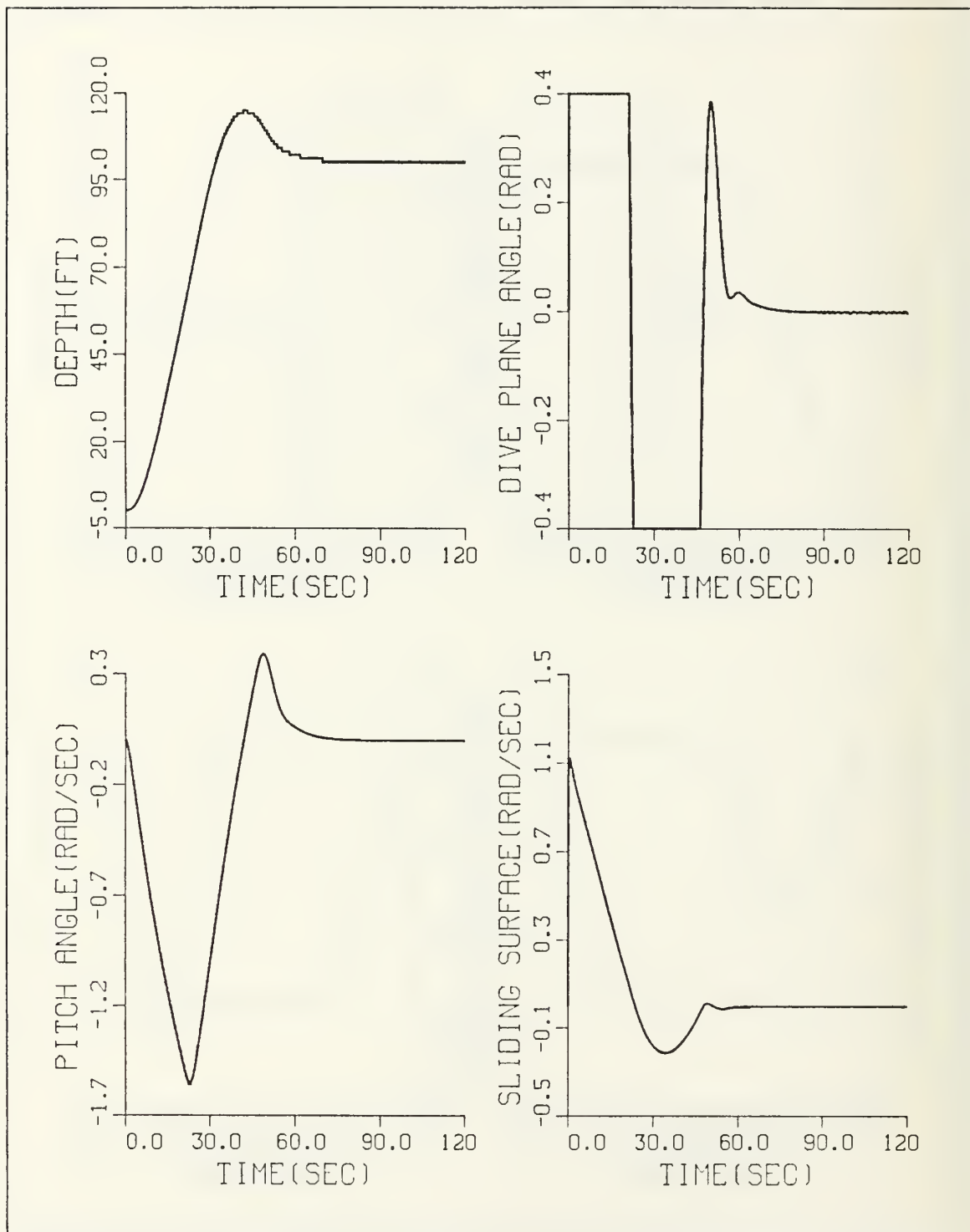
Figure 49. The dynamic response of nonlinear test 6 AUV

92

V. CONCLUSIONS AND RECOMMENDATIONS

A. SUMMARY

This thesis presented an application of variable structure systems for the robust control of linear and nonlinear systems in the presence of disturbances and parameter variations. The designed sliding mode compensator based on this methodology was successfully employed to provide a means for an unmanned underwater vehicle to control its depth under high nonlinearities. In this section, we summarize the sliding mode compensator design of the specified AUV:

1. The fully nonlinear equations of motion are linearized and simplified (as illustrated in section 3.C) in order to produce linear equations in the state space form.

2. The sliding surface, which provides desired dynamics of a closed-loop system, is designed by the standard pole placement method using the state space form.

3. The sliding mode control law, which consists of linear feedback and nonlinear switching feedback, can be obtained by satisfying the sliding condition.

4. Chattering due to piecewise discontinuous feedback is eliminated by replacing the switched control law at the sliding surface by continuous variations across a thin boundary layer neighboring the switching surface.

5. The nonlinear feedback gain (η^2) and boundary layer (ϕ) are optimized by a series of numerical experiments.

6. The state observer is designed using classical methods.

7. The sliding mode compensator is designed by combining the sliding mode control and state observer.

B. CONCLUSIONS

The objective of this work to design and analyze a sliding mode dive plane compensator for an autonomous underwater vehicle has been achieved. Realistic limitations due to pitch and pitch rate sensors non-availability were taken into account. The vehicle that was considered. the SDV is a typical AUV and its shape and characteristics greatly resemble the NPS vehicle.

The conclusions of this work are summarized below:

1. A procedure for computing the sliding plane was established. The procedure is very general and can be applied to a large class of linearized single input systems. Once the sliding plane coefficients have been determined, the switching feedback control law follows easily.

2. Chattering problems, characteristic of variable structure system, were reduced or eliminated by introducing a "boundary layer" in the switching logic, without violating the sliding condition.

3. Robustness of the design was demonstrated by a wide variation of parameters of the linear model. Similar robustness characteristics were established when a full order observer was incorporated in the design in order to provide estimates for pitch angle and pitch rate based on depth measurements only.

4. The control design that was based on a linear model was tested against the full nonlinear equations of motion. Numerical simulations demonstrated the ability of the design to handle unmodelled dynamics and variation of the hydrodynamic coefficients and geometric parameters of the vehicle.

5. A visual simulation using an IRIS graphics workstation was used [Ref. 13] in order to view the dynamic behavior of the AUV in real time under closed-loop sliding mode control. The vehicle response, Figure 50 on page 95, was seen to follow the predictions that were based on the linear model.

6. Finally, an experimental verification was attempted on the NPS protype vehicle with coefficients the same as the ones used in [Ref. 12]. A discrete-time sliding mode controller was designed based on 25 Hz sample rate with controller poles at $[0.9, 0.91, 1]$, observer poles at $[0.78, 0.79, 0.80]$, control law

$$u = -0.9\hat{q} - 1.789\hat{\theta} - 21.2976\eta^2 sign(\sigma)$$

$$\sigma = -0.3386\hat{q} - 1.6888\hat{\theta} + (z - z_{com}) \tag{5.1}$$

where $\eta^2 = 0.2$ and $\phi = 1.0$

The experimental results are shown in Figure 51 on page 96, where the commanded depth was 5 volts (1 ft corresponds to 3.1 volts).

The variable structure system was proven to be an attractive control system design method for autonomous underwater vehicles. The designed sliding mode compensator based on this methodology dealt with the dynamic problems of the underwater vehicle with sufficient accuracy.
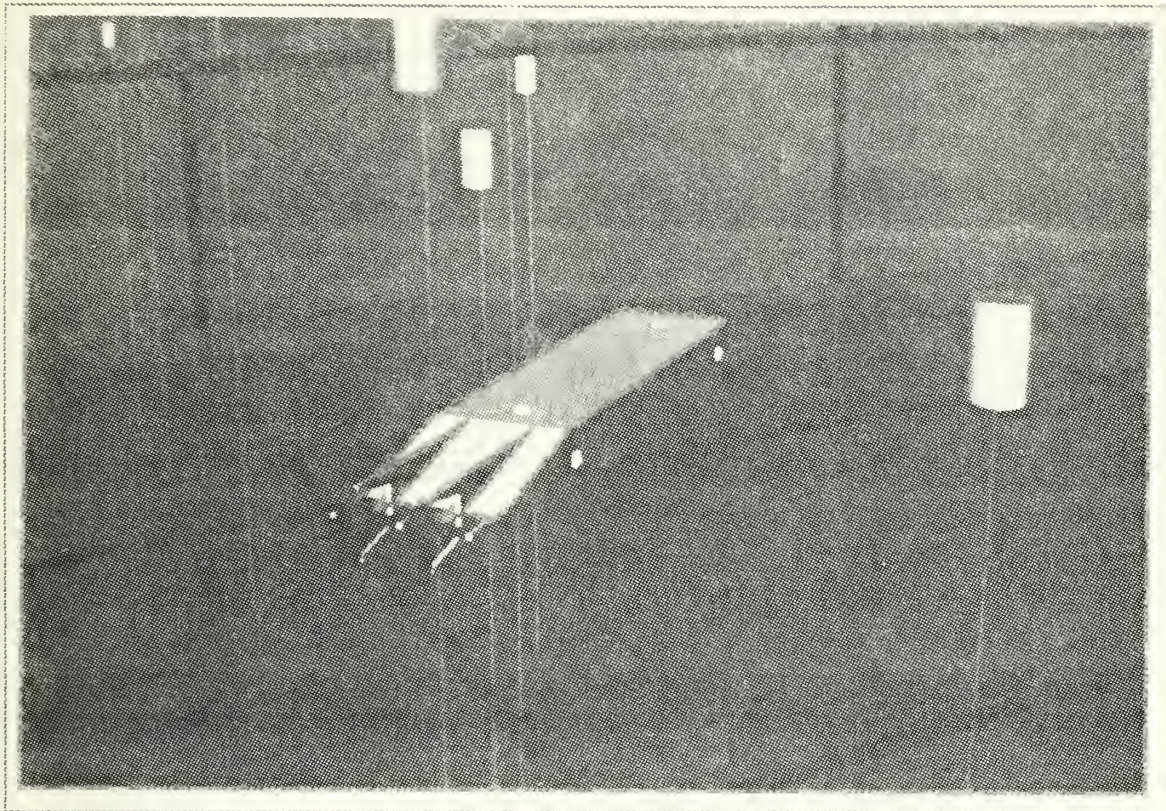
Figure 50. Graphic simulation display

C. RECOMMENDATIONS

Some suggestions for future research are as follows:

1. Design and analyze a nonlinear sliding mode compensator.

2. Evaluate the robustness characteristics of a digital (discrete time) sliding mode autopilot.

3. Extend the developed methodology in the problem of path following autopilots for the multiple input case under constant or random disturbance. Introduction of integral control action should help in this case to assure precise path tracking.
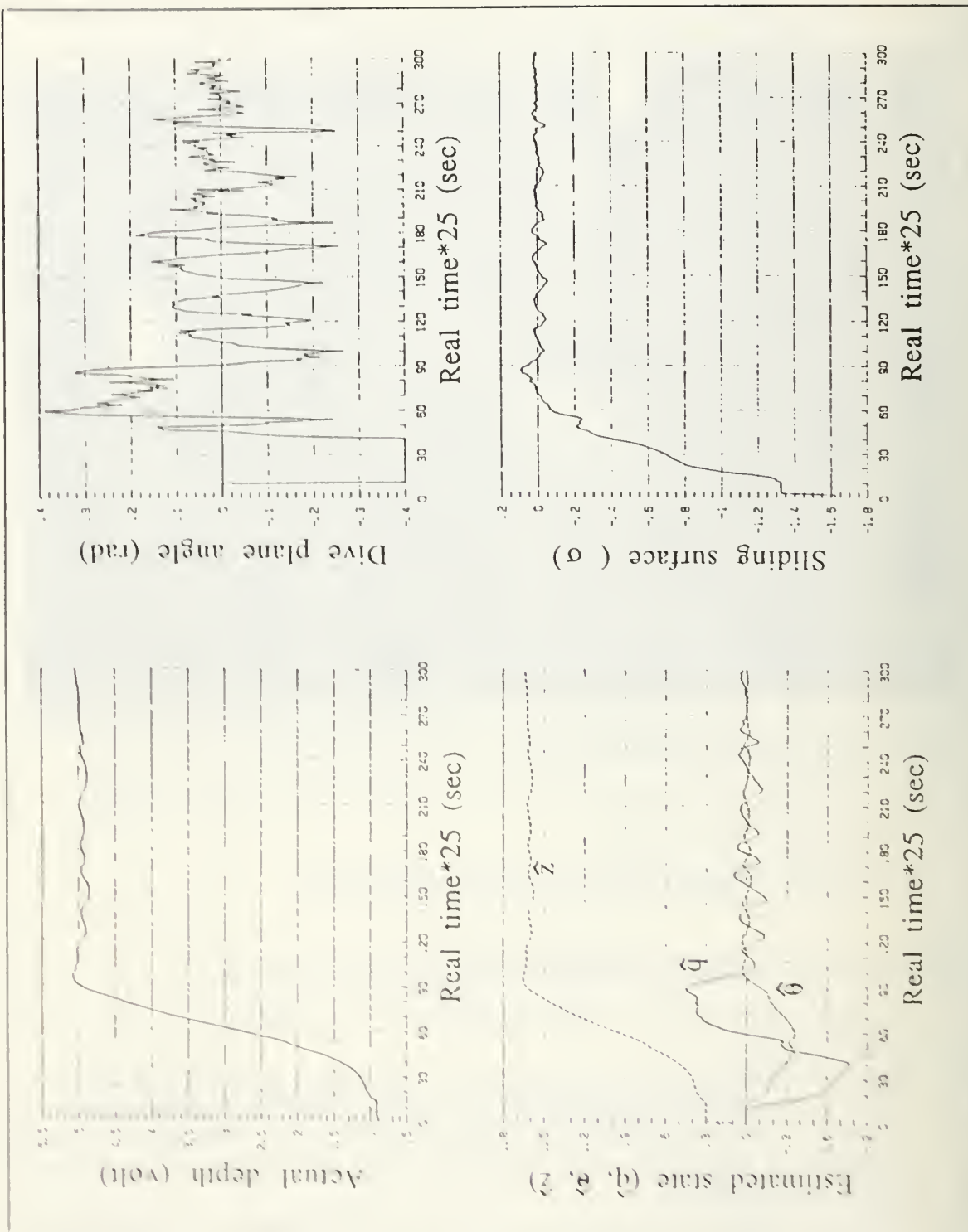
Figure 51. The experimental results of the sliding mode compensator

APPENDIX A. SIMULATION PROGRAM AND BLOCKDIAGRAM FOR LINEAR EQUATION

A. MATRIX-X(SMC) OF THE LINEAR EQUATION

```
****   MATRIX PROGRAM FOR SLIDING CONTROLLER   ***

UX=6;                           // FORWARD SPEED
CP1=0.25;                       // CLOSED LOOP POLE
CP2=0.27;                       // CLOSED LOOP POLE
S1=1.;                          // SLIDING SURFACE COEFFICIENT
S2=(CP1+CP2);                   // SLIDING SURFACE COEFFICIENT
S3=(CP1*CP2)/(-UX)              // SLIDING SURFACE COEFFICIENT
T=[0:0.1:150.]';
IETA =6.0;
GA3=-0.035;
GA4=-UX;
GA5=-0.7;
GA6=-0.03;
GA7=S2;
GA8=S3;
GA9=IETA;
GA10=1;
GA1=(GA6-S3*UX)/(-GA3);
GA2=(GA5+S2)/(-GA3);
INPUT(:,1)=100*ONES(T);
INPUT(:,2)=0.*ONES(T);
Y=SIM(T,INPUT);
PLOT(T,Y(:,1),'UPPER LEFT XLABEL/TIME(SEC)/ YLABEL/...
DEPTH RESPOSE/TITLE/   DEPTH COMMAND= 100 ,STANDARD AUV/')
PLOT(T,Y(:,2),'UPPER RIGHT XLABEL/TIME(SEC)/ YLABEL/ ...
PITCH ANGLE/TITLE/    CLOSED LOOP POLE=0.0,-0.35,-0.40/')
PLOT(T,Y(:,4),'LOWER LEFT XLABEL/TIME(SEC)/ YLABEL/ ...
DIVE PLANE ANGLE(radins)/TITLE/ SPEED=6/')
PLOT(T,Y(:,5),'LOWER RIGHT XLABEL/TIME(SEC)/YLABEL/ ...
SLIDING SURFACE/TITLE/ DIS=0.2, B, NLINEAR,IETA=6.0,PI=0.4/')
```

B. FORTRAN(SMC) OF THE LINEAR EQUATION

```
C              ****************************************************
C              *              LINEAR AUV MODEL                  *
C              *         SLIDING MODE CONTROL PROGRAM           *
C              *         DEPTH CONTROL IN DIVE PLANE            *
C              *       BY USING RUNGE-KUTTA FIFTH ORDER         *
C              ****************************************************
C
       REAL*8 TIME,QDOT, ZDOT, TDOT,THETA,ZPOS,Q,DS
       REAL*8 S, DE, UHAT, UBAR,PHI,SAT,EITA,COMZ
C      ********** INITIAL CONDITIONS **********
C

       TIME=0.0D0
       Q=0.0D0
       THETA=0.0D0
       ZPOS=0.0D0
C      ********** SLIDING MODE CONTROL PARAMETER ***********
       EITA=4.0D0
       DELT=0.02D0
       COMZ=100.0D0
       PHI=0.4D0
C      ******** SYSTEM PROGRAM ********
       WRITE (8,710)
       DO 100 I=0,6000
710    FORMAT (3X,'    TIME',5X,'    DEPTH ',6X,'      DIVE ',5X,'     PITCH
      *',5X,'      SLIDE')
C
       QDOT=-0.7D0*Q-0.03D0*THETA-0.035D0*DS
       TDOT=Q
       ZDOT=-12.0D0*THETA
C
       TIME=TIME+DELT
       Q=Q+DELT*QDOT
       THETA=THETA+DELT*TDOT
       ZPOS=ZPOS+DELT*ZDOT
       S=Q+0.52D0*THETA-0.0112D0*(ZPOS-COMZ)
       IF (ABS(S) .LT. PHI) SAT=(S/PHI)
       IF (S .LT. -PHI) SAT=-1.0D0
       IF (S .GT. PHI) SAT=1.0D0
       UHAT=-5.1429D0*Q+1.0714D0*THETA
       UBAR=EITA*SAT
       DE=UHAT+UBAR
       IF (DE .GE. 0.4D0) DS=0.4D0
       IF (DE .LE. -0.4D0) DS=-0.4D0
       IF ((DE .LT. 0.4D0) .AND. (DE .GT. -0.4D0)) DS=DE
       WRITE (8,720) TIME, ZPOS, DS, THETA, S
720    FORMAT (2X,E11.3,4X,E11.3,4X,E11.3,4X,E11.3,4X,E11.3)
100    CONTINUE
       STOP
       END
```

C. MATRIX-X(OBSERVER) OF THE LINEAR EQUATION

```
*** SIMULATION PROGRAM FOR SLIDING MODE COMPENSATOR ***


UX=6;                            // FORWARD SPEED
CP1=0.3                          // CLOSED LOOP POLE
CP2=0.40;                        // CLOSED LOOP POLE
S1=1.;                           // SLIDING SURFACE COEFFICIENT
S2=(CP1+CP2);                    // SLIDING SURFACE COEFFICIENT
S3=(CP1*CP2)/(-0.6);             // SLIDING SURFACE COEFFICIENT
EITA =6.0;
A=[-0.7,-0.03,0;1,0,0;0,-6,0];
B=[-0.035;0;0];
C=[0,0,1];
N=[C',A'*C',A'*A'*C'];
W=[1,0.7,0.03;0,1,0.7;0,0,1];
LA1=5.5;                         // DESIRE POLE OF OBSERVER
LA2=5.75;                        // DESIRE POLE OF OBSERVER
LA3=5.9;                         // DESIRE POLE OF OBSERVER
ABAR=[0.7;0.03;0];
AHAT=[LA1+LA2+LA3;LA1*LA2+LA2*LA3+LA1*LA3;LA1*LA2*LA3];
KC=INV((N*W)')*(AHAT-ABAR);
GA1=-1.4;
GA2=-0.06;
GA3=-2*UX;
GA4=KC(3,1);
GA5=KC(2,1);
GA6=KC(1,1);
GA7=-0.7;
GA8=-0.03;
GA9=-6;
GA10=-0.035;
GA16=-0.035;
GA11=0.75;
GA13=-0.0233;
GA14=(GA2-S3*UX)/(-GA10);
GA12=(GA7+S2)/(-GA10);
GA15=EITA;
T=[0:0.1:150.]';
INPUT(:,1)=100*ONES(T);
INPUT(:,2)=0.0*ONES(T);
Y=SIM(T,INPUT);
PLOT(T,[Y(:,1) Y(:,5)],'LINE STYLE 1 2 /UPPER LEFT XLABEL/
TIME(sec) / YLABEL/EST AND ACT DEPTH(ft)/')
PLOT(T,[Y(:,2) Y(:,4)],'LINE STYLE 1 2 /UPPER RIGHT XLABEL/
TIME(sec)/ YLABEL/EST AND ACT ANGLE(rad)/TITLE/  B, 2*A/')
PLOT(T,Y(:,3),'LOWER LEFT XLABEL/TIME(SEC)/ YLABEL/
DIVE PLANE ANGLE/TITLE/ S.F.C=1, 0.75, -0.0233, SPEED=6/')
PLOT(T,Y(:,6),'LOWER RIGHT XLABEL/TIME(SEC)/YLABEL/
SLIDING SURFACE/ TITLE/  SAT, DIS=0.2, IETA=6,PI=0.4/')
```

D. FORTRAN(OBSERVER) OF THE LINEAR EQUATION

```
C         ************************************************
C         *             LINEAR AUV MODEL                 *
C         *        SLIDING MODE CONTROL PROGRAM          *
C         *        DEPTH CONTROL IN DIVE PLANE           *
C         *            BY USING EULER-METHOD             *
C         ************************************************
C
      REAL*8 TIME,QDOT, ZDOT, TDOT,THETA,ZPOS,Q,DS
      REAL*8 S, DE, UHAT, UBAR,PHI,SAT,EITA,COMZ
      REAL*8 THADOT,QHADOT,ZHADOT,QHAT,THAT,ZHAT
C     ********** INITIAL CONDITIONS **********
C
      TIME=0.0D0
      Q=0.0D0
      THETA=0.0D0
      ZPOS=0.0D0
      QHADOT=0.0D0
      THADOT=0.0D0
      ZHADOT=0.0D0
      QHAT=0.0D0
      THAT=0.0D0
      ZHAT=0.0D0
C     ********** SLIDING MODE CONTROL PARAMETER ***********
      EITA=4.0D0
      DELT=0.02D0
      COMZ=100.0D0
      PHI=0.4D0
C     ******** SYSTEM PROGRAM ********
      WRITE (8,710)
      DO 100 I=0,6000
710   FORMAT (3X,'   TIME',5X,'   DEPTH ',6X,'      DIVE ',5X,'    PITCH
     *',5X,'     SLIDE')
C
      QDOT=-0.35D0*Q-0.015D0*THETA-0.0175D0*DS
      TDOT=0.5D0*Q
      ZDOT=-6.0D0*THETA
C
      TIME=TIME+DELT
      Q=Q+DELT*QDOT
      THETA=THETA+DELT*TDOT
      ZPOS=ZPOS+DELT*ZDOT
C     ********** SUBROUTINE OBSERVER **********
      CALL OBSER(QHADOT,THADOT,ZHADOT,QHAT,THAT,ZHAT,ZPOS,DELT)
C
C     ******** SLIDING MODE INPUT *********
C
      S=QHAT+0.52D0*THAT-0.0112D0*(ZHAT-COMZ)
      IF (ABS(S) .LT. PHI) SAT=(S/PHI)
      IF (S .LT. -PHI) SAT=-1.0D0
      IF (S .GT. PHI) SAT=1.0D0
      UHAT=-5.1429D0*QHAT+1.0714D0*THAT
```

```fortran
      UBAR=EITA*SAT
      DE=UHAT+UBAR
      IF (DE .GE.  0.4D0) DS=0.4D0
      IF (DE .LE.  -0.4D0) DS=-0.4D0
      IF ((DE .LT.  0.4D0) .AND. (DE .GT.  -0.4D0)) DS=DE
      WRITE (8,720) TIME, ZPOS, DS, THETA, S
720   FORMAT (2X,E11.3,4X,E11.3,4X,E11.3,4X,E11.3,4X,E11.3)
100   CONTINUE
      STOP
      END
C     ********** SUBROUTINE OBSER **********
C
      SUBROUTINE OBSER(QHADOT,THADOT,ZHADOT,QHAT,THAT,ZHAT,ZPOS,DELT)
      QHADOT=-0.7D0*QHAT-0.03D0*THAT-20.9293D0*(ZPOS-ZHAT)
      THADOT=QHAT-14.4092D0*(ZPOS-ZHAT)
      ZHADOT=-6.0D0*THAT+16.45D0*(ZPOS-ZHAT)

      QHAT=QHAT+DELT*QHADOT
      THAT=THAT+DELT*THADOT
      ZHAT=ZHAT+DELT*ZHADOT
      RETURN
      END
```

E. FORTRAN GRAPH

```
      DIMENSION TIME(6000),DEPTH(6000),DIVE(6000),PITCH(6000),
     *SLIDE(6000)
      REAL TIME,DEPTH,DIVE,PITCH,SLIDE
      DO 1 I=1,6000
    1 READ (8,*) TIME(I),DEPTH(I),DIVE(I),PITCH(I),SLIDE(I)
      CALL COMPRS

C ***** CREATES A DUMMY PLOT FOR POST PROCESSING******
      CALL NOBRDR
      CALL AREA2D(1.,1.)
      CALL GRAF(0.,1.,20.,0.,1.,10)
      CALL ENDPL(0)

C ***** PLOT COMMAND DEPTH *****
      CALL PAGE(3.,4.)
      CALL NOBRDR
      CALL AREA2D(2.3,3.0)
      CALL XNAME('TIME(SEC)$',100)
      CALL YNAME('COMMAND DEPTH(FT)$',100)
      CALL THKFRM(0.03)
      CALL GRAF(0.,30.0,120.,-5.0,25.0,120.0)
      CALL THKCRV(0.02)
      CALL CURVE(TIME,DEPTH,6000,0)
      CALL ENDPL(0)

C ***** PLOT DIVE PLANE ANGLE *****
      CALL PAGE(3.,4.)
      CALL NOBRDR
      CALL AREA2D(2.3,3.0)
      CALL XNAME('TIME(SEC)$',100)
      CALL YNAME('DIVE PLANE ANGLE(RAD)$',100)
      CALL THKFRM(0.03)
      CALL GRAF(0.,30.0,120.,-.4,.2,.4)
      CALL THKCRV(0.02)
      CALL CURVE(TIME,DIVE,6000,0)
      CALL ENDPL(0)

C ***** PLOT PITCH ANGLE ******
      CALL PAGE(3.,4.)
      CALL NOBRDR
      CALL AREA2D(2.3,3.0)
      CALL XNAME('TIME(SEC)$',100)
      CALL YNAME('PITCH ANGLE(RAD/SEC)$',100)
      CALL THKFRM(0.03)
      CALL GRAF(0.,30.0,120.,-1.0,0.3,0.2)
      CALL THKCRV(0.02)
      CALL CURVE(TIME,PITCH,6000,0)
      CALL ENDPL(0)

C ***** PLOT SLIDING SURFACE *****
      CALL PAGE(3.,4.)
      CALL NOBRDR
      CALL AREA2D(2.3,3.0)
      CALL XNAME('TIME(SEC)$',100)
      CALL YNAME('SLIDING SURFACE(RAD/SEC)$',100)
```

```
CALL THKFRM(0.03)
CALL GRAF(0.,30.0,120.,-0.5,0.5,1.5)
CALL THKCRV(0.02)
CALL CURVE(TIME,SLIDE,6000,0)
CALL ENDPL(0)

CALL DONEPL
STOP
END
```
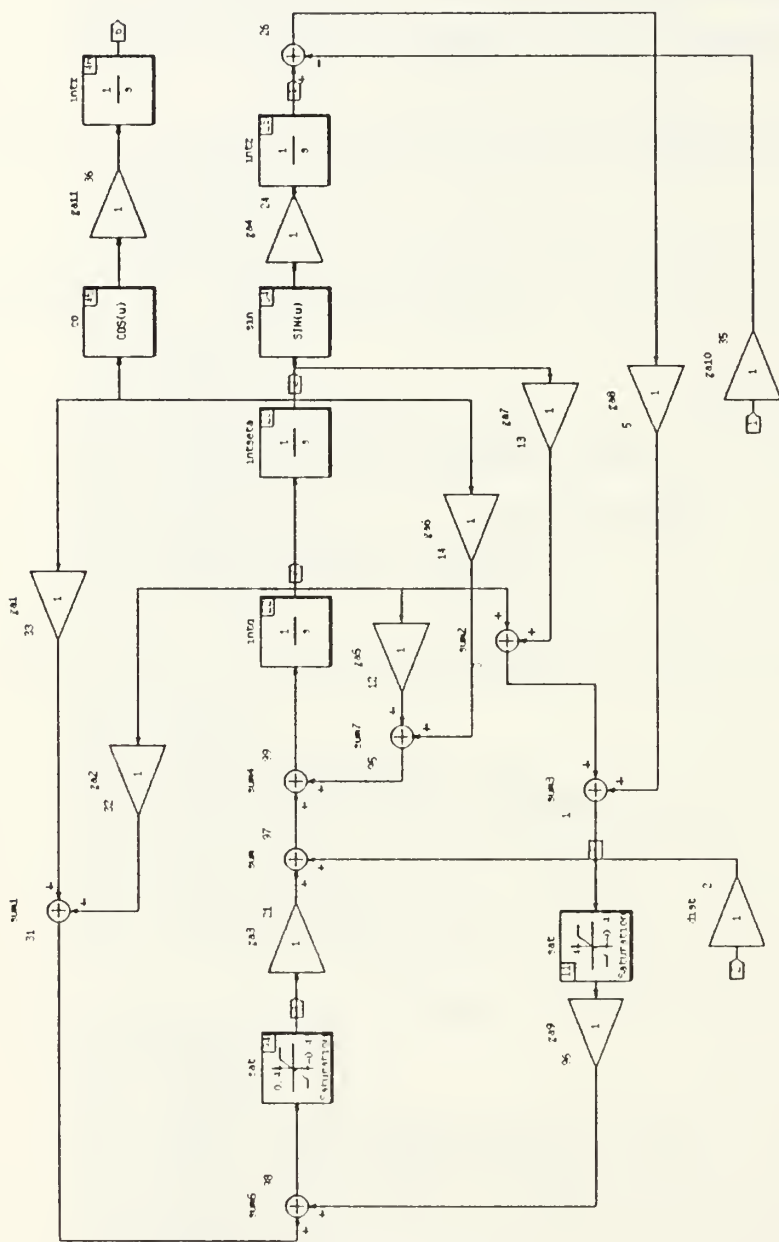
Figure 52. The block diagram of the SMC simulation
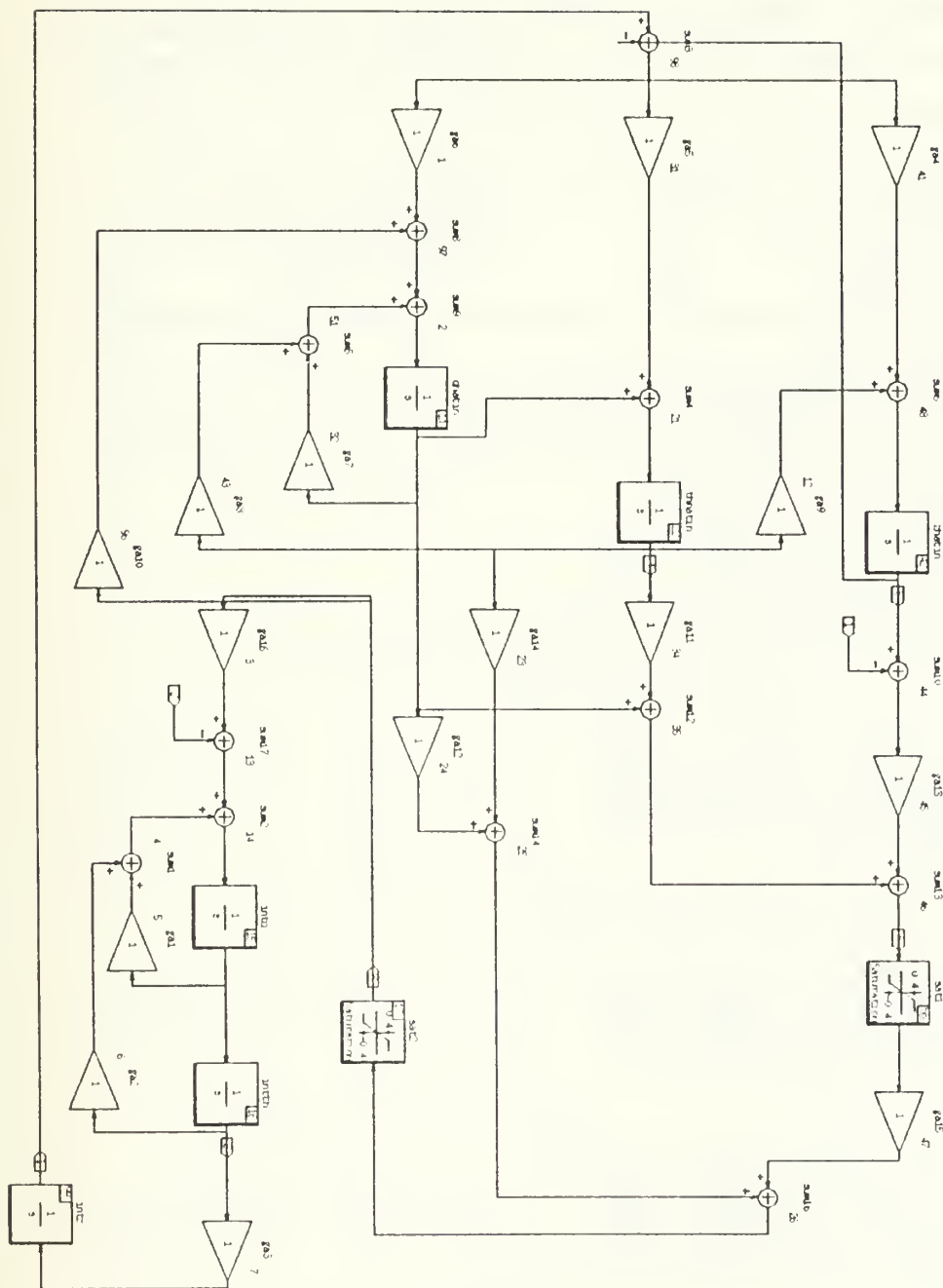
Figure 53. The block diagram of the SMO simulation

APPENDIX B. SIMULATION PROGRAM FOR NONLINEAR AUV

```
************************************************************************
*                                                                    *
*     NONLINEAR AUV MODEL / STERN PLANE AND BOW PLANE SEPARATED       *
*                                                                    *
*     VARIABLE DECLARATION 11        ** INPUTS **            248      *
*     CONSTANTS             70          PROPULSION MODEL     271      *
*     INITIAL CONDITIONS    128      ** OUTPUTS **           423      *
*     MASS MATRIX           206          INTEGRATION                  *
*     INVERT MATRIX         245                                       *
************************************************************************
      REAL AW(82,82)
      REAL MASS,LATYAW,NORPIT
      REAL MM(6,6),G4(4),GK4(4),BR(4),HH(4)
      REAL  B(6,6),BB(6,6)
      REAL A(12,12), AA(12,12)
      REAL XPP ,XQQ ,XRR ,XPR
      REAL XUDOT ,XWQ ,XVP ,XVR
      REAL XQDS ,XQDB ,XRDR  ,XVV
      REAL XWW  ,XVDR ,XWDS ,XWDB
      REAL XDSDS,XDBDB ,XDRDR ,XQDSN
      REAL XWDSN ,XDSDSN
      REAL TIME,S,EITA,UBAR,UHAT,COMZ,BAR,SIM,DE,SAT

      LATERAL HYDRODYNAMIC COEFFICIENTS

      REAL YPDOT ,YRDOT,YPQ   ,YQR
      REAL YVDOT ,YP    ,YR    ,YVQ
      REAL YWP   ,YWR ,YV ,YVW
      REAL YDR   ,CDY

      NORMAL HYDRODYNAMIC COEFFICIENTS

      REAL ZQDOT ,ZPP,ZPR ,ZRR
      REAL ZWDOT ,ZQ   ,ZVP    ,ZVR
      REAL ZW  ,ZVV    ,ZDS   ,ZDB
      REAL ZQN ,ZWN   ,ZDSN ,CDZ
      REAL ZHADOT,ZHAT

      ROLL HYDRODYNAMIC COEFFICIENTS

      REAL KPDOT ,KRDOT ,KPQ ,KQR
      REAL KVDOT , KP   ,KR      ,KVQ
      REAL KWP   , KWR   ,KV      ,KVW
      REAL KPN    , KDB

      PITCH HYDRODYNAMIC COEFFICIENTS

      REAL MQDOT ,MPP   ,MPR,MRR
      REAL MWDOT , MQ  ,MVP      ,MVR
      REAL MW  , MVV   ,MDS  ,MDB
      REAL MQN , MWN  ,MDSN
```

```
      REAL QHADOT,QHAT,THADOT,THAT

      YAW HYDRODYNAMIC COEFFICIENTS

      REAL NPDOT,NRDOT,NPQ ,NQR
      REAL NVDOT  , NP    ,NR      ,NVQ
      REAL NWP   , NWR  ,NV   ,NVW
      REAL NDR

      MASS CHARACTERISTICS OF THE FLOODED VEHICLE

      REAL  WEIGHT , BOY  ,VOL ,XG
      REAL YG  , ZG  ,XB    ,ZB
      REAL IX  , IY  ,IZ    ,IXZ
      REAL IYZ  , IXY     ,YB
      REAL L  , RHO ,G     ,NU
      REAL A0   ,KPROP ,NPROP ,    X1TEST
      REAL DEGRUD  ,DEGSTN
      COMMON /BLOCK1/ F(12), FP(6), XMMINV(6,6), UCF(4)
      INTEGER N,IA,IDGT,IER,LAST,J,K,M,JJ,KK,I
      REAL   WKAREA(54), X(12)

      RUDDER COEFFICIENTS

      PARAMETER ( DSMAX= -0.175)

      LONGITUDINAL HYDRODYNAMIC COEFFICIENTS

      PARAMETER(XPP = 7.E-3  ,XQQ = -1.5E-2 ,XRR = 4.E-3  ,XPR =7.5E-4,
     & XUDOT=-7.6E-3  ,XWQ = -2.E-1    ,XVP = -3.E-3   ,XVR = 2.E-2,
     & XQDS=2.5E-2    ,XQDB=-2.6E-3   ,XRDR= -1.E-3   ,XVV =5.3E-2,
     & XWW =1.7E-1    ,XVDR=1.7E-3    ,XWDS=4.6E-2    ,XWDB= 1.E-2,
     & XDSDS= -1.E-2  ,XDBDB= -8.E-3   ,XDRDR= -1.E-2  ,XQDSN= 2.E-3,
     & XWDSN=3.5E-3   ,XDSDSN= -1.6E-3 )

      LATERAL HYDRODYNAMIC COEFFICIENTS

      PARAMETER(YPDOT=1.2E-4 ,YRDOT=1.2E-3  ,YPQ = 4.E-3 ,YQR =-6.5E-3,
     & YVDOT=-5.5E-2  ,YP  = 3.E-3      ,YR = 3.E-2     ,YVQ =2.4E-2,
     & YWP =2.3E-1    ,YWR =-1.9E-2     ,YV = -1.E-1    ,YVW =6.8E-2,
     & YDR =2.7E-2    ,CDY =3.5E-1)

      NORMAL HYDRODYNAMIC COEFFICIENTS

      PARAMETER(ZQDOT=-6.8E-3 ,ZPP =1.3E-4  ,ZPR =6.7E-3  ,ZRR =-7.4E-3,
     & ZWDOT=-2.4E-1 ,ZQ =-1.4E-1     ,ZVP =-4.8E-2    ,ZVR =4.5E-2,
     & ZW =  -3.E-1   ,ZVV =-6.8E-2     ,ZDS =-7.3E-2    ,ZDB =-2.6E-2,
     & ZQN =-2.9E-3   ,ZWN =-5.1E-3     ,ZDSN= -1.E-2    ,CDZ = 1.0)

      ROLL HYDRODYNAMIC COEFFICIENTS

      PARAMETER(KPDOT= -1.E-3 ,KRDOT=-3.4E-5 ,KPQ =-6.9E-5 ,KQR =1.7E-2,
     & KVDOT=1.3E-4    , KP =-1.1E-2     ,KR =-8.4E-4     ,KVQ=-5.1E-3,
     & KWP =-1.3E-4    , KWR =1.4E-2     ,KV =3.1E-3       ,KVW =-1.9E-1,
     & KPN =-5.7E-4   , KDB = 0.0  )
```

PITCH HYDRODYNAMIC COEFFICIENTS

```
 PARAMETER(MQDOT=-1.7E-2    ,MPP =5.3E-5,MPR = 5.E-3,MRR =-2.9E-3,
& MWDOT=-6.8E-3  , MQ =-6.8E-2     ,MVP =1.2E-3    ,MVR =1.7E-2,
& MW = 1.E-1     , MVV =-2.6E-2    ,MDS =-4.1E-2   ,MDB =6.9E-3,
& MQN =-1.6E-3   , MWN =-2.9E-3    ,MDSN =-5.2E-3)
```

YAW HYDRODYNAMIC COEFFICIENTS

```
 PARAMETER(NPDOT=-3.4E-5 ,NRDOT=-3.4E-3,NPQ =-2.1E-2 ,NQR =2.7E-3,
& NVDOT=1.2E-3   , NP =-8.4E-4     ,NR =-1.6E-2     ,NVQ = -1.E-2,
& NWP =-1.7E-2   , NWR =7.4E-3     ,NV =-7.4E-3     ,NVW =-2.7E-2,
& NDR =-1.3E-2)
```

MASS CHARACTERISTICS OF THE FLOODED VEHICLE

```
 PARAMETER( WEIGHT =12000., BOY =12000. ,VOL =200. ,XG = 0.   ,
& YG = 0.0       , ZG = 0.2        ,XB = 0.         ,ZB =  0.0 ,
& IX = 1500.     , IY = 10000.     ,IZ = 10000.     ,IXZ = -10.  ,
& IYZ = -10.     , IXY = -10.      ,YB =  0.0 ,
& L = 17.4       , RHO = 1.94      ,G = 32.2        ,NU = 8.47E-4 ,
& A0 = 2.0       ,KPROP = 0.       ,NPROP = 0.  ,   X1TEST= 0.1 ,
& DEGRUD= 0.0    ,DEGSTN=  0.0)
```

INPUT INITIAL CONDITIONS HERE IF REQUIRED

```
 U0 = 12.0
 V0 = 0.0
 W0 = 0.0
 P0 = 0.0
 Q0 = 0.0
 R0 = 0.0
 PHI0 = 0.0
 THETA0 = 0.0
 PSI0 = 0.0
 XPOS0=0.0
 YPOS0=0.0
 ZPOS0=0.0
 DB= 0.0
 DS = 0.0
 DR = 0.0
 RPM = 1000.0
 LATYAW = 0.0
 NORPIT = 0.0
 RE = U0*L/NU

 U = U0
 V = V0
 W = W0
 P = P0
 Q = Q0
 R = R0
 XPOS = XPOS0
 YPOS = YPOS0
 ZPOS = ZPOS0
 PSI = PHI0
```

```
      THETA = THETA0
      PHI = PHI0
      QHADOT=0.0
      THADOT=0.0
      ZHADOT=0.0
      QHAT=0.0
      THAT=0.0
      ZHAT=0.0

      DEFINE LENGTH FRACTIONS FOR GAUSS QUADRATURE TERMS

      G4(1) = 0.069431844
      G4(2) = 0.330009478
      G4(3) = 0.669990521
      G4(4) = 0.930568155

      DEFINE WEIGHT FRACTIONS FOR GAUSS QUADRATURE TERMS

      GK4(1) = 0.1739274225687
      GK4(2) = 0.3260725774312
      GK4(3) = 0.3260725774312
      GK4(4) = 0.1739274225687

      DEFINE THE BREADTH BB AND HEIGHT HH TERMS FOR THE INTEGRATION

      BR(1) = 75.7/12
      BR(2) = 75.7/12
      BR(3) = 75.7/12
      BR(4) = 55.08/12

      HH(1) = 16.38/12
      HH(2) = 31.85/12
      HH(3) = 31.85/12
      HH(4) = 23.76/12

      MASS = WEIGHT/G



      N = 6
      DO 15 J = 1,N
         DO 10 K = 1,N
         XMM1NV(J,K) = 0.0
         MM(J,K) = 0.0
10         CONTINUE
15      CONTINUE




      MM(1,1) = MASS -((RHO/2)*(L**3)*XUDOT)
      MM(1,5) = MASS*ZG
      MM(1,6) = -MASS*YG
```

```
      MM(2,2) = MASS -((RHO/2)*(L**3)*YVDOT)
      MM(2,4) = -MASS*ZG -((RHO/2)*(L**4)*YPDOT)
      MM(2,6) = MASS*XG - ((RHO/2)*(L**4)*YRDOT)

      MM(3,3) = MASS - ((RHO/2)*(L**3)*ZWDOT)
      MM(3,4) = MASS*YG
      MM(3,5) = -MASS*XG -((RHO/2)*(L**4)*ZQDOT)

      MM(4,2) = -MASS*ZG - ((RHO/2)*(L**4)*KVDOT)
      MM(4,3) = MASS*YG
      MM(4,4) = IX - ((RHO/2)*(L**5)*KPDOT)
      MM(4,5) = -IXY
      MM(4,6) = -IXZ -((RHO/2)*(L**5)*KRDOT)

      MM(5,1) = MASS*ZG
      MM(5,3) = -MASS*XG -((RHO/2)*(L**4)*MWDOT)
      MM(5,4) = -IXY
      MM(5,5) = IY -((RHO/2)*(L**5)*MQDOT)
      MM(5,6) = -IYZ

      MM(6,1) = -MASS*YG
      MM(6,2) = MASS*XG -((RHO/2)*(L**4)*NVDOT)
      MM(6,4) = -IXZ - ((RHO/2)*(L**5)*NPDOT)
      MM(6,5) = -IYZ
      MM(6,6) = IZ - ((RHO/2)*(L**5)*NRDOT)


      LAST = N*N+3*N
      DO 20 M = 1,LAST
      WKAREA(M) = 0.0
20       CONTINUE

      IER = 0
      IA = 6
      IDGT = 4
      CALL LINV2F(MM,N,IA,XMMINV,IDGT,WKAREA,IER)


         ************        INPUTS        **************

      RUDDER AND DIVE PLANE COMMANDS

      DELT=0.1
      SIM= 800.0
      TIME= 0.0
      DS= 0.0
      DR= 0.0
      DB= 0.0
      RPM=1000.0
      EITA=6.0
      COMZ=100.0
      BAR=0.4
c SIZE OF OUTPUT DATA ARRAY FOR PLOTTING
c    NUMOUT=6
c    NUMPNT=4
c    WRITE (8,711) NUMPNT,NUMOUT
```

```fortran
      WRITE (8,710)
711   FORMAT (2I4)
      DO 100 I=1,SIM
C
C
C
C      PROPULSION MODEL
C
C
      SIGNU = 1.0
      IF (U.LT.0.0) SIGNU = -1.0
      IF (ABS(U).LT.X1TEST) U = X1TEST
      SIGNN = 1.0
      IF (RPM.LT.0.0) SIGNN = -1.0
      ETA = 0.012*RPM/U
      RE = U*L/NU
      CD0 =  .00385 + (1.296E-17)*(RE - 1.2E7)**2
      CT  = 0.008*L**2*ETA*ABS(ETA)/(A0)
      CT1 = 0.008*L**2/(A0)
      EPS = -1.0+SIGNN/SIGNU*(SQRT(CT+1.0)-1.0)/(SQRT(CT1+1.0)-1.0)
      XPROP = CD0*(ETA*ABS(ETA) - 1.0)



      CALCULATE THE DRAG FORCE, INTEGRATE THE DRAG OVER THE VEHICLE
      INTEGRATE USING A 4 TERM GAUSS QUADUTURE


      LATYAW = 0.0
      NORPIT = 0.0
      DO 500 K = 1,4
         UCF(K) = SQRT((V+G4(K)*R*L)**2 + (W-G4(K)*Q*L)**2)
         IF(UCF(K).GT.1E-10) THEN
         TERM0  = (RHO/2)*(CDY*HH(K)*(V+G4(K)*R*L)**2 +
     &           CDZ*BR(K)*(W-G4(K)*Q*L)**2)
         TERM1  = TERM0*(V+G4(K)*R*L)/UCF(K)
         TERM2  = TERM0*(W-G4(K)*Q*L)/UCF(K)
         LATYAW = LATYAW + TERM1*GK4(K)*L
         NORPIT = NORPIT + TERM2*GK4(K)*L
         END IF
500   CONTINUE
C
C      FORCE EQUATIONS
C
C
C      LONGITUDINAL FORCE
C
      FP(1) = MASS*V*R - MASS*W*Q + MASS*XG*Q**2 + MASS*XG*R**2-
     &        MASS*YG*P*Q - MASS*ZG*P*R + (RHO/2)*L**4*(XPP*P**2 +
     &        XQQ*Q**2 + XRR*R**2 + XPR*P*R) +(RHO/2)*L**3*(XWQ*W*Q +
     &        XVP*V*P+XVR*V*R+U*Q*(XQDS*DS+XQDB*DB)+XRDR*U*R*DR)+
     &        (RHO/2)*L**2*(XVV*V**2 + XWW*W**2 + XVDR*U*V*DR + U*W*
     &        (XWDS*DS+XWDB*DB)+U**2*(XDSDS*DS**2+XDBDB*DB**2+
     &        XDRDR*DR**2))-(WEIGHT -BOY)*SIN(THETA) +(RHO/2)*L**3*
     &        XQDSN*U*Q*DS*EPS+(RHO/2)*L**2*(XWDSN*U*W*DS+XDSDSN*U**2*
     &        DS**2)*EPS +(RHO/2)*L**2*U**2*XPROP
```

111

C

LATERAL FORCE

```
   FP(2) = -MASS*U*R - MASS*XG*P*Q + MASS*YG*R**2 - MASS*ZG*Q*R +
  &        (RHO/2)*L**4*(YPQ*P*Q + YQR*Q*R)+(RHO/2)*L**3*(YP*U*P +
  &        YR*U*R + YVQ*V*Q + YWP*W*P + YWR*W*R) + (RHO/2)*L**2*
  &        (YV*U*V + YVW*V*W +YDR*U**2*DR) -LATYAW +(WEIGHT-BOY)*
  &        COS(THETA)*SIN(PHI)+MASS*W*P+MASS*YG*P**2
```

NORMAL FORCE

```
   FP(3) = MASS*U*Q - MASS*V*P - MASS*XG*P*R - MASS*YG*Q*R +
  &        MASS*ZG*P**2 + MASS*ZG*Q**2 + (RHO/2)*L**4*(ZPP*P**2 +
  &        ZPR*P*R + ZRR*R**2) + (RHO/2)*L**3*(ZQ*U*Q + ZVP*V*P +
  &        ZVR*V*R) +(RHO/2)*L**2*(ZW*U*W + ZVV*V**2 + U**2*(ZDS*
  &        DS+ZDB*DB))-NORPIT+(WEIGHT-BOY)*COS(THETA)*COS(PHI)+
  &        (RHO/2)*L**3*ZQN*U*Q*EPS +(RHO/2)*L**2*(ZWN*U*W +ZDSN*
  &        U**2*DS)*EPS
```

ROLL FORCE

```
   FP(4) = -IZ*Q*R +IY*Q*R -IXY*P*R +IYZ*Q**2 -IYZ*R**2 +IXZ*P*Q +
  &        MASS*YG*U*Q -MASS*YG*V*P -MASS*ZG*W*P+(RHO/2)*L**5*(KPQ*
  &        P*Q + KQR*Q*R) +(RHO/2)*L**4*(KP*U*P +KR*U*R + KVQ*V*Q +
  &        KWP*W*P + KWR*W*R) +(RHO/2)*L**3*(KV*U*V + KVW*V*W) +
  &        (YG*WEIGHT - YB*BOY)*COS(THETA)*COS(PHI) - (ZG*WEIGHT -
  &        ZB*BOY)*COS(THETA)*SIN(PHI) + (RHO/2)*L**4*KPN*U*P*EPS+
  &        (RHO/2)*L**3*U**2*KPROP +MASS*ZG*U*R
```

PITCH FORCE

```
   FP(5) = -IX*P*R +IZ*P*R +IXY*Q*R -IYZ*P*Q -IXZ*P**2 +IXZ*R**2 -
  &        MASS*XG*U*Q + MASS*XG*V*P + MASS*ZG*V*R - MASS*ZG*W*Q +
  &        (RHO/2)*L**5*(MPP*P**2 +MPR*P*R +MRR*R**2)+(RHO/2)*L**4*
  &        (MQ*U*Q + MVP*V*P + MVR*V*R) + (RHO/2)*L**3*(MW*U*W +
  &        MVV*V**2+U**2*(MDS*DS+MDB*DB))+ NORPIT -(XG*WEIGHT-
  &        XB*BOY)*COS(THETA)*COS(PHI)+(RHO/2)*L**4*MQN*U*Q*EPS +
  &        (RHO/2)*L**3*(MWN*U*W+MDSN*U**2*DS)*EPS-
  &        (ZG*WEIGHT-ZB*BOY)*SIN(THETA)
```

YAW FORCE

```
   FP(6) = -IY*P*Q +IX*P*Q +IXY*P**2 -IXY*Q**2 +IYZ*P*R -IXZ*Q*R -
  &        MASS*XG*U*R + MASS*XG*W*P - MASS*YG*V*R + MASS*YG*W*Q +
  &        (RHO/2)*L**5*(NPQ*P*Q + NQR*Q*R) +(RHO/2)*L**4*(NP*U*P+
  &        NR*U*R + NVQ*V*Q +NWP*W*P + NWR*W*R) +(RHO/2)*L**3*(NV*
  &        U*V + NVW*V*W + NDR*U**2*DR) - LATYAW + (XG*WEIGHT -
  &        XB*BOY)*COS(THETA)*SIN(PHI)+(YG*WEIGHT)*SIN(THETA)
  &        +(RHO/2)*L**3*U**2*NPROP-YB*BOY*SIN(THETA)
```

NOW COMPUTE THE F(1-6) FUNCTIONS

```
   DO 600 J = 1,6
          F(J) = 0.0
   DO 600 K = 1,6
```

112

```
              F(J) = XMMINV(J,K)*FP(K) + F(J)
600     CONTINUE

      THE LAST SIX EQUATIONS COME FROM THE KINEMATIC RELATIONS

      FIRST SET THE DRIFT CURRENT VALUES

      UCO = 0.0
      VCO = 0.0
      WCO = 0.0

      INERTIAL POSITION RATES F(7-9)

      F(7) = UCO + U*COS(PSI)*COS(THETA) + V*(COS(PSI)*SIN(THETA)*
     &       SIN(PHI) - SIN(PSI)*COS(PHI)) + W*(COS(PSI)*SIN(THETA)*
     &       COS(PHI) + SIN(PSI)*SIN(PHI))

      F(8) = VCO + U*SIN(PSI)*COS(THETA) + V*(SIN(PSI)*SIN(THETA)*
     &       SIN(PHI) + COS(PSI)*COS(PHI)) + W*(SIN(PSI)*SIN(THETA)*
     &       COS(PHI) - COS(PSI)*SIN(PHI))

      F(9) = WCO - U*SIN(THETA) +V*COS(THETA)*SIN(PHI) +W*COS(THETA)*
     &       COS(PHI)

      EULER ANGLE RATES F(10-12)

      F(10) = P + Q*SIN(PHI)*TAN(THETA) + R*COS(PHI)*TAN(THETA)

      F(11) = Q*COS(PHI) - R*SIN(PHI)

      F(12) = Q*SIN(PHI)/COS(THETA) + R*COS(PHI)/COS(THETA)


      UDOT = F(1)
      VDOT = F(2)
      WDOT = F(3)
      PDOT = F(4)
      QDOT = F(5)
      RDOT = F(6)
      XDOT = F(7)
      YDOT = F(8)
      ZDOT = F(9)
      PHIDOT = F(10)
      THETAD = F(11)
      PSIDOT = F(12)
CCCCCCCCCCCCCCCCCCCCCCCCCCCCCCCCCCCCCCCCCCCCCCCCCCCC
C       CREATE OUTPUT DATA FILE
C
C     TESTER=MOD(FLOAT(I),100.)
C     IF (TESTER .EQ. 0.0) THEN
      TIMER=FLOAT(I)/2.
C     WRITE (8,730)  DS,DR,XPOS,YPOS,ZPOS,ROLL,PITCH,YAW
C     WRITE (8,730)  FP(5)
C     WRITE (8,730)  U,V,W,P,Q,R
C     WRITE (8,730)  IX,IZ,IXY,IYZ,IXZ
C     WRITE (8,730)  MASS,XG,ZG
```

```
C      WRITE (8,730)   RHO,L,MPP,MPR,MRR
C      WRITE (8,730)   MQ,MVP,MVR,MW
C      WRITE (8,730)   MVV,MDS,DS,MDB,DB,NORPIT,WEIGHT
C      WRITE (8,730)   XB,BOY,THETA,PHI,MQN,EPS
C      WRITE (8,730)   MWN,MDSN,ZB
C      WRITE (8,730)   TIME,DEPTH,DS,THETA,S
C20    FORMAT (1X,'TIME',3X,'COMMAND DEPTH',3X,'DIVE P ANG',
C     *3X,'PITCH ANGLE',3X,'SLIDING SURFACE'/)
C30    FORMAT (1X,F6.2,2X,E11.3,3X,E11.3,4X,E10.3,3X,E11.3)
710    FORMAT (1X,'   TIME',3X,'  U ',3X,' ETA',3X,'  XPROP',
      *3X,  'DS')
       WRITE (8,730) TIME,U,ETA,XPROP,DS
730    FORMAT (1X,F6.2,2X,F6.2,2X,F6.3,2X,F8.4,2X,E11.3)
C      ENDIF
CCCCCCCCCCCCCCCCCCCCCCCCCCCCCCCCCCCCCCCCCCCCCCCCCCC
C       FIRST ORDER INTEGRATION
C
       U = U + DELT*UDOT
C                                         U = SURGE RATE
       V = V + DELT*VDOT
C                                         V = SWAY RATE
       W = W + DELT*WDOT
c                                         W = HEAVE RATE
       P = P + DELT*PDOT
C                                         P = ROLL RATE
       Q = Q + DELT*QDOT
C                                         Q = PITCH RATE
       R = R + DELT*RDOT
C                                         R = YAW RATE
       XPOS = XPOS + DELT*XDOT
C                                         X = SURGE
       YPOS = YPOS + DELT*YDOT
C                                         Y = SWAY
       ZPOS = ZPOS + DELT*ZDOT
C                                         Z = HEAVE
       PHI = PHI + DELT*PHIDOT
C                                         PHI = ROLL
       THETA = THETA + DELT*THETAD
C                                         THETA = PITCH
       PSI = PSI + DELT*PSIDOT
C                                         PSI = YAW

C
C         ********** OBSERVER OF SLIDING CONTROLLER **********
       CALL OBSER(QHADOT,THADOT,ZHADOT,QHAT,THAT,ZHAT,DELT,ZPOS,DS,U0)
C
C
C         ********** SLIDING MODE CONTROL INPUT **********
       S=QHAT+0.75*THAT-0.0233*(ZHAT-COMZ)
       IF (ABS(S) .LT. BAR) SAT=(S/BAR)*ABS(S)
       IF (S .LE. -BAR) SAT=-1
       IF (S .GE. BAR)  SAT=1
       UHAT=1.4286*QHAT+3.1429*THAT
       UBAR=EITA*SAT
       DE=UHAT+UBAR
       IF (DE .GE. 0.4) DS=0.4
```

114

```fortran
      IF (DE .LT. -0.4) DS=-0.4
      IF( (DE .LT. 0.4) .AND. (DE .GE.-0.4) ) DS=DE
      DB=-DS*1.0
      TIME=TIME+DELT
C
      PHIANG = PHI/0.0174532925
      THEANG = THETA/0.0174532925
      PSIANG = PSI/0.0174532925
C
      TRAC=-YPOS
      ROLL=PHIANG
      YAW=PSIANG
      DEPTH=-ZPOS
      DEPTH=ZPOS
      PITCH=THEANG
      BOWANG=(DB/.01745)
      STNANG=(DS/.01745)



100   CONTINUE
      STOP
      END

C     ******** OBSERVER SUBROUTINE ********
      SUBROUTINE OBSER(QHADOT,THADOT,ZHADOT,QHAT,THAT,ZHAT,DELT,
     *ZPOS,DS,U)
C
      QHADOT=-0.7*QHAT-0.03*THAT-0.035*DS-20.9293*(ZPOS-ZHAT)
      THADOT=QHAT-14.4092*(ZPOS-ZHAT)
      ZHADOT=-6*THAT+16.45*(ZPOS-ZHAT)
C
      QHAT=QHAT+DELT*QHADOT
      THAT=THAT+DELT*THADOT
      ZHAT=ZHAT+DELT*ZHADOT
      RETURN
      END
```

LIST OF REFERENCES

1. Vadim I. Utkin *Variable Structure System with Sliding Mode* IEEE Tractions on Automatic control, April 1977.

2. Jean-Jacques E. Slotine *Tracking Control of Nonlinear System Using Sliding Surface* Massachusetts Institute of Technology 1983.

3. Dana R. Yoerger and Jean-Jacques E. Slotine *Robust Trajectory Control of Underwater Vechicles* IEEE Journal of Oceanic Engineering, VOL. OE-10, NO 4, Oct 1985.

4. Katsuhiko, Ogata *Modern Control Engineering* Prentice-hall electrical engineering series, Prentice-hall, Inc, Englewood Cliffs, N.J., 1970.

5. U. Itkis *Control Systems of Variable Structure* Israel Universities press, Jerusalem.

6. Raymond A. Decarlo, Stanislaw H. Zak, and Gregory P. Matthews *Variable Structure Control of Nonlinear Multivariable System* Proceeding of the IEEE, VOL. 76, NO.3, March 1988.

7. Richard J. Boncal *A Study of Model Based Maneuvering Controls for Autonomous Underwater Vehicles* Master's Thesis, Naval Postgraduate School, Monterey, California, December 1987.

8. M. Gertler and G. R. Hagen *"Standard Equation of Motionfor Submarine Simulation"* NSRDC Report 2510, June 1967.

9. Kevin P. Larsen *Reduced Hydrodynamic Modeling for a Surmersible Vehicle* Master's Thesis. Naval Postgraduate School, Monterey, California. 1988

10. Michael A. Schwartz *Kalman Filtering for Adaptive Depth, Steering and Rolling Control of An Autonomous Underwater Vehicle* Master's Thesis, Naval Postgraduate School, Monterey, California, March 1989.

11. Bernard Friendland *Control System Design* Mc Graw-Hill Book Company, 1986.

12. Gordon S. MacDonald *Model Based Design and Verification of Rapid Dive Controller for Autonomous Underwater Vehicle* Master's Thesis, Naval Postgraduate School, Monterey, California, March 1989.

13. F.A. Papoulias, R. Cristi, D. Marco, A.J. Healey *Modeling, Sliding Mode Control Design, and Visual Simulation of AUV Dive Plane Dynamics Response* Proceeding. 6th International Symposium on Unmanned Untethered Submersible Technology. Washington D. C., June 1989.

INITIAL DISTRIBUTION LIST

No. Copies

1. Defense Technical Information Center   2
   Cameron Station
   Alexandria, VA 22304-6145

2. Library, Code 0142   2
   Naval Postgraduate School
   Monterey, CA 93943-5002

3. Professor F. A. Papoulias, Code 69Pa   3
   Department of Mechanical Engineering
   Naval Postgraduate School
   Monterey, CA 93943

4. Chairman, Code 69Hy   5
   Department of Mechanical Engineering
   Naval Postgraduate School
   Monterey, CA 93943

5. Professor R. McGhee, Code 52Mz   1
   Department of Computer Science
   Naval Postgraduate School
   Monterey, CA 93943

6. Professor R. Christi, Code 62Cx   1
   Department of Electrical and Computer Engineering
   Naval Postgraduate School
   Monterey, CA 93943

7. Naval Shipyard   1
   Hyun Dong, Jinhae City, Gyungnam 602-00
   Republic of Korea

8. Library of the Naval Academy   1
   Anggok Dong, Jinhae City, Gyungnam 602-00
   Republic of Korea

9. Professor Seo, Young-Tae   1
   Anggok Dong, Jinhae City, Gyungnam 602-00
   Republic of Korea

10.   Professor Park, Chil-Seung   1
      Anggok Dong, Jinhae City, Gyungnam 602-00
      Republic of Korea

11.   Sur Joo No   8
      Naval Academy, Jinhae, Ggungnam 602-02
      Republic of Korea

12.   Professor L. Chang, Code 69Ch   1
      Department of Mechanical Engineering
      Naval Postgraduate School
      Monterey, CA 93943

13.   Hal Cook, Code U25   1
      Naval Surface Warfare Center
      White Oak Laboratories
      Silver Spring, MD 20910-5000

14.   D. Steiger,   1
      Naval Research Laboratory
      Washington, D.C.

15.   RADM Evans, Code 9ZR   1
      Naval Sea Systems Command
      Washington, D.C. 20362-5101